ENERGY BAND STRUCTURES AND HIGH-FIELD CARRIER DISTRIBUTION FUNCTIONS IN SEMICONDUCTORS

A Thesis
Submitted in Partial Fulfilment
of the Requirements
for the Degree of

DOCTOR OF PHILOSOPHY

In the Department of
Electrical Engineering
University of Manitoba

by

WAFIK AZIZ WASSEF

October, 1973

ENERGY BAND STRUCTURES AND HIGH-FIELD CARRIER DISTRIBUTION FUNCTIONS IN SEMICONDUCTORS

By

Wafik Aziz Wassef

A dissertation submitted to the Faculty of Graduate Studies of the University of Manitoba in partial fulfillment of the requirements of the degree of

DOCTOR OF PHILOSOPHY

© 1973

Permission has been granted to the LIBRARY OF THE UNIVERSITY OF MANITOBA to lend or sell copies of this dissertation, to the NATIONAL LIBRARY OF CANADA to microfilm this dissertation and to lend or sell copies of the film, and UNIVERSITY MICROFILMS to publish an abstract of this dissertation.

The author reserves other publication rights, and neither the dissertation nor extensive extracts from it may be printed or otherwise reproduced without the author's written permission.

To My Mother

and

In Memory of My Father

ABSTRACT

A new method is presented for deriving a general expression for the energy band structure of a crystal under various conditions. Only two parameters, the energy splitting and effective electron mass at the extremum, which can easily be measured experimentally, are required for the calculations. The effect of temperature on the energy band structure is shown explicitly.

A general expression of the carrier distribution function is also presented. This general expression can be used to analyze any carrier transport phenomena at high or low fields in both nondegenerate and degenerate semiconductors with either parabolic or nonparabolic band structures. Using this expression, the Boltzmann transport equation has been solved analytically for low and high temperatures.

The effect of nonparabolic energy band structures on the high field distribution functions are briefly discussed.

ACKNOWLEDGEMENTS

The author wishes to express his grateful appreciation to Professor K.C. Kao for suggesting the topic of this thesis and for his supervision throughout the entire work.

The Graduate Fellowships awarded to the author by the University of Manitoba Research Board, and the financial support of the National Research Council of Canada through the research grants awarded to Professor K.C. Kao are deeply appreciated.

ACKNOWLEDGEMENT

(erratum)

The auther wishes to express his thanks to the Faculty of Engineering, Alexandria University, EGYPT, for the study leave offered to him, during which this work has been done.

TABLE OF CONTENTS

ABSTRACT iii

ACKNOWLEDGEMENTS iv

LIST OF PRINCIPAL SYMBOLS vii

CHAPTER 1 INTRODUCTION 1

CHAPTER 2 REVIEW OF PREVIOUS AND CONTEMPORARY WORK 4

2.1 Physical Properties of III-V Compounds 4

2.1.1 Mixed Crystals of III-V Compounds 8

2.1.2 Impurities and Defects 12

2.2 Energy Band Structures 12

2.2.1 The Cellular Method 14

2.2.2 The Variational Methods 15

2.2.3 The Augmented Plane Wave Method 17

2.2.4 The Tight Binding Method 19

2.2.5 The $\vec{k} \cdot \vec{p}$ Method 21

2.2.6 The Orthogonalized Plane Waves (OPW) Method 23

2.2.7 The Pseudopotential Method 26

2.3 High Field Transport Phenomena in Semiconductors 28

2.3.1 Scattering Mechanisms 30

2.3.2 The Boltzmann Equation 36

2.3.3 Electron Transport in Polar Semiconductors 38

CHAPTER 2 (continued)

2.4 Applications of III-V Compound Semiconductors 42

CHAPTER 3 ENERGY BAND STRUCTURES 43

3.1 Theory 44

3.2 Determination of the One Electron State Function, $\psi_{\vec{k}}$ 46

3.3 Determination of the Energy Eigenvalue, $E_{\vec{k}}$ 50

3.4 Computed Results 57

CHAPTER 4 HIGH-FIELD DISTRIBUTION FUNCTIONS OF CARRIERS IN SEMICONDUCTORS 65

4.1 General Expression of the Distribution Function 66

4.2 Boltzmann Equation and Scattering Mechanisms 71

4.3 Analytical Solution of Boltzmann Equation 79

4.4 Computed Results and Discussion 87

CHAPTER 5 THE EFFECT OF NONPARABOLIC ENERGY BAND STRUCTURES ON THE HIGH-FIELD CARRIER DISTRIBUTION FUNCTIONS 97

5.1 Distribution Function of Carriers in Nonparabolic Energy Band Structures 97

5.2 Physical Interpretation of the Complex Distribution Function 104

CHAPTER 6 CONCLUSIONS 107

REFERENCES 109

APPENDIX I EVALUATION OF ε 112

APPENDIX II 118

LIST OF PRINCIPAL SYMBOLS

a	lattice constant
A	normalization constant
B	constant
$C_1, C_2, \ldots$	constants
$C_{ij}^{(s)}$	magnitude of scattering due to phonons of type s
$\vec{d}$	displacement vector used in the displaced Maxwellian distribution function
d_t	interaction constant
D	dielectric tensor
D_o	diffusion coefficient
D_{ij}	interaction constant for intervalley scattering
$\tilde{D}_{ij}$	deformation potential field for intervalley scattering
e	electronic charge
e^*	effective charge
$\tilde{e}$	average of the strain tensor
$E(\vec{k})$	electron energy as a function of $\vec{k}$ in an energy band
ε	normalized energy defined by Eq.(3.44)
ε_1	shift of band edge per unit dilation
$f(\vec{k})$	distribution function of carriers
$f_o(E)$	Maxwellian distribution function
$\vec{F}$	external electric field
$g(\vec{k})$	perturbation part of the distribution function

G_i	number of states having energy E_i
$G_{\vec{k}}(\vec{r}-\vec{r}')$	Green's function
$\vec{G}_N$	reciprocal lattice vector defined by Eq. (3.31)
h	Planck's constant divided by 2π
H	the Hamiltonian operator
H_B	Boltzmann H-function
J	current density
$J_\ell(\rho)$	spherical Bessel function
$\vec{k}$	wave vector
K_B	Boltzmann constant
$\vec{K}$	$\vec{G}_N/N$ = reciprocal lattice vector
$\Delta\ell/\ell$	relative elongation
m_o	rest mass of the electron
m^*	anisotropic effective mass of the electron
$\langle m^*_{\vec{G}_N} \rangle$	isotropic average effective mass in the direction $\vec{G}_N$
M	number of atomic cells in the fundamental domain in a crystal
n,N	integers, used as band index
n_i	carrier concentration in the ith subband
N_i	number of electrons with energy E_i
N_q	number of phonons having wave vector q per unit volume
$\tilde{p}$	average of piezoelectric tensor
$\vec{p}$	momentum
$P_k(E_{\vec{k}},\vec{r})$	nonparabolicity factor defined by Eq. (3.18)
$P_n(u)$	Legendre polynomials of order n
$\vec{q}$	wave vector of phonons

Q	constant
$\vec{r}$	position vector
R_ℓ	operator degined by Eq. (3.10)
$\vec{R}_n$	lattice translation vector
s	superscript used for a particular type of phonons
T	temperature in degrees Kelvin
T_e	effective electron temperature
T_o	lattice temperature
u	velocity of sound
$u_{\vec{k}}(\vec{r})$	part of the wave function with lattice periodicity
u_ℓ	longitudinal sound velocity
$u_\ell(\vec{r})$	radial wave function
U	unitary operator
$\vec{v}$	drift velocity
$\langle\vec{v}\rangle_i$	average drift velocity of carriers in the ith subband
v_s	velocity of phonons of type s
$V(\vec{r})$	lattice potential
V_p	pseudo-potential
V_{F_i}	velocity of carriers in the direction of the applied field and having energy E_i
$w_{\vec{k},\ell}$	operator defined by Eq. (3.21)
$W_{\vec{k}}$	operator defined by Eq. (3.2)
x	normalized wave vector defined by Eq. (3.45)
$Y_\ell^m(\theta,\phi)$	spherical harmonic functions
α,β,γ	Lagrange multipliers
$\delta_{m,n}$	Kronecker delta function

Δ_i	extremum energy of the ith subband
$\square$	difference operator
ε	infinitesimal quantity
ε_o	interaction constant
θ	angle measured from the z-axis in spherical coordinates
μ_i	carrier mobility in the ith subband
ρ	$\lvert\vec{k}\rvert\lvert\vec{r}\rvert$
ρ_d	density of the crystalline solid
τ	nonprimitive translation (a/4, a/4, a/4)
τ_a	momentum relaxation time for acoustic scattering
τ_{ij}	relaxation time tensor elements
τ^i_{iV}	relaxation time for intervalley scattering in the ith subband
τ_{op}	relaxation time for nonpolar optical scattering
ϕ	azimuthal angle in spherical coordinates
$\{\phi_{\vec{k},m}\}$	set of orthonormal functions
$\Phi_{\vec{k}}(\vec{r})$	wave function defined by Eq. (2.18)
$\psi_{\vec{k}}(\vec{r})$	wave function defined by Eq. (2.4)
ω	angular frequency of phonons
ω_{ij}	angular frequency of phonons for intervalley scattering
ω_ℓ	longitudinal angular frequency for optical phonons
ω_o	angular frequency of optical phonons
Ω	volume of a unit cell in the crystal

LIST OF TABLES

Table 2.1 Mobilities of electrons and holes in some III-V compounds. 9

2.2 Energy gaps and effective masses of some III-V Compounds. 11

2.3 Diffusion coefficients of some materials in GaAs. 13

3.1 Parameters for GaAs. 60

3.2 Computed results for GaAs. 61

LIST OF FIGURES

Figure 2.1 Symmetry axes in a cube (o) 6

2.2 The energy gap a a function of x in the ternary compound $Ga(As_{1-x}P_x)$ [Folberth, 1955]. 10

3.1 The normalized energy band structure (a) on the base of Eq. (3.43); (b) on the base of the parabolic structure. 59

3.2 The energy band structure of the lower conduction band of GaAs with the extremum at Γ_i in the direction 100 (a) the result transformed from Fig. 3.1 for $< 1/m^*_{\vec{G}_N} > = 1/0.084m_o$ at 4°K; (b) the result transformed from Fig. 3.1 for $< 1/m^*_{\vec{G}_N} > = 1/0.065\ m_o$ at 300°K; (c) the result transformed from Fig. 3.1 for $< 1/m^*_{\vec{G}_N} > = 1/0.084\ m_o$ at 300°K; (d) the result of Pollak, Higginbotham and Cardona [1966] for $< 1/m^*_{\vec{G}_N} > 1/0.065m_o$ at 300°K. 63

4.1 Distribution function of electrons in (000) valley in n-GaAs for $C_{ij} = 2 \times 10^{-18} |\vec{K}-\vec{K}'|^{-2}$, $\theta = 0°$ and $h\omega_s = 0.01$ eV. (a) F = 2 kV/cm, n = 1; (b) f = 1 kV/cm, n = 1; (c) F = 1 kV/cm, n = 1.02; (d) Maxwellian distribution at F = 0 and T = 30°K for comparison purposes. 90

4.2 Distribution function of electrons in the (000) valley in n-GaAs for $C_{ij} = 1 \times 10^{-18} |\vec{K}-\vec{K}'|^{-2}$, $\theta = 0°$, and $h\omega_s = 0.01$ eV. (a) F = 2 kV/cm, n = 1; (b) F = 1 kV/cm, n = 1. 92

Figure 4.3 Distribution function of electrons in the (000) valley in n-GaAs for $C_{ij} = 1 \times 10^{-18} |\vec{k}-\vec{k}'|^{-1.98}$, $\theta = 0°$ and $h\omega_s = 0.01$ eV. (a) F = 2 kV/cm, n = 1; (b) F = 1 kV/cm, n = 1. 93

4.4 Distribution function of electrons in the (000) valley in n-GaAs for $C_{ij} = 1 \times 10^{-18} |\vec{k}-\vec{k}'|^{-2}$, F = 1 kV/cm, $h\omega_s = 0.01$ eV and n = 1. (a) $\theta = 0°$; (b) $\theta = 10°$. 94

4.5 Distribution function of electrons in the (000) valley in N-GaAs for $C_{ij} = 2 \times 10^{-18}|\vec{k}-\vec{k}'|^{-2}$, F = 2.4 kV/cm, $h\omega_s = 0.01$ eV, n = 1.05, and $\theta = 0°$. (a) Wassef and Kao; (b) Vassell and Conwell [1966]; (c) Maxwellian distribution (F = 0) at T = 293°K corresponding to n = 1.05 for comparison purposes. 96

CHAPTER 1

INTRODUCTION

The motion of carriers in a crystalline solid is one of the most important problems in solid state physics. The exact solution of this problem requires the solution of a many body problem under the influence of external fields. In most cases of interest the following two properties are of prime importance to this problem and they are:

1. The one electron energy band structure from which the allowed energy levels of a single electron in the field of all other charges and their interactions can be calculated.

2. The carrier distribution function, by which the distribution of all the available carriers over the energy bands can be calculated.

For the first property the relation between the energy and the wave vector (E-$\vec{k}$) of the electron under consideration is to be determined. This relation can usually be found by solving the Schrödinger equation and consequently all the interactions can be treated on the basis of the quantum theory. Chapter 3 will be devoted to a new

approach for the calculation of the one electron energy band structures.

The second property concerning the carrier distribution function can normally be found by solving the Boltzmann transport equation based on statistical mechanical concepts. The calculation of the distribution function of carriers is not only useful for determining the density of carriers in momentum space, but also for determining the average of any physical quantity shared by all of the carriers. Chapter 4 presents a new method for obtaining a general expression for the carrier distribution function for non-degenerate or degenerate semiconductors with parabolic or nonparabolic energy band structures under high or low electric fields.

In fact, these two properties are not completely separable. The knowledge of the energy band structure in the vicinity of any extremum is necessary for a complete determination of the carrier distribution function.

Since a great deal of work has been done about these two properties a brief account of the most important work in this field will be given in Chapter 2. Gallium Arsenide is used as a model semiconductor throughout this thesis to demonstrate any phenomena under consideration.

The effect of nonparabolic energy band structures on the high field distribution function together with the possible mechanisms for current instabilities will be

discussed briefly in Chapter 5. The general conclusions are given in Chapter 6.

CHAPTER 2

REVIEW OF PREVIOUS AND CONTEMPORARY WORK

The field of energy band structures and high field transport phenomena in semiconductors is very broad, and therefore the present review has to be confined to the energy band structures and certain aspects of transport phenomena in III - V compound semiconductors and particularly GaAs which are relevant to present investigations being reported in this thesis.

In this review, three major areas will be considered, namely: (i) the physical properties of the III - V compounds; (ii) the different approaches to the calculations of the energy bands; and (iii) the high field transport phenomena with particular emphasis on GaAs, and they are discussed separately in the following sections.

2.1 Physical Properties of III - V Compounds

The important features of these compounds are the low effective mass and high mobility. To study the chemical binding in these compounds we may define an effective charge e^* to be the charge around an atom in the group III elements; then $e^* = 0$ for neutral binding, $e^* = +e$ for covalent binding

and $e^* = -3e$ for ionic binding, where e is the electronic charge. For GaAs, $e^* = +0.51e$ and for InSb $e^* = +0.54e$. The effective charge can be measured by means of the infrared reflectivity, the X-ray diffraction or the piezoelectric effect.

In general, the chemical binding in group IV semiconductors is homopolar binding (the two neighbour atoms share two electrons centered halfway between them with opposite spin), but in III - V compounds the binding is partly homopolar and partly heteropolar by sharing between one electron of group III atom and three electrons of group V atoms [Madelung, 1964]. An increase in ionicity of the binding usually results in an increase in melting point and forbidden energy gap.

Most of the III - V compounds have the zinc-blende lattice structure. Some compounds of this category are: BP, AlP, GaP, InP, BAs, AlAs, GaAs, InAs, BSb, AlSb, GaSb and InSb. The others may have the Wurtzite lattice structure or the Hexagonal lattice or NaCl lattice structure, such as BN (distorted Wurtzite) and graphite.

Rotations and reflections, combined or not combined with nonprimitive translations, form the point group of the crystal. Primitive translations form an invariant subgroup of the space group, which constitutes the point lattice such as F.C.C. for diamond and zinc-blende structures. The point group of the zinc-blende structure which does not

contain all the symmetry elements of the F.C.C. lattice is designated by O_h [Hamermesh, 1962]

$$O_h : E,\ C_4^2(3),\ C_4(6),\ C_2(6),\ C_3(8),\ I,\ IC_4^2(3),\ IC_4(6),\ IC_2(6),\ IC_3(8),\ \text{total of 48 elements.}$$

The point group of the zinc-blende structure containing 24 elements which leaves the tetrahedron invariant is normally designated by T_d

$$T_d : E,\ C_4^2(3),\ C_3(8),\ IC_2(6),\ IC_4(6),$$

where E is the identity; C_n is a rotation around an axis with an angle of $\frac{2\pi}{n}$, in which n=1,2,3,4, or 6; I is an inversion; and the number inside the brackets indicate the number of such equivalent elements. Figure 2.1 shows some symmetry axes in a cube (designated by O)

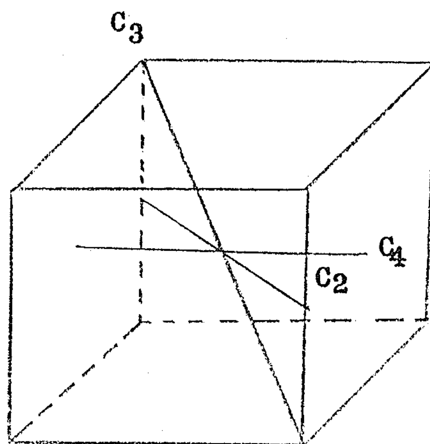

Fig. 2.1. Symmetry axes in a cube (O)

There are no inversion elements in T_d and no nonprimitive translations connected with the rotations and reflections-rotations in the space group of the zinc-blende lattice (T_d^2). Consequently, the space group is a direct product of the point group T_d and the translation group. The symmetry properties and their relation with the energy bands of the zinc-blende structures have been discussed in detail by Parmenter [1955] and Dresselhaus [1955].

The point group of the diamond structure contains all elements in O_h. In its space group (O_h^7), the operations IC_4^2, IC_3, C_2 and C_4 which are the elements not contained in T_d are combined with nonprimitive translations $\tau = (\frac{a}{4}, \frac{a}{4}, \frac{a}{4})$.

The lattice constants a of GaAs and InSb are, respectively, 5.6535 Å and 6.4789 Å. The change of the lattice constant with temperature can be calculated from the thermal properties of the materials [Novikova, 1966]. The relative elongation of GaAs can be expressed as:

$$\frac{\Delta l}{l} = 5.88 \times 10^{-6}\, T(°C) - 0.2 \times 10^{-3} \qquad (2.1)$$

This expression is valid for a very wide range of temperatures.

The melting points of some of the III - V compounds are InSb (530°C), InAs (942°C), GaSb (706°C) and GaAs (1238°C). The energy gap in II - VI compounds are larger than that of group IV elements but smaller than that of

I - VII compounds. In III - V compounds the lightest compound is BN which has the largest energy gap (5.3 ev), while the heaviest compound InSb has the smallest gap (0.08 ev).

In III - V compounds the atoms are more tightly bound due to the partial ionic bond, therefore the interaction of carriers with the lattice is weaker and hence the carriers have a larger mobility than that for group IV semiconductors.

In general, the mobility increases with increasing atomic weight in both group IV semiconductors and III - V compounds [Madelung, 1964]. The mobilities of some of the III - V compounds are given in Table 2.1 [Hilsum, 1966]. The calculated mobilities are based on polar optical scattering as a dominant mechanism. The discrepancy between the calculated and measured mobilities may be due to the effect of other types of scattering mechanisms which are not taken into account in the mobility calculations.

From the Hall effect experiments in GaAs, the mobility and the number of carriers have been found to decrease with the increase of pressure [Sladek, 1964].

2.1.1. Mixed Crystals of III - V Compounds

Most of the mixed crystals which have been extensively studied [Long, 1966] are ternary compounds such as $(In_{1-x}Ga_x)As$ and $Ga(As_{1-x}P_x)$, where x represents the mole

Table 2.1 Mobilities of electrons and holes in some III-V compounds.

Compound	Calculated Mobilities (cm /v.sec.)		Measured Mobilities (cm /v.sec.)	
	Electrons	Holes	Electrons	Holes
InSb	130,000	850	78,000	750
GaSb	33,000	3000	4,000	1,400
GaAs	10,400	520	8,800	400

fraction. The variation of the energy gap and the effective mass with x is of great importance to the development of suitable materials to meet the requirements for some particular devices, specially for infrared or optical devices. Also, it would help in the study of energy band structures of each of the binary compounds.

Some useful parameters for III - V compounds which can be interpolated for the case of ternary compounds are given in Table 2.2, where m* is the effective mass, m_o is the rest mass of the electron and [0,0,0] indicates the position of the band extremum in $\vec{k}$-space.

For $Ga(As_{1-x}P_x)$ it has been found [Long, 1966] that there is a kink in the relation of energy gap versus x at x ≃ 0.5 as shown in Fig. 2.2.

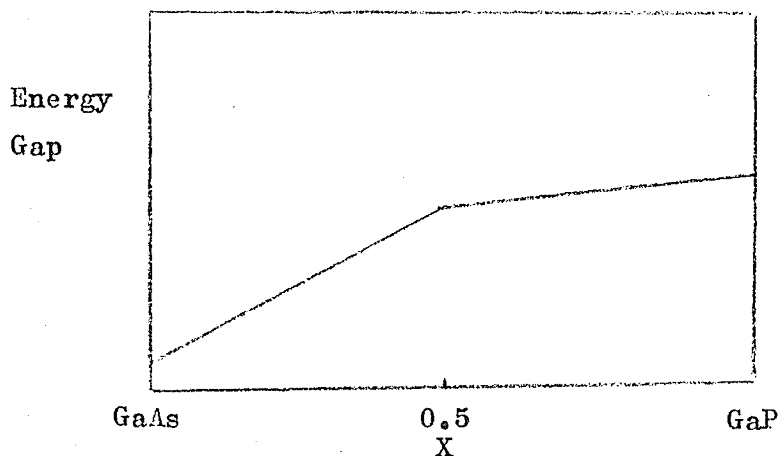

Fig. 2.2. The energy gap a a function of x in the ternary compound $Ga(As_{1-x}P_x)$ [Folberth,1955]

The change of the slope occurs when the [0,0,0] conduction band minimum (lowest in GaAs) and the [1,0,0] minima

Table 2.2 Energy gaps and effective masses of some III-V compounds

Compound	Energy Gaps (eV)			(m^*/m_o)		
	0 K	77 K	300 K	Electron	Light Hole	Heavy Hole
InSb 000	0.235	0.225	0.17	0.0155	0.02	0.4
GaSb 000	0.810	0.77-0.82	0.7-0.74	0.047	0.052	0.35
GaAs 000	1.530	1.49-1.52	1.37-1.43	0.07	0.12	0.68

(lowest in GaP) lie at the same energy, assuming no other changes to occur to the valence band. It has also been found that [Lang, 1966] the effective mass and the valence band spin-orbital splitting increase monotonically with x.

2.1.2. Impurities and Defects

Almost all the defects found in element semiconductors can also be found in III - V compounds such as vacancies, interstituals, grain boundaries, substitutionals, ... etc. Impurities of group II (zinc or cadmium) can be doped substitutionally in the trivalent lattice as acceptors and impurities of group VI (selenium or tellurium) in the pentavalent lattice as donors. Sulfur can also be used as donors and oxygen usually constitute a deep trap level.

The diffusion coefficients for self diffusion of some materials in GaAs at certain temperatures are listed in Table 2.3.

2.2. Energy Band Structures

One of the most important relations in solid state physics is the energy-wave vector relation, $E(\vec{k})$, which is usually referred to as the energy band. This relation not only indicates whether the material is a conductor or an insulator but also determines the binding forces and, hence, the transport coefficients. We usually ignore the problem

Table 2.3 Diffusion coefficients of some materials in GaAs

Diffusing Element	D_o (cm^2/sec)	Temperature °C
Cd	0.05 ± 0.04	868 - 1149
Zn	15 ± 7	800
Se	3×10^3	1000 - 1200
Sn	6×10^{-4}	1069 - 1215
Cu	0.03	100 - 600

of many particles and the effect of the motion of nuclei in the calculations of the energy band structures of semiconductors. In this section we shall give a short account of the different methods employed in the energy band calculations.

2.2.1. The Cellular Method

It was suggested by Wigner and Seitz [1933] that in order to solve the Schrödinger equation in a crystalline solid it is sufficient to confine the solution in a limited space in the crystal since the wave function will repeat itself due to the symmetry of the crystal. Consequently the derivative of the wave function at the symmetry plane will be zero normal to the plane. This argument was used as a boundary condition. The crystal space is divided by polyhedra constructed by the bisecting planes normal to the lines connecting the lattice points. As an approximation the polyhedral cell is replaced by a sphere of the same volume and as boundary conditions are taken to be that the derivative of the wave function vanishes at the boundary of this sphere.

For a spherically symmetric potential we can write the one electron wave function in the form [Wigner and Seitz, 1933; Slater, 1934; Callaway, 1964]

$$\psi_{\vec{k}} = \sum_{l=0}^{\infty} A_{\vec{k},l} \left[\sum_{m=-l}^{l} C^{m}_{\vec{k},l} \, Y^{m}_{l}(\theta,\phi) \right] u_{l}(E,r) \qquad (2.2)$$

where $A_{\vec{k},l}$ and $C^{m}_{\vec{k},l}$ are constants, $Y^{m}_{l}(\theta,\phi)$ are the spherical harmonics and $u_{l}(E,r)$ satisfies the radial equation

$$\{\frac{\hbar^2}{2m}[\frac{d^2}{dr^2} + \frac{2}{r}\frac{d}{dr} - \frac{l(l+1)}{r^2}] + (E-V)\}u_l(E,r) = 0 \qquad (2.3)$$

The constants in Eq. (2.2) can be determined by the boundary conditions of $\psi_{\vec{k}}$ and its derivatives based on Bloch's theorem. This is a complicated method even for the simplest cases. As an approximation the polyhedral cell is usually replaced by a sphere of the same volume.

Once the one electron wave function is completely determined, the energy eigenvalues can be found by evaluating the expectation value of the Hamiltonian of the system under consideration between two normalized wave functions similar to that given by Eq. (2.2).

2.2.2. The $\vec{k} \cdot \vec{P}$ Method

This method was first pointed out by Elliott [1954] and then developed and put in its present known form by Kane [1957] and applied to GaAs (the model semiconductor used in this thesis by Cardona and Pollak [1966]). As usual we begin by solving Schrödinger equation

$$[\frac{p^2}{2m} + V(\vec{r})]\,\psi_{n,\vec{k}} = E\,\psi_{n,\vec{k}} \qquad (2.4)$$

where n is the band index for a complete set of bands and the wave function $\psi_{n,\vec{k}}$ satisfies Bloch's theorem:

$$\psi_{n,\vec{k}} = e^{i\,\vec{k}\cdot\vec{r}}\,U_{n,\vec{k}}(\vec{r}) \qquad (2.5)$$

Suppose the set $U_{n,\vec{k}}$ is complete for $\vec{k} = \vec{k}_o$. The $U_{n,\vec{k}}$ can be expanded in the form

$$U_{n,\vec{k}}(\vec{r}) = \sum_{n'} C_{n,n'}(\vec{k} - \vec{k}_o)\, U_{n',\vec{k}_o}(\vec{r}) \qquad (2.6)$$

Substituting Eq. (2.5) into Eq. (2.4) we get:

$$\left[\frac{P^2}{2m} + \frac{h^2}{m}\vec{k}_o \cdot \vec{P} + \frac{h^2 k_o^2}{2m} + V(\vec{r})\right] U_{n,\vec{k}_o} = E_n(\vec{k}_o)\, U_{n,\vec{k}_o} \qquad (2.7)$$

which can be written in the form:

$$H_{\vec{k}_o} U_{n,\vec{k}_o} = E_n(\vec{k}_o)\, U_{n,\vec{k}_o} \qquad (2.8)$$

Substituting Eq. (2.6) into Eq. (2.7) we get

$$\sum_{n'} \left[\left\{E_n(\vec{k}_1) + \frac{h^2}{2m}(k^2 - k_o^2)\right\}\delta_{n,n'} + \frac{h}{m}(\vec{k} - \vec{k}_o) \cdot P_{n,n'}\right] C_{n'n}$$

$$= E_n(\vec{k})\, C_{n,n} \qquad (2.9)$$

where

$$\vec{P}_{n,n'} = \int_\Omega U^*_{n,\vec{k}_o}(\vec{r})\, \vec{P}\, U_{n',\vec{k}_o}(\vec{r})\, d^3r \qquad (2.10)$$

The radial wave functions $U_{n,\vec{k}_o}$ are normalized within the unit cell. If the nondiagonal part of the Hamiltonian $\frac{h}{m}(\vec{k} - \vec{k}_o) \cdot P_{n,n'}$ is small, we can treat it as a perturbation term. Then the eigenvalues $E(\vec{k})$ will be given by:

$$E_n(\vec{k}) = E_n(\vec{k}_o) + \frac{h^2}{2} \sum_{i=1} \frac{(k_i - k_{oi})^2}{m_i} \qquad (2.11)$$

where

$$\frac{1}{m_i} = \frac{1}{m} + \frac{2}{m^2} \sum_{n'} \frac{|\vec{i} \cdot \vec{P}_{n,n'}|^2}{E_n(\vec{k}_o) - E_{n'}(\vec{k}_o)} \qquad (2.12)$$

and $\vec{i}$ is a unit vector in the direction of the ith principal axis and $\vec{k}_o$ is the wave vector at an extremum.

As a critirian for the use of the $\vec{k} \cdot \vec{P}$ method, the validity of applying the perturbation theory must be satisfied in the semiconductor under consideration.

2.2.3 The Orthogonal Plane Waves (OPW) Method

This method was first suggested by Harring [1940]. The lattice potential is expanded in the form

$$V(\vec{r}) = \sum_{j\alpha} U_\alpha (\vec{r} - \vec{R}_{j\alpha}) \tag{2.13}$$

where α refers to the different ions in the unit cell, and j is an index integral to refer to the different cells. The Schrödinger equation for a particular ion α can be written in the form:

$$[- \frac{h^2}{2m} \nabla^2 + U_\alpha (\vec{r})] \phi_{\alpha t}(\vec{r}) = E_{\alpha t_o} \phi_{\alpha t} (\vec{r}) \tag{2.14}$$

The ionic wave function through the crystal may be written in the form:

$$|\alpha t,\vec{k} > = M^{-\frac{1}{2}} \sum_j \exp(i \vec{k} \cdot \vec{R}_{j\alpha}) \phi_{\alpha t} (\vec{r} - \vec{R}_{j\alpha}) \tag{2.15}$$

where t refers to the ionic state.

The ionic eigenvalues can therefore be calculated by

$$E_{\alpha t}(\vec{k}) = \frac{< \alpha t, \vec{k} |H| \alpha t, \vec{k}>}{<\alpha t, \vec{k} |\alpha t, \vec{k} >} \simeq E_{\alpha t_o} \tag{2.16}$$

A plane wave can be written in the form:

$$| \vec{k} > = \Omega^{\frac{1}{2}} \exp (i \vec{k} \cdot \vec{r}) \tag{2.17}$$

The fundamental step in this method is to construct a wave function (OPW) in the form:

$$|OPW, \vec{k} > = |\vec{k} > - \sum_{\alpha,t} |\alpha t, \vec{k} ><\alpha t, \vec{k}| \vec{k} > \tag{2.18}$$

which satisfies the orthogonality relation

$$< \alpha t, \vec{k} \mid OPW, \vec{k} > = o \qquad (2.19)$$

The energy eigenvalues can be determined by solving the determinantal equation:

$$\det \mid < OPW, \vec{k} + \vec{K} |H| OPW, \vec{k} + \vec{K}' >$$

$$- E(\vec{k}) < OPW, \vec{k} + \vec{K} \mid OPW, \vec{k} + \vec{K}' > \mid = o \qquad (2.20)$$

The disadvantage of this method is the lack of knowledge of the lattice potential. However, Herman [1969] found that it is sufficient to use a trial crystal potential having the form of a spatial superposition of overlapping atomic potentials. By iterating the solutions, he obtained self consistent crystal potentials.

Bassani and Yoshimine [1963] have also used the OPW method to calculate the energy bands of zinc-blende lattice. They used the Hartree-Fock atomic core states and a model crystal potential constructed as a sum of atomic potentials in which they used Slater approximation for the exchange potential. However, they found that the s-like conduction states does not agree with the experimental results.

2.2.4. The Variational Method

The potential inside the inscribed spheres is assumed to be spherically symmetric and constant in the space between them. This condition may be considered the main limitation in this method. It was found that the convergence of the numerical techniques used in this method is very good. As a rule, variational techniques based on integral equations, as is the case here, give more accurate results than those based on differential equations.

Consider the Schrödinger equation given by

$$(H-E)\psi = 0 \tag{2.21}$$

where H is the Hamiltonian of the system under consideration. If we define

$$I = \int \psi^* (H-E)\psi d^3r = 0 \tag{2.22}$$

then the variational principle gives the relation

$$\delta I = 0 \tag{2.23}$$

By setting $\psi' = \psi + \delta\psi$ (2.24)

and applying Green's theorem, we obtain

$$\delta I = \int (\delta\psi\nabla\psi^* - \psi^*\nabla\delta\psi)\cdot d\vec{s} \tag{2.25}$$

The integration is performed over the surface of an atomic cell.

A different approach [Callaway, 1964] may be given in terms of Green's function which satisfies the equation

$$(\frac{\hbar^2}{2m}\nabla^2 + E)G_{\vec{k}} - (\vec{r} - \vec{r}\,') = \delta(\vec{r} - \vec{r}\,') \tag{2.26}$$

which is subject to the boundary condition

$$G_{\vec{k}}(\vec{r} + \vec{R}_n) = e^{i\,\vec{k}.\vec{R}_n}\, G_{\vec{k}}(\vec{r}) \tag{2.27}$$

where $\vec{R}_n$ is the lattice translation vector.

If we designate the eigenfunctions of the operator $(-\frac{\hbar^2}{2m}\nabla^2)$ by ψ_j and the corresponding eigenvalues by E_j we have

$$G(\vec{r},\vec{r}\,') = - \sum_j \psi_j^* (\vec{r}\,') \frac{1}{E_j - E} \psi_j(\vec{r}) \tag{2.28}$$

where

$$\psi_j(\vec{r}) = \frac{1}{\Omega^{\frac{1}{2}}} e^{i(\vec{k} + \vec{K}_n)\cdot\vec{r}} \tag{2.29}$$

and Ω is the volume of the unit cell and $\vec{K}_n$ is the reciprocal lattice vector.

The variational method can be reformulated in a different way and this is generally referred to as the Kohn Korringa and Rostoka method [Kohn and Rostoker, 1954; and Korringa, 1947].

If we rewrite Schrödinger equation in the form

$$(\frac{\hbar^2}{2m}\nabla^2 + E)\ \psi_{\vec{k}}(\vec{r}) = V\,\psi_{\vec{k}}(\vec{r}) \tag{2.30}$$

then a solution can be found as

$$\psi_{\vec{k}}(\vec{r}) = \int_\Omega G_{\vec{k}}(\vec{r}-\vec{r}\,')\ V(\vec{r}\,')\ \psi_{\vec{k}}(\vec{r}\,')\ d^3\vec{r}\,' \tag{2.31}$$

This solution may be derived from the variational principle

$$\delta\Lambda = 0 \tag{2.32}$$

where

$$\Lambda = \int_{\Omega} \psi^{*}_{\vec{k}}(\vec{r})\ V(\vec{r})\ \psi_{\vec{k}}(\vec{r})\ d^{3}\vec{r} - \int_{\Omega}\int_{\Omega'} \psi^{*}_{\vec{k}}(\vec{r})\ V(\vec{r})\ G_{\vec{k}}(\vec{r}-\vec{r}\,')\ V(\vec{r}\,')\ \psi_{\vec{k}}(\vec{r}\,')\ d^{3}\vec{r}\,'\ d^{3}\vec{r} \tag{2.33}$$

We may choose $\psi_{\vec{k}}(\vec{r})$ as a linear combination of plane waves and adjust the coefficients in order to satisfy the variational principle.

2.2.5. The Augmented Plane Wave Method

In this method [Slater, 1937] the wave function is expanded into a set of functions composed of plane waves in the outer regions of the atomic cell and a sum of spherical waves in the interior [Loucks, 1967];

$$\Phi_{\vec{k}} = a\cdot\varepsilon(r-r_i)e^{i\ \vec{k}\cdot\vec{r}} + \sum_{l,m} a_{l,m}\ \varepsilon(r_i-r)\ Y_l^m(\theta,\phi)R_l(E,r) \tag{2.34}$$

where

$$\varepsilon(x) = 1 \quad \text{for} \quad x\geq 0$$

$$\varepsilon(x) = 0 \quad \text{for} \quad x<0$$

r_i is the radius of the inscribed sphere, $a_{l,m}$ are chosen such that $\Phi_{\vec{k}}$ is continuous across the sphere. However, its derivative cannot be made continuous. But we can calculate the energy from the expectation value of the Hamiltonian between two Augmented Plane waves.

The crystal potential is calculated using the muffin-tin model [Loucks, 1967] for which two nonoverlapping spheres are constructed on each site of a unit cell. Inside the spheres the potential is assumed to be spherically symmetric and outside it to be constant. For group IV semiconductors with diamond lattice, the muffin-tin model is not as good as it is for III - V compounds.

It can be shown [Loucks, 1967] that both the Augmented Plane Wave method and Green's function method give the same result if the same muffin-tin potential is used. The advantage of the Green's function method is that the secular determinant used there is smaller than that used in the APW method.

The relativistic effect is important for semiconductors with atomic number greater than 32 and thus it must be taken into consideration for atomic numbers greater than 71.

2.2.6. The Tight Binding Method

The main approximation in this method is that the one-electron wave functions belonging to bound atomic states do not form a complete set of functions. In this method [Bloch, 1929] we construct the functions

$$\Phi_{\vec{k}} = M^{-\frac{1}{2}} \sum_{n} e^{i\,\vec{k}\cdot\vec{R}_n}\, u(\vec{r}-\vec{R}_n) \qquad (2.35)$$

where M is the number of atomic cells in the crystal. The Hamiltonian can be expressed in the form

$$H = H_o(\vec{r}) + \sum_{n\neq 0} V(\vec{r}-\vec{R}_n) \qquad (2.36)$$

where

$$H_o(\vec{r}) = -\frac{\hbar^2}{2m}\nabla^2 + V(\vec{r}) \qquad (2.37)$$

We suppose that u satisfies the equation

$$H_o u(\vec{r}) = E_o\, u(\vec{r}) \qquad (2.38)$$

Then the energy eigenvalues can be calculated by the following equation

$$E(\vec{k}) = \frac{\int \phi^*_{\vec{k}}\, H\, \phi_{\vec{k}}\, d^3r}{\int \phi^*_{\vec{k}}\, \phi_{\vec{k}}\, d^3r}$$

$$= E_o + \frac{Q + \sum_{n} J(|\vec{R}_n|)\, e^{-i\,\vec{k}\cdot\vec{R}_n}}{1 + \sum_{n} S(|\vec{R}_n|)\, e^{-i\,\vec{k}\cdot\vec{R}_n}} \qquad (2.39)$$

where

$$Q = \sum_{n\neq 0} \int |u(\vec{r})|^2\, V(\vec{r}-\vec{R}_n)\, d^3r$$

$$S(|\vec{R}_n|) = \int u^*(\vec{r}-\vec{R}_n)\, u(\vec{r})\, d^3r \qquad (2.40)$$

$$J(|\vec{R}_n|) = \int u^*(\vec{r})\, V(\vec{r})\, u(\vec{r}-\vec{R}_n)\, d^3r$$

Generally, the nearest neighbour overlap terms are included. However, this approximation is not always valid. It was found [Bartling and Craig, 1971] that for many-centre calculations the series expressions in Eq. (2.22) converge slowly.

In the III - V compounds we have two different atoms per unit cell, therefore the tight-binding method may be rederived by writing Eq. (2.18) as

$$\psi_n(\vec{k},\vec{r}) = M^{-\frac{1}{2}} \sum_{\vec{R}_j} e^{i\,\vec{k}\cdot\vec{R}_j}\, u_n(\vec{r}-\vec{R}_j) \quad ,$$
$$\psi_m(\vec{k},\vec{r}) = M^{-\frac{1}{2}} \sum_{\vec{R}_j} e^{i\,\vec{k}\cdot(\vec{R}_j+\vec{\tau})}\, u_m(\vec{r}-\vec{R}_j-\vec{\tau}) \qquad (2.41)$$

The Hamiltonian is given by

$$H(\vec{r}) = -\frac{\hbar^2}{2m}\nabla^2 + \sum_{\vec{R}_j} [V_A(\vec{r}-\vec{R}_j) + V_B(\vec{r}-\vec{R}_j-\vec{\tau})] \qquad (2.42)$$

and the overlap matrix element by

$$I_{n,m}(\vec{k}) = \int_{-\infty}^{\infty} \psi_n^*(\vec{k},\vec{r})\ \psi_m(\vec{k},\vec{r})\ d^3r \qquad (2.43)$$

The Hamiltonian matrix element is given by

$$H_{n,m}(\vec{k}) = \int_{-\infty}^{\infty} \psi_n^*(\vec{k},\vec{r})H(\vec{r})\ \psi_m(\vec{k},\vec{r})\ d^3r \quad , \qquad (2.44)$$

The lattice potential may be expanded in the following form

$$V(\vec{K}) = \Omega^{-1} \int_{\Omega} V(\vec{r})\ e^{i\,\vec{K}\cdot\vec{r}}\ d^3r \qquad (2.45)$$

Thus, the eigenvalues $E(\vec{k})$ can be calculated by solving the determinantal equation

$$\det \left| H_{n,m}(\vec{k}) - E\, I_{n,m}(\vec{k}) \right| = 0 \qquad (2.46)$$

2.2.7. The Pseudopotential Method

In this method [Phillips, 1958; Phillips and Kleinman, 1959; and Falicov, 1968], an operator P defined by

$$P = \sum_{\alpha t} |\alpha t, \vec{k}\rangle\langle \alpha t, \vec{k}| \qquad (2.47)$$

is used in the description of the wave function

$$|\psi_{\vec{k}}\rangle = |X_{\vec{k}}\rangle - \sum_{\alpha t} |\alpha t, \vec{k}\rangle\langle \alpha t, \vec{k}|X_{\vec{k}}\rangle = (1-P)\,|X_{\vec{k}}\rangle \qquad (2.48)$$

The Schrödinger equation takes the form

$$(H-HP)\,|X_{\vec{k}}\rangle = E_{\vec{k}}(1-P)\,|X_k\rangle \qquad (2.49)$$

or

$$H_p|X_{\vec{k}}\rangle = E_{\vec{k}}|X_k\rangle \qquad (2.50)$$

where

$$H_p = H - (H-E_{\vec{k}})P$$

$$= -\frac{\hbar^2}{2m}\nabla^2 + V_p(\vec{k}) \qquad (2.51)$$

The pseudopotential V_p is given by

$$V_p = V - \sum_{\alpha t} (E(\vec{k}) - E_{\alpha t})\,|\alpha t, \vec{k}\rangle\langle \alpha t, \vec{k}| \qquad (2.52)$$

The pseudopotential is usually so large such that the perturbation theorem cannot be applied satisfactorily.

However, using the cancellation theorem [Cohen and Heine, 1961;Pendry, 1971] the pseudopotential is considerably reduced. The potential in this case may be written in the form

$$V_{pc} = (1 - \sum_{c} |c\rangle\langle c|)V \qquad (2.53)$$

where $|c\rangle$ represents the core states. Equation (2.54) can easily be interpreted for low energy electrons near the core region, since for such electrons only the fraction of charge included in a sphere of radius equal to their separation from the nucleus, will constitute their potential energy.

The pseudopotential method was used to calculate the energy band structures for semiconductors of the diamond and zinc-blende structures [Cohen and Bergstresser, 1966]. In this case, the potential may be expressed in the form

$$V(\vec{r}) = \sum_{K \leq K_o} (S^S(\vec{K})V_K^S + iS^A(\vec{K})V_K^A)\ e^{-i\ \vec{K}\cdot\vec{r}} \qquad (2.54)$$

where

$$S^S(\vec{K}) = \cos \vec{K}\cdot\vec{\tau}$$

$$S^A(\vec{K}) = \sin \vec{K}\cdot\vec{\tau}$$

$$V_K^S = \tfrac{1}{2}\ [V_1(\vec{K}) + V_2(\vec{K})] \qquad (2.55)$$

$$V_K^A = \tfrac{1}{2}\ [V_1(\vec{K}) - V_2(\vec{K})]$$

$$V_1(\vec{K}) = \frac{2}{\Omega} \int V_1(\vec{r})\, e^{i\,\vec{K}\cdot\vec{r}}\, d^3r$$

All the methods given above have two main disadvantages:

(1) the calculations are tedious;

(2) the lattice potential is unknown and has to be assumed to follow some form before the calculations can be done.

The investigation into a new method to remove these shortcomings and to simplify the calculation process forms part of the present thesis and this will be discussed in Chapter 3.

2.3 High Field Transport Phenomena in Semiconductors

The application of a high electric field in semiconductors [Conwell, 1967] causes a change in mobility of carriers, dielectric constant, photo-absorption, carrier distribution, magnetoresistance and recombination rate of excess carriers. The high field introduces also new effects such as anisotropy of conductivity, a potential due to a gradient in electric field intensity and negative differential resistance, ... etc. Two main problems which must be well studied before any transport phenomena at high fields can be investigated. These are the distribution function of carriers $f(\vec{k})$ and the energy band structures $E(\vec{k})$.

At very low temperatures (few degrees Kelvin) we should use Fermi-Dirac distribution instead of Maxwell-Boltzmann distribution. But the disturbance of Bose-Einstein distribution of phonons must be well studied at this low temperature range. To distinguish between different mechanisms of scattering we must study their temperature dependence. For n-type GaAs it is believed that polar optical scattering dominates at room temperature while piezoelectric scattering dominates at very low temperatures.

The energy band structure of a material is of great importance to the study of high field transport phenomena because

(a) the conductivity is an anisotropic quantity in most materials; and

(b) the carriers may occupy states in momentum space which may be empty at low fields.

One of the most important phenomena at high fields is the negative differential resistance. This can be caused by one of the following mechanisms

(a) scattering mechanism

Kogan [1963] showed that a material in which the energy loss of carriers is due to piezoelectric scattering while the momentum relaxation is due to impurity scattering should show negative differential resistance

(b) electron transfer mechanism

In this mechanism the carriers are heated by an

external field such that they make a transition to higher states in which their mobilities are smaller [Ridley and Watkins, 1961].

(c) electron capturing mechanism

This mechanism depends on the existence of impurity or other defect levels in which the capture cross section increases with the increase of the carrier energy [Ridley and Watkins, 1961].

There are several experimental methods to study the energy distribution of carriers in semiconductors [Conwell, 1967] and some of the important ones are:

(1) the electrical noise of carriers;

(2) the Faraday rotation (the rotation of the plane of polarisation of an electromagnetic wave when it passes through a substance with a static magnetic field along the direction of propagation);

(3) the electron emittance from the sample surface. This method is used to measure the tail of the distribution function;

(4) the shift in electron spin resonance. This is used to determine the variation of the average electron energy with the field.

2.3.1 Scattering Mechanisms

There are two branches in the dispersion curves of lattice vibrations, and they are the acoustic

branch and the optical branch. In the acoustic branch, scattering of carriers due to lattice strain is called deformation potential scattering, and that due to polarization is called piezoelectric scattering. In the following, we shall briefly discuss each type of scattering mechanism [Conwell, 1967].

(i) Acoustic mode scattering

The momentum relaxation time for acoustic scattering is given by

$$\frac{1}{\tau_a} = \frac{m^*\Omega M}{2\pi\hbar^3 k} \Big[\int_0^{2k+2m^*u/\hbar} |<\vec{k}+\vec{q}|H'|\vec{k}>|^2 \, q \, dq + \int_0^{2k-2m^*u/\hbar} |<\vec{k}-\vec{q}|H'|\vec{k}>|^2 \, q \, dq \qquad [2.66]$$

where Ω is the volume of the unit cell, M is the number of cells in the crystal, u is the velocity of sound and $\vec{q}$ is the wave vector of phonons.

For deformation potential scattering only longitudinal lattice waves scatter the carriers. If the equipartition law is assumed to hold for this case, the relaxation time can be written in the form

$$\frac{1}{\tau_{ae}} = \frac{\sqrt{2}}{\pi} \frac{\varepsilon_1^2 \, m^{*3/2} \, K_B \, T}{\hbar^4 \, C_l} E^{\frac{1}{2}} \qquad (2.67)$$

where

$$C_l = \frac{\rho_d \, u^2{}_l}{\sqrt{2m^*}} \qquad (2.68)$$

ε_1 is the shift in the band edge per unit dilation, K_B is the Boltzmann constant, ρ_d is the crystal density, u_l is the longitudinal sound velocity and E is the carrier energy.

In general, for the nonequipartition case we have

$$\frac{1}{\tau_a} = \frac{\hbar^2 u_l}{4 l_{ae} m^* K_B T} \frac{1}{k^3} \int_0^{2k} (N_q + \tfrac{1}{2})\, q^4\, dq \qquad (2.69)$$

where

$$l_{ae} = \frac{\pi \hbar^4 \rho_d u_l^2}{m^{*2} \varepsilon_1^2 K_B T} \qquad (2.70)$$

and N_q is the number of phonons per unit volume.

For piezoelectric scattering the relaxation time can be written in the form

$$\frac{1}{\tau_{PZ}} = \frac{m^{*1/2}\, \tilde{e}^2\, K_B\, T}{2^{3/2}\, \pi\, \hbar^2\, E^{1/2}} \quad \frac{\tilde{p}^2}{D^2 C_l} \qquad (2.71)$$

where $\tilde{p}$ is the average of the piezoelectric tensor, $\tilde{e}$ is the average of the strain tensor and D is the dielectric tensor.

(A) The rate of energy loss to acoustic modes

If we assume that the distribution function obeys Maxwell-Boltzmann distribution at temperature T_e, then the energy loss of carriers to acoustic phonons obeying equipartition law is given by

$$\left\langle \frac{dE}{dt} \right\rangle_a = - \frac{8\sqrt{2}}{\pi^{3/2}} \frac{\varepsilon_1^2\, m^{*5/2}}{\hbar^4 \rho_d} (K_B T_e)^{3/2} \left(1 - \frac{T}{T_e}\right) \qquad (2.72)$$

It is worthy to mention here two approaches for calculating the effect of an applied electric field on the scattering processes. One way of handling this problem [Bardeen and Schockley, 1950] is to begin with the time dependent Schrödinger equation

$$[-\frac{\hbar^2}{2m}\nabla^2 + V_o(\vec{r}) - \vec{F}\cdot\vec{r} + H_I]\psi = i\hbar\frac{\partial\psi}{\partial t} \qquad (2.73)$$

where $V_o(\vec{r})$ is the periodic crystal field, $\vec{F}$ the electric field force and H_I is the interaction operator which describes the scattering process. It was found that the probability per unit time of a transition from a state $\vec{k}$ to a state $\vec{k}'$ is

$$S(\vec{k},\vec{k}') = \frac{2\pi}{h}|M(\vec{k},\vec{k}')|^2\ \delta(E(\vec{k}) - E'(\vec{k}')) \qquad (2.74)$$

where $M(\vec{k},\vec{k}')$ is the matrix element for transition, and $E(\vec{k})$ and $E'(\vec{k}')$ are respectively, the energies of the initial and final states which are independent of the field. The approximations used in reaching such a conclusion was found to be valid under the condition

$$\tau\omega > 1 \qquad (2.75)$$

where τ is the relaxation time between two collisions and ω is the angular frequency of the phonon participating in the collision process. An equivalent limit for this

treatment is found to be given for the upper limit of the applied electric field of the value 6×10^5 volts/cm.

A different approach [Sharma, 1971] handles the same problem by solving the Boltzmann transport equation

$$\frac{\partial f}{\partial t} + \vec{v}\cdot\vec{\nabla}_r f + \frac{\vec{F}}{m^*}\cdot\vec{\nabla}_V f = \left(\frac{\partial f}{\partial t}\right)_{coll} \qquad (2.76)$$

where m^* is the effective mass of the electron and $\left(\frac{\partial f}{\partial t}\right)_{coll}$ is considered to be for acoustic scattering mechanisms. By calculating the absorption coefficient, it was found that the threshold drift velocity of the electrons that changes absorption into amplification is equal to the velocity of sound. The main difference between the above mentioned two approaches is the electron-velocity-dependent collision frequency which was neglected in the first approach.

(B) Spontaneous and stimulated emission of phonons

At low temperatures the lifetime of phonons will increase and the effect of external fields will be considerable in distorting their thermal equilibrium distribution function. Therefore, we can express the phonon distribution as

$$N_{\vec{q}} = N_{\vec{q}o} + N_{\vec{q}} \qquad (2.77)$$

where $N_{\vec{q}o}$ is the spontaneous part (at thermal equilibrium) and $N_{\vec{q}}$ is the stimulated part.

(ii) Optical mode scattering

For nonpolar optical scattering the relaxation time is given by [Conwell, 1967]

$$\frac{1}{\tau_{op}} = \frac{d_t^2 K^2 m^{*3/2}}{\sqrt{2}\pi\hbar^3 \rho_d \omega_o} [N_{\vec{q}}(E + h\omega_o)^{\frac{1}{2}} + (N_{\vec{q}} + 1)(E - \hbar\omega_o)^{\frac{1}{2}}] \quad (2.78)$$

where d_t is an interaction constant having the dimensions of energy, $\vec{K}$ is the reciprocal lattice vector, and ω_o is the angular frequency of the optical phonons.

The polar optical scattering is the dominant mechanism of scattering in compound semiconductors such as in InSb and GaAs at temperatures higher than 100°K. In this case we cannot define a relaxation time for the carriers. However, the rate of change of carrier energy due to polar optical scattering is given by

$$\left(\frac{dE}{dt}\right)_{po} = \frac{2e\varepsilon_o \hbar\omega_l}{(2mE)^{\frac{1}{2}}}[N_{\bar{q}} \sinh^{-1}\left(\frac{E}{\hbar\omega_l}\right)^{\frac{1}{2}} - (N_{\bar{q}} + 1)\sinh^{-1}\left(\frac{E-\hbar\omega_l}{\hbar\omega_l}\right)^{\frac{1}{2}}] \quad \ldots (2.79)$$

where e is the electronic charge, ε_o is an interaction constant and ω_l is the longitudinal angular frequency of the optical phonons.

(iii) Intervalley scattering

Similar to the optical scattering the relaxation time for the ith valley is given by [Conwell, 1967]

$$\frac{1}{\tau_{iV}^{i}} = \sum_{\substack{j \\ j\neq i}} \frac{D_{ij}^2 m_j^{*3/2}}{\sqrt{2}\pi\hbar^3 \rho_d \omega_{ij}}[N_{\vec{q}}(E-\Delta E^j+\hbar\omega_{ij})^{\frac{1}{2}} + (N_{\vec{q}}+1)(E-\Delta E^j-\hbar\omega_{ij})^{\frac{1}{2}}] \quad \ldots (2.80)$$

where D_{ij} is an interaction constant, m_j is the isotropic effective mass of the jth valley and $N_{\vec{q}}$ represents the steady state number of phonons with energy $\hbar\omega_{ij}$ which follows the Bose-Einstein distribution function.

2.3.2 The Boltzmann Equation

The Boltzmann equation is mainly used to determine the carrier distribution function under the effects of externally applied electric field and different types of scatterings. The mathematical theorems connected with the general solutions of Boltzmann equation are discussed by F.A. Grünbaum [1972]. However, we are interested in the special cases under which this equation will take the form of Eq. (2.76).

One of the most important consequences of this equation is the Boltzmann H-theorem [Mazo, 1967] which states that if

$$H_B = \int f \ln f \, d\vec{r} \, d\vec{V} \qquad (2.81)$$

where f is the distribution function. It can be proved that

$$\frac{dH_B}{dt} \leq 0 \qquad (2.82)$$

This result is different from that indicated by the equations of motion which are invariant under time reversal. The irreversible behaviour of Boltzmann equation is due to

the separation of streaming and collision terms and also due to the assumption of the molecular chaos. This implies that there is no correlation between positions and momenta of particles before and after collision.

In constructing the collision term in the Boltzmann equation we usually make the following assumptions [Mazo, 1967]:

(i) only two particles participate in the collision process;

(ii) the distribution function describing both particles can be expressed as a multiplication of two functions, one for each particle alone;

(iii) during the time of collision the explicit dependence of time in the distribution function can be neglected;

(iv) any gradient of inhomogeneities in the range of intermolecular distance is neglected.

Boltzmann equation is valid for low concentration since it does not take into consideration the Pauli exclusion principle. However, this deficiency can be corrected by using the distribution function to obey Fermi-Dirac statistics before applying it to Boltzmann equation [Rode, 1971; Wassef and Kao, 1972]. Besides, the distribution function must be coarse-grained in space and time by suitable averaging processes.

It is worthy to mention that assumption (ii) above-

mentioned introduces the principle of molecular chaos.

2.3.3. Electron Transport in Polar Semiconductors

A large amount of work on the transport phenomena in polar semiconductors has been carried out in the last few years (Conwell 1967). Perhaps one of the earliest and most important articles for the band structure and electron transport in GaAs is that by Ehrenreich [1960]. He found that the most important mechanism of scattering in GaAs above room temperature is the polar scattering. However, for large concentrations of electrons in the semiconductor the polar scattering is reduced considerably due to the screening effect.

Acoustic, polar and impurity scattering are almost always anisotropic. This suggests the importance of studying the transport phenomena with anisotropic scattering [Żukotyński and Grynberg, 1965]. In this case, both the effective mass and relaxation time should be used in tensor forms. The distribution function is expressed as

$$f = f_o + \chi_i(E) k_i \left(\frac{df_o}{dE}\right) \tag{2.83}$$

while the scattering term in the Boltzmann equation is written in the form

$$\left(\frac{df}{dt}\right)_{scatt} = - \sum_j \chi_i(E)\ \tau_{ij}^{-1}\ k_j \left(\frac{df_o}{dE}\right) \tag{2.84}$$

where $\chi_i(E)$ is a function of energy and τ_{ij} is the relaxation time tensor element.

The nonparabolicity of the energy bands plays a major role in the calculations of the high field transport phenomena. An approximate relation for the energy bands was derived from the $\vec{k}\cdot\vec{P}$ method to take the form [Conwell and Vassell, 1968]

$$\frac{\hbar^2 k^2}{2m_1^*} = E(1 + \alpha E + \beta E^2 + \ldots) \qquad (2.85)$$

where m_1^* is the effective mass of electrons at the bottom of the conduction band and α and β are constants.

It has also been shown [Conwell and Vassell, 1968] that in the cases where a relaxation time for the polar optical scattering can be defined, the decrease in the relaxation time due to nonparabolicity of energy bands may reach 35 percent at $E/\hbar\omega_l = 20$. Similarly, it has been found that the relaxation time due to acoustic scattering decreases by more than 50 percent when nonparabolic energy band is considered at $E/\hbar\omega_l = 20$.

An experimental approach to the study of the transport properties of GaAs has been reported by Rush and Kino [1968]. In their experiment they used a reverse-biased Schottky barrier-i-n^+ diode. The transit time of the carriers in the uniform-field intrinsic region is the measure of the drift velocity. To avoid injection problems

the diode is held in a cathode ray tube and injection of electrons was performed by a short pulse (0.1 nsec) high-energy (14kV) electron beam. For a sample of the mobility of 7500 cm /vsec at low fields the threshold field for the occurrence of a negative differential mobility was found to be 3.3 kV/cm approximately. They observed also that the negative differential mobility stays almost constant when the temperature of the sample changes from 210°K to 340°K; but the threshold field for the occurrence of a negative differential mobility decreases monotonically as the temperature of the sample is increased.

A great deal of work has been done for calculating the transport properties of InAs. Curby and Ferry [1971] have given a brief account of the previous work in this field. In their work they calculated the change in mobility versus applied electric field for n-type InAs at 77°K for fields below impact ionization level. They used the $\vec{k}\cdot\vec{p}$ method expression for the energy band structure together with the following balance equations

$$\left\langle\frac{dE}{dt}\right\rangle_{field} + \left\langle\frac{dE}{dt}\right\rangle_{po} = 0 \qquad (2.86)$$

$$\left\langle\frac{d\vec{P}}{dt}\right\rangle_{field} + \left\langle\frac{d\vec{P}}{dt}\right\rangle_{po} + \left\langle\frac{d\vec{P}}{dt}\right\rangle_{imp} = 0 \qquad (2.87)$$

where the energy loss due to ionized-impurities (imp) and the energy and momentum loss due to acoustic scattering

mechanism are neglected. However, the calculated mobilities are in good agreement with the corresponding experimental results for fields below 100 v/cm. For higher fields, the agreement was not as good as for low fields, possibly due to the assumptions made in the energy band calculations and distribution function form.

Another approach for calculating transport properties of electrons in direct-gap semiconductors can be achieved by solving Boltzmann equation [Rode, 1971]. To allow for high impurity concentration, that is to say for electron degeneracy, the distribution function must satisfy Fermi-Dirac statistics as well as Boltzmann equation. In fact, the Fermi-Dirac distribution function does not hold for high fields [Wassef and Kao, 1972] and for this reason some modifications must be introduced. This will be shown in Chapter 4. However, Rode [1971] used the approximate expression for the distribution function

$$f_t(\vec{k}) = f(\vec{k}) + g(\vec{k}) \cos(\theta) \tag{2.88}$$

where $f(\vec{k})$ is the Fermi-Dirac distribution function, $g(\vec{k})$ is a perturbation part and θ is the angle between $\vec{k}$ and the applied field. Taking into account the scattering by ionized impurities as well as by polar optical, piezo-electric and acoustic scattering, Rode [1971] has found that the calculated mobilities for InSb agrees with the

corresponding experimental results for a wide range of temperature extending from 200°K ($\mu \simeq 1.2 \times 10^5$ cm^2/vsec) up to 600°K ($\mu \simeq 2 \times 10^4$ cm^2/vsec).

2.4 Applications of III - V Compound Semiconductors

The p-n junctions of III - V compounds [Madelung, 1964] are of greater interest. They have been used as photo-diodes and radiation detectors and as tunnel diodes. Metal semiconductor contacts can be used for the study of band structures of semiconductors.

Transistors made of GaAs operate at higher temperatures than Ge and Si transistors and at a higher cut-off frequency than Ge transistors.

Laser action has been observed in p-n junctions of different III - V compounds because they are direct gap semiconductors.

CHAPTER 3

ENERGY BAND STRUCTURES

Energy band calculations are of great importance to the field of solid state physics. One of the earliest applications of the quantum theory was to calculate the energy levels in crystalline solids. The cellular method [Wigner and Seitz, 1933; Slater, 1934] was the first method introduced for such calculations. Since then, several methods have been put forward either to improve or to simplify the computations involved. Some of the well-known methods have been briefly discussed in Chapter 2. Most of the aforementioned methods, except the $\vec{k} \cdot \vec{P}$ method, depend greatly on the knowledge of the lattice potential which usually constitutes a fundamental problem for such calculations. However, the $\vec{k} \cdot \vec{P}$ method removes this shortcoming and makes use of the group theory, the perturbation theory and some experimental results including effective masses, spin-orbit splittings and energy splittings. It should be noted that it is absolutely necessary to check the validity of the use of the perturbation theory for each case separately before applying the $\vec{k} \cdot \vec{P}$ method.

In this chapter a new method is presented for deriving an analytical expression for the wave functions and energy band structures for crystalline solids. In this method only two parameters namely the effective mass and the energy splitting at a particular extremum under investigation have to be known. These two parameters can easily be determined experimentally. However, the shortcoming concerning the doubtful assumptions for the lattice potential is removed.

The expression for the eigenfunctions applicable to both periodic and aperiodic potentials is presented, and some computed results based on this method for the energy band structure and the effect of temperature for GaAs and a comparison of these results with those of other investigators are also given.

In the case of aperiodic potentials it will be shown that the expression for the eigenfunction predicts correctly the assymptotic behaviour of the eigenfunctions in collision problems.

3.1 Theory

The energy band structure of a crystal can be calculated by solving Schrödinger equation

$$H|\psi_{\vec{k}}\rangle = E_{\vec{k}}\,|\psi_{\vec{k}}\rangle \qquad (3.1)$$

where $\psi_{\vec{k}}$ represents the one electron state function corresponding to the energy eigenvalue $E_{\vec{k}}$ with the wave vector $\vec{k}$. The Hamiltonian H consists of the kinetic energy operator $-\frac{\hbar^2}{2m}\nabla^2$, and the total potential energy $V(\vec{r})$ which is due to all charges and all types of interactions in the crystal.

To solve Eq. (3.1) we introduce an operator $W_{\vec{k}}$ defined by

$$W_{\vec{k}} = \sum_m |\psi_{\vec{k}}><\phi_{\vec{k},m}| \tag{3.2}$$

where $\phi_{\vec{k},m}$ represents an arbitrary set of orthonormal functions which have no direct relation with $\psi_{\vec{k}}$. We also assume that $\psi_{\vec{k}}$ is normalized so that $<\psi_{\vec{k}}|\psi_{\vec{k}}> = 1$

The operator $W_{\vec{k}}$ has the following properties:

(i) The orthonormality of the set $\{\phi_{\vec{k},m}\}$ implies that $<\phi_{\vec{k},m}|\phi_{\vec{k},n}> = \delta_{m,n}$, where $\delta_{m,n}$ is the Kronecker delta function. Therefore, the operation of $W_{\vec{k}}$ on any ket of this orthonormal set generates the one electron state function. Thus

$$W_{\vec{k}} |\phi_{\vec{k},n}> = |\psi_{\vec{k}}> \tag{3.3}$$

(ii) The Hermitian adjoint operator of $W_{\vec{k}}$ is given by

$$W^{\dagger}_{\vec{k}} = \sum_m |\phi_{\vec{k},m}><\psi_{\vec{k}}| \tag{3.4}$$

Thus, the operation of $W^{\dagger}_{\vec{k}}$ on any ket of the one electron state function dissociates it into a sum of $|\phi_{\vec{k},m}\rangle$

$$W^{\dagger}_{\vec{k}} \, |\psi_{\vec{k}}\rangle = \sum_{m} |\phi_{\vec{k},m}\rangle \tag{3.5}$$

(iii) The matrix elements of $W^{\dagger}_{\vec{k}}W_{\vec{k}}$ between any two elements of the orthonormal set is given by

$$\langle \phi_{\vec{k},t} |W^{\dagger}_{\vec{k}}W_{\vec{k}}| \phi_{\vec{k},s}\rangle = \sum_{m,n} \langle\phi_{\vec{k},t}|\phi_{\vec{k},m}\rangle\langle \psi_{\vec{k}}|\psi_{\vec{k}}\rangle\langle \phi_{\vec{k},n}|\phi_{\vec{k},s}\rangle$$

$$= (\sum_{m} \delta_{t,m})(\sum_{n} \delta_{ns}) = 1 \tag{3.6}$$

Therefore, $W_{\vec{k}}$ is not a unitary operator since a unitary operator U must satisfy the condition

$$\langle \phi_{\vec{k},t} |U^{\dagger}U| \phi_{\vec{k},s}\rangle = \langle \phi_{\vec{k},t} | \phi_{\vec{k},s}\rangle$$

$$= \delta_{t,s} \tag{3.7}$$

3.2 Determination of the One Electron State Function, $\psi_{\vec{k}}$

We choose a set of plane wave functions to represent the orthonormal set $\{\phi_{\vec{k},n}\}$

$$|\phi_{\vec{k},n}\rangle = \frac{1}{\Omega^{\frac{1}{2}}} \exp\,(i\,\vec{k}\cdot\vec{r})$$

$$= \frac{4\pi}{\Omega^{\frac{1}{2}}} \sum_{\ell=0}^{\infty} \sum_{p=-\ell}^{\ell} i^{\ell} J_{\ell}(\rho) \left[Y^{p}_{\ell}(\theta_{k},\phi_{k})\right]^{*} Y^{p}_{\ell}(\theta_{r},\phi_{r}) \tag{3.8}$$

where Ω is the volume of a unit cell in the crystal lattice; θ_{k} and θ_{r} are, respectively, the angles of directions of $\vec{k}$

and $\vec{r}$ with respect to the z axis; ϕ_k and ϕ_r are, respectively, the azimuthal angles about the z axis for $\vec{k}$ and $\vec{r}$; Y_ℓ^p are the spherical harmonic functions; and $J_\ell(\rho)$ are the spherical Bessel function defined by

$$R_\ell J_\ell(\rho) = 0 \tag{3.9}$$

where

$$R_\ell = \frac{d^2}{d\rho^2} + \frac{2}{\rho}\frac{d}{d\rho} + 1 - \frac{\ell(\ell+1)}{\rho^2} \tag{3.10}$$

and

$$\begin{aligned} \rho &= kr \\ k &= |\vec{k}| \\ r &= |\vec{r}| \end{aligned} \tag{3.11}$$

The one electron state function can be expressed as the sum of products of the spherical harmonic functions $Y_\ell^p(\theta_r, \phi_r)$ and radial wave functions $\mu_\ell(\rho)$

$$|\psi_{\vec{k}}> = \sum_{\ell=0}^{\infty} \sum_{p=-\ell}^{\ell} C_{\vec{k},\ell,p} \; \mu_\ell(\rho) \; Y_\ell^p(\theta_r, \phi_r) \tag{3.12}$$

where $C_{\vec{k},\ell,p}$ are the coefficients of the expansion and $\mu_\ell(\rho)$ satisfies the following radial equation

$$\{R_\ell + \frac{2m}{\hbar^2 k^2} [E_{\vec{k}} - V(\vec{r})] - 1\} \; \mu_\ell(\rho) = 0 \tag{3.13}$$

The expansion given by Eq. (3.12) can be derived also by expanding $\psi_{\vec{k}}$ in Legendre polynomials and then using the addition theorem of the spherical harmonic functions. Due to the completeness of Legendre polynomials we can always expand any function like $\psi_{\vec{k}}$ in terms of them. However, the degree of spherical symmetry of the potential $V(\vec{r})$ gives an indication as to how many terms in the expansion given by Eq. (3.12) are sufficient for describing the one electron state ψ_k fairly accurately. In the following analysis we are not going to truncate this expansion but we will use a different technique to get the unknown quantities in it.

We can imagine that the application of the nonunitary operator $W_{\vec{k}}$ on any plane wave function will distort it in a certain manner. This distortion is developed due to the distortion of each term in the expansion of Eq. (3.8) with a different amount as compared with the other terms. This idea can be expressed mathematically by introducing a new operator $w_{\vec{k},\ell}$ such that the left hand side of Eq. (3.3) can be written as

$$W_{\vec{k}} \,|\phi_{\vec{k},n}> = \frac{4\pi}{\Omega^{\frac{1}{2}}} \sum_{\ell=0}^{\infty} \sum_{p=-\ell}^{\ell} i^{\ell}\, w_{\vec{k},\ell}\, J_{\ell}(\rho) \left[Y_{\ell}^{p}(\theta_k, \phi_k)\right]^{*} Y_{\ell}^{p}(\theta_r, \phi_r) \quad (3.14)$$

and comparing Eq. (3.12) with Eq. (3.14) based on Eq. (3.3), we can write

$$C_{\vec{k},\ell,p} = \frac{4\pi}{\Omega^{\frac{1}{2}}} i^{\ell}\left[Y_{\ell}^{p}(\theta_k, \varphi_k)\right]^{*} \tag{3.15}$$

$$\mu_{\ell}(\rho) = w_{\vec{k},\ell} J_{\ell}(\rho) \tag{3.16}$$

by choosing the operator $w_{\vec{k},\ell}$ such that it operates on functions of ρ only. Thus, by substituting Eq. (3.16) into Eq. (3.13) we obtain

$$[R_{\ell} + P_k(E_{\vec{k}},\vec{r}) - 1]\, w_{\vec{k},\ell} J_{\ell}(\rho) = 0 \tag{3.17}$$

where

$$P_k(E_{\vec{k}},\vec{r}) = \frac{2m}{\hbar^2 k^2}[E_{\vec{k}} - V(\vec{r})] \tag{3.18}$$

To avoid mathematical singularity, we may rewrite Eq. (3.9) in the form

$$\lim_{\varepsilon\to 0} (R_{\ell} + \varepsilon) J_{\ell}(\rho) = 0 \tag{3.19}$$

Because of the uniqueness of the spherical Bessel functions $J_{\ell}(\rho)$ the comparison between Eqs. (3.17) and (3.19) gives

$$[R_{\ell} + P_k(E_{\vec{k}},\vec{r}) - 1]\, w_{\vec{k},\ell} = \lim_{\varepsilon\to 0}(R_{\ell} + \varepsilon) \tag{3.20}$$

This equation can be solved for $w_{\vec{k},\ell}$ by iteration method [Messiah, 1969]. Thus

$$w_{\vec{k},\ell} = - \{1 + \sum_{q'=1}^{\infty} [R_\ell + P_k (E_{\vec{k}},\vec{r})]^{q'}\} [\lim_{\varepsilon\to 0} (R_\ell + \varepsilon)] \qquad (3.21)$$

and by substituting Eqs. (3.15), (3.16) and (3.21) into Eq. (3.12) we obtain

$$|\psi_{\vec{k}}> = - \frac{4\pi\varepsilon}{\Omega^{1/2}} \sum_{\ell=0}^{\infty} \sum_{p=-\ell}^{\ell} i^\ell \{1 + P_k (E_{\vec{k}},\vec{r}) + \sum_{q=1}^{\infty} [R_\ell + P_k (E_{\vec{k}},\vec{r})]^q P_k (E_{\vec{k}},\vec{r})\} J_\ell (\rho) \times [Y_\ell^p (\theta_k, \varphi_k)]^* Y_\ell^p (\theta_r,\phi_r) \qquad (3.22)$$

The infinitesimal quantity ε will disappear in the process of normalization of $\psi_{\vec{k}}$.

3.3 Determination of the Energy Eigenvalue, $E_{\vec{k}}$

It is clear from Eq. (3.22) that there is only one quantity which determines the one electron state function, which is the dimensionless quantity $P_k(E_{\vec{k}},\vec{r})$. As defined by Eq. (3.18), $P_k(E_{\vec{k}},\vec{r})$ is a measure of the degree of the nonparabolicity of an energy band structure. It is clear that for $V(\vec{r})$ = constant, $P_k(E_{\vec{k}},\vec{r}) = 1$, $w_{\vec{k},\ell} = 1$ and $|\psi_{\vec{k}}> = |\phi_{\vec{k},n}>$. This means that under such a condition $\psi_{\vec{k}}$ reduces to a plane wave function and the energy band becomes purely parabolic as expected.

The bracket in Eq. (3.22) can be written as

$$\{1 + P_k + \sum_{q=1}^{\infty} (R_\ell + P_k)^q P_k\} J_\ell(\rho)$$

$$= \frac{1}{1 - P_k} \{1 + R_\ell P_k + R_\ell P_k^{\,2} + R_\ell R_\ell P_k + R_\ell P_k^{\,3} \ldots\} J_\ell(\rho) \quad (3.23)$$

The dimensionless quantity P_k has two features which can be used to approximate and to simplify Eq. (3.23). These are:

(i) For bound electrons, $P_k < 1$, which is the case for any electron in a crystal whatever small the binding force is. This condition is equivalent to $E_{\vec{k}} - V(\vec{r}) < \frac{\hbar^2 k^2}{2m}$. Thus, for $k \geq 0.1 \, (\frac{2\pi}{a})$, where a is the lattice constant, this case is valid if the kinetic energy of the electron is less than 1 eV which corresponds to an effective electron temperature smaller than $10{,}000\,^\circ$K. Therefore, for low temperatures this condition is usually encountered.

(ii) The quantity P_k changes more slowly than the function $J_\ell(\rho)$, specially at high energies for a given k and ℓ; which can be expressed in mathematical form as $R_\ell \, P_k \, J_\ell(\rho) \simeq P_k \, R_\ell \, J_\ell(\rho) = 0$. With any one or both of the aforementioned features Eq. (3.23) reduces to

$$\{1 + P_k + \sum_{q=1}^{\infty} (R_\ell + P_k)^q P_k\} J_\ell(\rho) \simeq \frac{1}{1 - P_k} J_\ell(\rho) \quad (3.24)$$

From Eqs. (3.8), (3.22) and (3.24) we obtain

$$|\psi_{\vec{k}}> = A \left[\frac{1}{1 - P_k \, (E_{\vec{k}}, \vec{r})} \right] \exp\,(i \, \vec{k} \cdot \vec{r}) \quad (3.25)$$

where A is a normalization constant. According to Eq. (3.18), (V(r) is periodic so is P_k and also the quantity in bracket in Eq. (3.25) with the same periodicity. Therefore Eq. (3.25) satisfies Bloch's theorem in case of periodic potential V(r). However, it should be noted that it is applicable also to aperiodic potentials and this will be discussed later. By comparing Eq. (3.25) with Eq. (3.3), we obtain

$$W_{\vec{k}} = \frac{1}{1 - P_k\ (E_{\vec{k}}, \vec{r})} \tag{3.26}$$

For the case $P_k << 1$ we may use the approximation

$$\frac{1}{1 - P_k} \simeq 1 + P_k \tag{3.27}$$

By substitution of Eq. (3.27) into Eq. (3.25) and then into Eq. (3.1), Schrödinger equation takes the following form

$$[- \frac{\hbar^2}{2m} \nabla^2 + V(\vec{r})]\ (1 + P_k)\ \exp\ (i\ \vec{k} \cdot \vec{r}) =$$

$$= E_{\vec{k}}(1+P_k)\ \exp\ (i\ \vec{k} \cdot \vec{r}) \tag{3.28}$$

Since $P_k^2 << 1$, Eq. (3.28) becomes

$$\nabla^2 P_k + 2i\ \vec{k} \cdot \nabla P_k - k^2 = 0 \tag{3.29}$$

For periodic lattice potential $P_k(E_{\vec{k}}, \vec{r})$ may be expressed as

follows

$$P_k\,(E_{\vec{k}},\vec{r}) = \sum_N g_{\vec{k},N}\, e^{-i\vec{G}_N \cdot \vec{r}} \qquad (3.30)$$

where $G_{\vec{N}}$ is the reciprocal lattice vector and is given by

$$G_N = N\left(\frac{2\pi}{a}\right) \qquad (3.31)$$

where N is an integer. By substituting Eq. (3.30) into Eq. (3.29) we obtain for any value of N

$$g_{\vec{k},N} = \frac{-k^2}{G_N^{\,2} - 2\vec{k}\cdot\vec{G}_N} \qquad (3.32)$$

since $\exp(-i\,\vec{G}_N \cdot \vec{r})$ are linearlv independent. The quantity $g_{\vec{k},N}$ can also be expressed as Fourier coefficients as given in Eq. (3.30). Therefore by the use of Eq. (3.18), we obtain

$$g_{\vec{k},N} = \frac{1}{\Omega}\int \frac{2m[E_{\vec{k}} - V(\vec{r})]}{\hbar^2 k^2}\, e^{i\,\vec{G}_N \cdot \vec{r}}\, dr^3 \qquad (3.33)$$

where dr^3 is the volume element in the ordinary lattice space and the integration is to be performed over a unit cell of volume Ω in the crystal lattice. From Eqs. (3.32) and (3.33) we obtain

$$E_{\vec{k},N} = \frac{1}{\Omega m_N}\int m\,(\vec{r})\; V\,(\vec{r})\, e^{i\,\vec{G}_N \cdot \vec{r}}\, dr^3$$

$$- \frac{\hbar^2}{2m_N}\,\frac{k^4}{\left(G_N^{\,2} - 2\vec{k}\cdot\vec{G}_N\right)}$$

$$= E_{o,N} - \frac{\hbar^2}{2m_N} \frac{k^4}{\left(G_N^2 - 2\vec{k}\cdot\vec{G}_N\right)} \qquad (3.34)$$

where $m(\vec{r})$ is the effective electron mass which is, in general, a function of $\vec{r}$, and m_N is given by

$$m_N = \frac{1}{\Omega} \int m(\vec{r})\, e^{i\vec{G}_N \cdot \vec{r}} dr^3 \qquad (3.35)$$

Where $m(\vec{r})$ is the electron mass, which infact is the rest mass of electron and not dependent on $\vec{r}$. However, to facilitate mathematical procedures we write it to be a function of r. This will help in getting rid of singularities in Eq. (3.34). It is obvious that m_N in Eq. (3.35) would reduce to m_o if $m(\vec{r})$ is not dependent on $\vec{r}$. Since the integral tends to zero except when $\vec{G}_N = o$.

The quantity $E_{o,N}$ shown by Eq. (3.34), is the energy level at $\vec{k} = 0$. Equation (3.34) shows also that the energy is quantized and depends on the quantum number N which can be used as a band index. This equation has the following features:

(a) An energy band $E_{\vec{k},N}$ can be determined within the approximations given in Eqs. (3.24) and (3.27) if the two parameters $E_{o,N}$ and m_N are known. The energy splittings between $E_{o,N}$ and $E_{o,N+1}$ can easily be measured by spectroscopy methods or other means. However, m_N is not the measured effective mass for the Nth band, but it can be related to this value which is denoted by $\langle m^*_{\vec{G}_N} \rangle$. Consider the reciprocal lattice vector $\vec{G}_N$ to be in the x-direction say. Then the effective mass of carriers are defined by

$$\frac{1}{m^*_{\vec{G}_N}} = \frac{1}{\hbar^2} \frac{\partial^2 E_{\vec{k},N}}{\partial k_x^2}$$

$$= \frac{1}{2m_N} \frac{\partial^2}{\partial k_x^2} \left[\frac{(k_x^2 + k_y^2 + k_z^2)^2}{2k_x G_N - G_N^2}\right] \qquad (3.36)$$

where the x-direction is one of the principal axes of the crystal. However, this is not the measured effective mass since it is a function of the wave vector $\vec{k}$. To find the measured value of the effective mass we have to find the average value of $1/m^*_{\vec{G}_N}$ with respect to the distribution function $f(\vec{k})$. Thus

$$\left\langle \frac{1}{m^*_{\vec{G}_N}} \right\rangle = \frac{\int_{-\infty}^{\infty} \frac{1}{m^*_{\vec{G}_N}} f(\vec{k}) d^3k}{\int_{-\infty}^{\infty} f(\vec{k}) d^3k} \qquad (3.37)$$

Using Eq. (3.36) we get

$$\frac{1}{m_N} = 2\left\langle \frac{1}{m^*_{\vec{G}_N}} \right\rangle \frac{\iiint_{-\infty}^{\infty} f(\vec{k}) d^3k}{\iiint_{-\infty}^{\infty} \left\{\frac{\partial^2}{\partial k_x^2} \left[\frac{(k_x^2 + k_y^2 + k_z^2)^2}{2k_x G_N - G_N^2}\right]\right\} f(\vec{k}) d^3k} \qquad (3.38)$$

The evaluation of Eq. (3.38) is given in Appendix I. Now it is clear that the energy band structure $E_{\vec{k},N}$ given by Eq. (3.34) can be completely determined in terms of the two measureable quantities namely the energy splittings at $\vec{k} = 0$ denoted by $E_{o,N}$ and the measured effective mass $\langle m^*_{\vec{G}_N} \rangle$.

(b) Another feature of Eq. (3.34) is that there exists a singular point in the energy band $E_{\vec{k},N}$ at

$$2\vec{k} \cdot \vec{G}_N = G_N^2 \qquad (3.39)$$

It should be noted that $P_k(E_{\vec{k}},\vec{r})$ can be treated as a slowly varying function with respect to $\vec{r}$ and thus Eq. (3.24) is satisfied, if $E_{\vec{k},N}$ (which is invariant in space) is much greater than $V(\vec{r})$ (which is variant in space).

Therefore this singularity may exist only in high energy bands, that is, for large values of N. Therefore if $\vec{k}$ becomes very large and very far from the energy band extremum, then this analysis is not suitable for this case. It should be noted that Eq. (3.34) is valid only in the region of the values of k: $0.01 (\frac{2\pi}{a})_2 < k < 0.08 (\frac{2\pi}{a})$. The lower limit is determined by the condition $P_k^2 \ll 1$ and can be neglected for higher values of k and the upper limit which corresponds to about 1 eV as shown by Fig. (3.2) at 300°K is determined by the diminishing of the distribution function used in Eq. (3.37).

However, it should be noted that the E - k relation at k below $0.01 (\frac{2\pi}{a})$ is close to parabolic form and that the region of $0.01 (\frac{2\pi}{a}) < k < 0.08 (\frac{2\pi}{a})$ is most important to high field transport phenomena because at high electric field more electrons tend to have energies in the corresponding range (see chapter 4).

Finally, it would be of interest to apply Eq. (3.25) to a case with aperiodic potential $V(\vec{r})$ as mentioned before. For example, we treat the collision problem with the analysis given in this chapter. Consider the potential in this case is given by

$$V(\vec{r}) = \frac{B}{r} \qquad (3.40)$$

where B is a constant. Equation (3.25) becomes

$$\left|\psi_{\vec{k}}\right\rangle \simeq A[1 + P_k(E_{\vec{k}},\vec{r})] \exp(i\,\vec{k}\cdot\vec{r})$$

$$= A[\,1 + \frac{2m}{\hbar^2 k^2}\,(E_{\vec{k}} - \frac{B}{r})]\exp(i\,\vec{k}\cdot\vec{r})$$

$$= D[1 + \frac{Q}{r}]\exp(i\,\vec{k}\cdot\vec{r}) \qquad (4.41)$$

where D is a constant and

$$Q = -\frac{B}{E_{\vec{k}} + \frac{\hbar^2 k^2}{2m}} \qquad (3.42)$$

It is obvious that as $r \to \infty$, $V(\vec{r}) \to 0$ and $P_k \to$ constant with respect to $\vec{r}$. Then Eq. (3.41) gives the correct asymptotic solution of the Schrödinger equation in this particular case if we take the direction of $\vec{k}$ to be in the z-direction of the spherical coordinates.

3.4 Computed Results

Equation (3.34) can be written in the following normalized form (see Appendix I)

$$\mathcal{E} = \frac{X^4}{1 - 2X} \qquad (3.43)$$

where

$$\mathcal{E} = \frac{(E_{\vec{k},N} - E_{o,N})5k_B T}{\left(\frac{\hbar^2 G_N^2}{2 < m^*_{\vec{G}_N} >}\right)^2} \tag{3.44}$$

and

$$X = k/|G_N| \tag{3.45}$$

$\vec{k}$ is taken in $\vec{G}_N$ direction, K_B is the Boltzmann constant, and T is the absolute temperature. For small values of $k/|\vec{G}_N|$ or for large N, Eq. (3.43) reduces to the simple form

$$\mathcal{E} = X^4 \tag{3.46}$$

Figure 3.1 shows the normalized energy band ε-x as given by Eq. (3.43). The parabolic energy band is included also for comparison purposes.

It is clear from Eq. (3.38) that when the measured value of the effective mass $<m^*_{\vec{G}_N}>$ changes its sign, m_N changes its sign accordingly and in this case the energy band shown in Fig. 3.1 will be reflected on the other side of the x axis. This is the situation between the upper valence band and the lower conduction band or vice versa. Therefore curve a in Fig. 3.1 can be considered as a

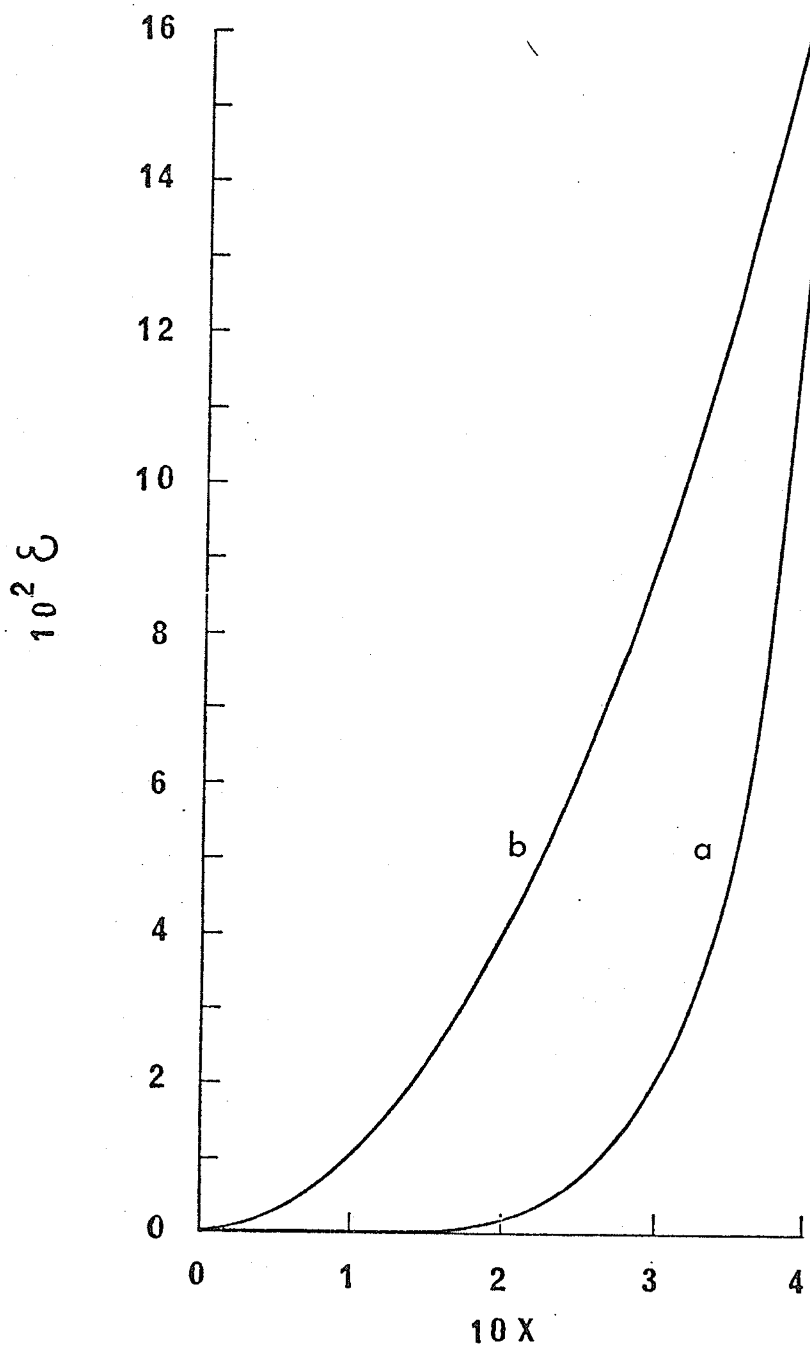

Fig. 3.1. The normalized energy band structure
(a) on the base of Eq. (3.43); (b) on the base of the parabolic structure

Table 3.1. Parameters for GaAs

Temperature	4°K	300°K
a	4.581 Å (Novikova, 1966)	5.653 Å (Ozolin'sh *et al.*,1963)
$E_{o,N}$	1.517 eV (Madelung, 1964)	1.430 eV (Nadelung, 1964)
$1/m^{*}_{\vec{G}_N}$	1/0.081 m_o (Piller, 1966)	1/0.08 m_o (Madelung, 1964)
	1/0.063 m_o (Piller, 1966)	1/0.65 m_o (Pollak *et al.*,1966)

m_o is the rest mass of the electron

Table 3.2. Computed results for GaAs

Temperature	4°K	300°K
$G_N = N\ (2\pi/a)$	45.2619 Å^{-1}	36.6787 Å^{-1}
$\frac{1}{5k_BT}\ (\frac{h^2 G_N^2}{2<m^*_{G_N}>})^2$	5.3327 x 10^{12} eV	2.8805 x 10^{10} eV

$<1/m^*_{G_N}> = 1/0.081\ m_o$ was used for 4°K and $1/0.084\ m_o$ for 300°K.

universal curve for the energy bands in the range $0.01(\frac{2\pi}{a}) < k < 0.08(\frac{2\pi}{a})$ measured from the band extremum provided that the appropriate scales for ε and x corresponding to the appropriate values of $E_{o,N}$ and $< m^*_{\vec{G}_N} >$ at the extremum in each band are used.

The effect of temperature on the energy band structures can be deduced easily from Fig. 3.1 if the temperature dependance of the lattice constant a, the distribution function $f(\vec{k})$, the energy splittings at the band extremum $E_{o,N}$ and the measured effective mass $<m^*_{\vec{G}_N}>$ are known. Using the parameters for GaAs given in Table 3.1 and choosing the top of the upper valence band at Γ_{15} as the zero energy level, the scales for the lowest empty conduction band with extremum at Γ_1 in the direction [100] can be calculated easily for temperatures 4°K and 300°K and the results are given in Table 3.2. Since the atomic number of Ga is 31 and that of As is 33, there are 64 electrons per molecule corresponding to 32 filled bands and therefore, we use $N = 33$ for the first empty band in the above mentioned calculations. Using Eqs.(3.44) and (3.45) the curve a in Fig. 3.1 can be transformed into E-k curves: curve (a) with $<1/m^*_{\vec{G}_N}> = 1/0.081\ m_o$ at 4°K and curves (b) and (c) corresponding, respectively, to $<1/m^*_{\vec{G}_N}> = 1/0.065\ m_o$ and $1/0.084\ m_o$ at 300°K as shown in Fig. 3.2. Another E-k curve (d) is included in Fig. 3.2 with $<1/m^*_{\vec{G}_N}> = 1/0.065\ m_o$ at 300°K computed by the $\vec{k} \cdot \vec{p}$ approximation [Pollak, Higginbotham and Cardona, 1966] for comparison purposes.

It should be noted that the curves a, b, c in Fig. 3.2 are only for $0.01\ (\frac{2\pi}{a}) < K < 0.08\ (\frac{2\pi}{a})$ because the afore mentioned analysis is valid only in this range.

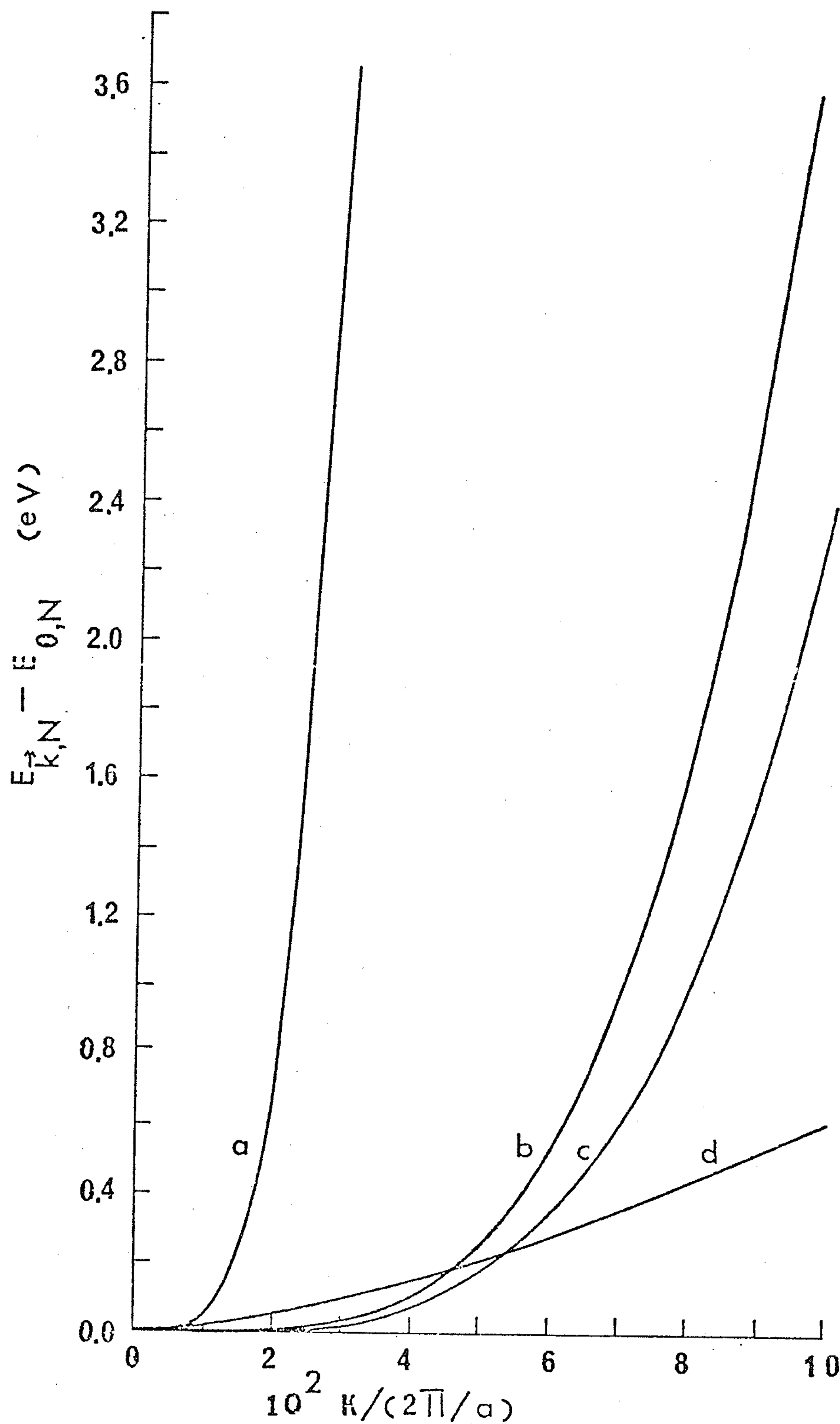

Fig. 3.2. The energy band structure of the lower conduction band of GaAs with the extremum at Γ_i in the direction 100 (a) the result transformed from Fig. 3.1 for $< 1/m^*_{\vec{G}_N} > = 1/0.084 m_o$ at 4°K; (b) the result transformed from Fig. 3.1 for $< 1/m^*_{\vec{G}_N} > = 1/0.065\ m_o$ at 300°K; (c) the result transformed from Fig. 3.1 for $< 1/m^*_{\vec{G}_N} > = 1/0.084\ m_o$ at 300°K; (d) the result of Pollak, Higginbotham and Cardona [1966] for $< 1/m^*_{\vec{G}_N} > = 1/0.065 m_o$ at 300°K.

General features of the energy band structures can be deduced from Fig. 3.2 such as the nonparabolicity, the strong temperature dependence, and the sensitivity to the measured value of the effective mass $<1/m^*_{G_N}>$. These features have naturally considerable effect on the transport phenomena in any material. The discrepancy between the energy band structure according to the method described in this chapter and that given by Pollak, Higginbotham and Cardona [1966] may be attributed to the different approximations used in the two different approaches.

It is worthy to mention that for the case of known lattice potential the one electron state given by Eq. (3.22) become completely known and the energy band structures can be calculated by the expectation value of the Hamiltonian of the system between two of such wave functions. In this case no approximations are needed. Therefore it becomes a matter of compromise between the approximations introduced in this chapter; the approximations for the case of unknown lattice potentials on one hand, and the approximations needed in assuming the lattice potential on the other. The uncertainity of the assumptions of constructing the lattice potential may suggest the use of this method. It should also be realized that as each method has its own advantages, it is not easy at present to compare one method with others from the accuracy or sophistication point of view just simply based on the presently available experimental results.

We should like to emphasize that the advantage of our expression is that it is analytic, simple and no assumptions concerning the lattice potential are involved. The effect of temperature is explicitly shown in Eq. (3.44). We do not need experimental data other than $<m^*_{G_N}>$ and $E_{o,N}$ for our analysis. This reduces possible errors introduced by the involvement of many experimental data

CHAPTER 4

HIGH-FIELD DISTRIBUTION FUNCTIONS OF CARRIERS IN SEMICONDUCTORS

The carrier distribution function f is one of the most important quantities which has to be determined before the study of the transport phenomena is possible. The distribution function varies with time, and is governed by the externally applied field, carrier diffusion, and the scattering of the carriers with the carriers, the phonons, and the impurities. These factors constitute the main features of the Boltzmann equation. Generally, we obtain f by solving this equation with certain boundary conditions and some necessary assumptions. In the absence of external fields and in thermal equilibrium, f for degenerate semiconductors must be the Fermi-Dirac distribution function. But in the presence of external fields the net carrier transport will disturb the equilibrium condition and hence f will be altered. At low fields the effect of all scattering effects are usually treated by the relaxation time approximation [Conwell, 1967]. There are many shortcomings of the relaxation time approximation and they have been discussed in detail by Law and Kao [1971]. To avoid using this approximation, several methods have been introduced to

solve this problem, such as the variational method [Howarth and Sandheimer, 1953; Ehrenreich, 1959], the iterative technique [Rode, 1970], the Monte Carlo method [Kurosawa, 1966; Rees, 1969; Fawcett, Boardman and Swain, 1970]. In this chapter we present a new method to derive a general expression for the distribution function as a function of applied electric field for fields of any strength and for parabolic and nonparabolic energy bands as well as for non-degenerate and degenerate semiconductors. This method is based on the principle of deriving the Fermi-Dirac distribution function. With the general expression for f we have solved analytically the Boltzmann transport equation for low and high temperatures. We also present some computed results to show the field dependence of f, the effect of mixed scattering, and the effect of temperature; and to compare our results with those calculated by other investigators.

4.1 General Expression of the Distribution Function

With the flow of carriers in a semiconductor under the influence of applied fields, the carrier distribution function will depend on the applied field and temperature; and in the steady state it will be formed under such a condition that the number of ways for arranging all carriers in all available energy states is a maximum [Huang, 1963]. By taking into account the effect of applied electric field,

the carrier distribution function is derived as follows.

Suppose the energy states are divided into many compartments with N_1 electrons and G_1 states of energy E_1 in the first compartment, N_2 electrons and G_2 states of energy E_2 in the second compartment, N_i electrons and G_i states of energy E_i in the ith compartment, and so on. Then the number of ways for arranging the total N electrons in the total G states is given by

$$W = \prod_{i=1} \frac{G_i!}{N_i!\,(G_i - N_i)!} \tag{4.1}$$

The total number of electrons in the system is

$$N = \sum_{i=1} N_i \tag{4.2}$$

and the total energy of the system is

$$E = \sum_{i=1} N_i E_i \tag{4.3}$$

If there is a net carrier transport, an additional condition must be added, and it is

$$J = e \sum_{i=1} N_i V_{F_i} \tag{4.4}$$

where J is the current density, e is the electronic charge, and V_{F_i} is the velocity of the carriers of the ith

compartment in the direction of the applied electric field $\vec{F}$. In thermal equilibrium and in the absence of the externally applied electric field we should use only the conditions given by Eqs. (4.2) and (4.3). These conditions imply that the carriers in each compartment have the same energy. Therefore, these compartments are simply the constant energy surfaces in the momentum space. However, in the presence of an external field these surfaces will be distorted, and for isotropic materials they will be symmetric around the direction of the field. For this reason, a question may arise as to the correctness of considering the compartments for carriers in the presence of external fields as the constant energy surfaces. However, if we divide each compartment into many subcompartments in a way that the carriers in each subcompartment not only have the same energy but also the same velocity component in the direction of the applied field, then all the conditions given by Eqs. (4.2), (4.3) and (4.4) will be satisfied. The subcompartment is formed by the intersection of a cone with the constant energy surface, the axis of the cone being in the direction of the applied field and the cone is confined within an angle θ from its slant height. Equation (4.3) is the necessary condition for a system to have a constant total energy, while Eq. (4.4) is the necessary condition for a system to have a steady current flow. Based on this argument the velocity component V_{Fi} in the ith subcompartment

is thus given by

$$V_{F_i} = \left(\frac{\hbar k_i}{m^*}\right) \cos \theta \tag{4.5}$$

where m* is the effective mass, $\hbar$ is Planck's constant divided by 2π, k_i is the magnitude of the wave vector $\vec{k}_i$, and θ is the angle between $\vec{k}_i$ and $\vec{F}$, the latter being taken in the z-direction only.

Using the method of Lagrange multipliers, the condition for the number of ways for arranging N electrons in G states to be a maximum is

$$\frac{d}{dN_i} \{\ln W + \alpha (N - \sum_{i=1} N_i) + \beta (E - \sum_{i=1} N_i E_i) + \gamma (J - e \sum_{i=1} N_i V_{Fi})\} = o \tag{4.6}$$

Using Stirling's formula, the solution of Eq. (4.6) gives

$$\frac{N_i}{G_i} = \frac{1}{1 + e^{\alpha + \beta E_i + \gamma e V_{Fi}}} \tag{4.7}$$

Hence, the carrier distribution function is

$$f = \frac{1}{1 + e^{\alpha + \beta E + \frac{\gamma e \hbar k}{m^*} \cos \theta}} \tag{4.8}$$

This is the carrier distribution function under an externally applied electric field. For thermal equilibrium conditions and under no external fields, the condition given by

Eq. (4.4) does not exist, that is $\gamma = 0$, and Eq. (4.8) reduces to the Fermi-Dirac distribution function as expected However, when $\vec{F} \neq 0$, γ must be field dependent. Since Eq. (4.8) is valid for any E-k relationship, this distribution function should be applicable for both non-degenerate and degenerate semiconductors with either parabolic or nonparabolic band structure.

Equation (4.8) can be reduced to some forms which have been generally used under similar conditions in the past. For nondegenerate semiconductor with a parabolic band structure, Eq. (4.8) can be approximated to

$$f \simeq e^{-\alpha - \beta E - \frac{\gamma e \hbar k}{m^*} \cos\theta}$$

$$\simeq e^{-\alpha + \frac{\gamma^2 e^2 \cos^2\theta}{2\beta m^*} - \frac{\beta \hbar^2}{2m^*}\left(k + \frac{\gamma e \cos\theta}{\beta\hbar}\right)^2} \qquad (4.9)$$

The first two terms in the exponential of Eq. (4.9) are independent of k. Equation (4.9) is generally referred to as the displaced Maxwellian distribution function [Fröhlich and Paranjape, 1956] with the displacement vector given by

$$d = -\frac{\gamma e \cos\theta}{\beta\hbar} \qquad (4.10)$$

where $\beta = 1/K_B T$; K_B is the Boltzmann constant and T is the temperature of the electrons.

By rewriting Eq. (4.9) in the form

$$
\begin{aligned}
f &\simeq e^{-\alpha - \beta E} \, e^{-\frac{\gamma e\hbar k}{m^*}\cos\theta} \\
&= f_o(E)\, e^{-\frac{\gamma e\hbar k}{m^*}\cos\theta} \\
&\simeq f_o(E)\left(1 - \frac{\gamma e\hbar k}{m^*}\cos\theta\right) \\
&= f_o(E) + k_F g(E)
\end{aligned}
\qquad (4.11)
$$

with $f_o(E) = e^{-\alpha - \beta E}$, $k_F = k \cos\theta$ and $g = -f_o \gamma e h/m^*$. Equation (4.11) is the distribution function used by Conwell and Vassell [1966] for their study of the transport phenomena, but they obtained this by expanding f in a series of Legendre polynomials and cutting off the series after the second term.

It is clear that the displaced Maxwellian function cannot be used for nonparabolic energy band structures, while Eq. (4.11) cannot be used for high fields. Besides, both of the two approximations cannot be used for degenerate semiconductors. In the following we shall determine the carrier distribution function based on the general expression given in Eq. (4.8) by solving the Boltzmann transport equation.

4.2 Boltzmann Equation and Scattering Mechanisms

The Boltzmann equation for a many-valley semiconductor is given by [Butcher, 1967]

$$\frac{\partial f_i(\vec{k})}{\partial t} = [\frac{\partial f_i(\vec{k})}{\partial t}]_F + \sum_j [\frac{\partial f_i(\vec{k})}{\partial t}]_{ij} \qquad (4.12)$$

where i and j stand for the ith and the jth valley, the diffusion term being neglected as usual for the high field conditions. The first term on the right-hand side is the rate of change of $f_i(\vec{k})$ due to the applied field, which is given by

$$[\frac{\partial f_i(\vec{k})}{\partial t}]_F = -\frac{e}{\hbar}\vec{F} \cdot \nabla_k f_i(\vec{k}) \qquad (4.13)$$

The second term is the rate of change of $f_i(\vec{k})$ due to various scattering processes.

To simplify the matter, it is necessary to introduce some assumptions. These assumptions would not affect getting a realistic picture of the distribution function in a semiconductor under consideration. These assumptions are

(a) The semiconductor is nondegenerate, so that the effect of carrier-carrier scattering can be ignored because the carrier concentration is so small that the carriers are mostly scattered by the lattice vibrations [Fröhlich and Paranjape, 1956].

(b) The energy-band structure is parabolic. This assumption has been shown in the previous chapter to be not true. However, by choosing the appropriate effective mass the error will be decreased to a minimum.

(c) The external applied field $\vec{F}$ is uniform across the sample. This means that the applied electric field is

not high enough to cause space-charge effects such as the formation of domains. So we confine ourselves to scattering mechanisms due to phonons of different types denoted by s. Thus the second term on the right-hand side of Eq. (4.12) may be written in the form [Butcher, 1967].

$$\left[\frac{\partial f_i(\vec{k})}{\partial t}\right]_{ij} = \int_j C_{ij}^{(s)}(\vec{k},\vec{k}')[\{N_s f_j(\vec{k}') - (N_s+1) f_i(\vec{k})\}\delta\{E_i(\vec{k}) - E_j(\vec{k}') - \hbar\omega_s\} - \{N_s f_i(\vec{k}) - (N_s+1) f_j(\vec{k}')\}\delta\{E_j(\vec{k}') - E_i(\vec{k}) - \hbar\omega_s\}]d\vec{k}' \tag{4.14}$$

The four terms in the integrand represent the transition from state $\vec{k}$ in the ith valley to state $\vec{k}'$ in the jth valley, and vice versa by emission and absorption of one phonon of type s with wave vector $\pm(\vec{k}-\vec{k}')$ and angular frequency ω_s. By assuming that the phonons remain in termal equilibrium at the lattice temperature T_o, the number of phonons of type s follows the Bose-Einstein statistics

$$N_s = [\exp(\frac{\hbar\omega_s}{k_B T_o}) - 1]^{-1} \tag{4.15}$$

The strength of the scattering is controlled by the function $C_{ij}^{(s)}$ which depends on the type of phonon and the magnitude $|\vec{k}-\vec{k}'|$. Therefore $C_{ij}^{(s)}$ can be written in the form

$$C_{ij}^{(s)} = D_{ij}^{(s)} |\vec{k} - \vec{k}'|^r \tag{4.16}$$

For different types of scatterings the (s) and r are changed as follows:

when $r = -2$, $(s) \rightarrow (0)$ for optical-mode scattering;

when $r = 1$, $(s) \rightarrow (a)$ for acoustic-mode scattering;

when $r = 0$, $(s) \rightarrow (ij)$ for intervalley scattering.

The general form of Eq. (4.16) enables us to make corrections for the assumptions made in deducing the values of $C_{ij}^{(s)}$ for different types of scatterings. It also helps in mixing various types of scatterings together by taking the value of the parameter r between -2 and 1, and the quantity $D_{ij}^{(s)}$ would be different from that for a single type of scattering. The discrepancy between the theoretical and experimental results for the transport parameters [Ehrenreich, 1960] may be attributed to some factors, one of which is the inaccuracy in determining the scattering parameters. The simple form of Eq. (4.16) helps in evaluating or measuring both $D_{ij}^{(s)}$ and r.

The magnitude of the wave vector of the phonons may be written as

$$|\vec{k} - \vec{k}'| = [k^2 + k'^2 - 2kk'u]^{\frac{1}{2}} \tag{4.17}$$

in which

$$u = \cos\theta\cos\theta' + \sin\theta\sin\theta'\cos(\phi - \phi')$$

where k and k' are the magnitudes of the wave vectors $\vec{k}$ and $\vec{k}'$ whose directions are θ and θ' from the z axis, and ϕ and ϕ' are their azimuthal angles about the z axis, respectively.

For mathematical simplicity, it is advantageous to divide the energy range of phonons into three regions as follows.

(i) High-energy phonons

For this case $\hbar\omega_s >> K_B T_o$. Therefore, $N_s << 1$ and Eq. (4.14) reduces to

$$\left(\frac{\partial f_i(\vec{k})}{\partial t}\right)_{ij}^{(s)} = \int_j C_{ij}^{(s)}(\vec{k},\vec{k}')[f_j(\vec{k}')\delta_+ - f_i(\vec{k})\delta_-]\, d\vec{k}' \quad (4.18)$$

with

$$\delta_+ = \delta[E_j(\vec{k}') - E_i(\vec{k}) - h\omega_s]$$

and

$$\delta_- = \delta[E_i(\vec{k}) - E_j(\vec{k}') - \hbar\omega_s]$$

In this range of phonon energies, optical, polar-optical, and intervalley scatterings may play a role in the transport phenomena, and at very low temperatures the acoustic scattering may also become important. This case is usually encountered at low temperatures.

(ii) Low-energy phonons

For this case $\hbar\omega_s << K_B T_o$. Therefore, $N_s >> 1$ and Eq. (4.14) reduces to

$$\left[\frac{\partial f_i(\vec{k})}{\partial t}\right]_{ij}^{(s)} = \int_j N_s C_{ij}^{(s)}(\vec{k},\vec{k}')\,(\delta_+ + \delta_-)[f_j(\vec{k}') - f_i(\vec{k})]d\vec{k}' \quad (4.19)$$

where

$$N_s \approx \frac{k_B T_o}{\hbar\omega_s} , \tag{4.20}$$

$$\omega_s \simeq |\vec{k} - \vec{k}'| v_s , \tag{4.21}$$

and v_s is the velocity of sound which may be considered to be constant for this case - the linear portion of the dispersion curve for phonons. This case is usually encountered at high temperatures and the dominant scattering is of the acoustic type.

(iii) Intermediate-energy phonons

For this case $\hbar\omega_s \approx K_B T_O$; no approximations of the type made in the previous two cases can be made to simplify Eq. (4.14). This case is general and complicated, and will not be dealt with in this chapter.

We shall begin with case (i) for low temperature and case (ii) will be treated in a similar manner later.

A High-Energy Phonons

From Eqs. (4.16) and (4.17) we have

$$C_{ij}^{(s)} = D_{ij}^{(s)} \left[k^2 + k'^2 - 2kk' u\right]^{r/2} \tag{4.22}$$

The function $C_{ij}^{(s)}$ can be expanded in a series of Legendre polynomials $P_n(u)$ as

$$C_{ij}^{(s)} = \sum_{n=0}^{\infty} a_n P_n(u) \tag{4.23}$$

Using Eqs. (4.22) and (4.23), the coefficients a_n can be determined and expressed as

$$a_n(k, k') = \frac{(2n+1)}{2} D_{ij}^{(s)} \int_{-1}^{1} [k^2 + k'^2 - 2kk'u]^{r/2} P_n(u)du \tag{4.24}$$

Using the addition theorem of the spherical harmonics, namely

$$P_n(u) = \frac{4\pi}{(2n+1)} \sum_{\ell=-n}^{n} Y_n^{\ell *}(\theta,\phi)\, Y_n^{\ell}(\theta',\phi') \tag{4.25}$$

Eq. (4.18) becomes

$$\begin{aligned}[\frac{\partial f_i}{\partial t}]_{ij}^{(s)} = &- \sum_{n=o}^{\infty} \sum_{\ell=-n}^{n} \frac{4\pi}{2n+1} Y_n^{\ell *}(\theta,\phi) f_i(\vec{k}) \int_j a_n Y_n^{\ell}(\theta',\phi')\delta_- k'^2 \sin\theta' d\theta' dk' d\phi' \\ &+ \sum_{n=o}^{\infty} \sum_{\ell=-n}^{n} \frac{4\pi}{2n+1} Y_n^{\ell *}(\theta,\phi) \int_j a_n Y_n^{\ell}(\theta',\phi') f_j(\vec{k}')\delta_+ k'^2 \sin\theta' d\theta' dk' d\phi'\end{aligned} \tag{4.26}$$

We denote some integrals as follows

$$W_n(k,k') = \int_{-1}^{1} [k^2 + k'^2 - 2kk'u]^{r/2} P_n(u)du \tag{4.27}$$

$$y_n^{\ell} = \int_o^{2\pi} \int_o^{\pi} \sin\theta'\, Y_n^{\ell}(\theta',\phi') d\theta' d\phi' \tag{4.28}$$

$$S_n(k)_{ij} = \int_j \delta_- W_n(k,k') k'^2 dk' \tag{4.29}$$

$$Z_n^{\ell}(k')_{ij} = \int_o^{2\pi} \int_o^{\pi} \frac{\sin\theta' Y_n^{\ell}(\theta',\phi') d\theta' d\phi'}{1 + e^{\alpha_j + \beta_j E_j' + \gamma_j \frac{e\hbar}{m_j^*} k_j' \cos\theta'}} \tag{4.30}$$

$$T_n^{\ell}(k)_{ij} = \int_j \delta_+ W_n(k, k') \; Z_n^{\ell}(k')_{ij} k'^2 dk' \qquad (4.31)$$

the evaluation of the above integrations being shown in Appendix II. It is shown that the integrals $W_n(k,k')$ are appreciable only when n=0 and n=1 (Appendix II). Therefore Eq. (4.26) takes the form

$$\left[\frac{\partial f_i}{\partial t}\right]_{ij}^{(s)} = -\, 2\pi\, D_{ij}^{(s)} \left[f_i(\vec{k})\, S_o(k)_{ij} - \frac{1}{\sqrt{4\pi}}\, T_o^o(k)_{ij} - \sqrt{\frac{3}{4\pi}}\cos\theta\; T_1^o(k)_{ij}\right] \qquad (4.32)$$

By substituting Eq. (4.8) into Eq. (4.13) we obtain:

$$\left[\frac{\partial f_i}{\partial t}\right]_F = \frac{e}{\hbar} F\left(\frac{\gamma_i e\hbar}{m_i^*} + \beta_i \hbar^2 \frac{(k - K_i)}{m_i^*}\cos\theta\right)[1 - f_i(\vec{k})] f_i(\vec{k}) \qquad (4.33)$$

where $\vec{K}_i$ is the wave vector at the extremum of the ith valley. By substituting Eqs. (4.32) and (4.33) into Eq. (4.12) we obtain the general Boltzmann equation.

$$\frac{e}{\hbar} F\left[\frac{\gamma_i e\hbar}{m_i^*} + \beta_i \hbar^2 \frac{(k - K_i)}{m_i^*}\cos\theta\right][1 - f_i(\vec{k})] f_i(\vec{k})$$

$$- 2\pi \sum_j D_{ij}^{(s)} \left[f_i(\vec{k}) S_o(k)_{ij} - \frac{1}{\sqrt{4\pi}} T_o^o(k)_{ij} - \sqrt{\frac{3}{4\pi}}\cos\theta\; T_1^o(k)_{ij}\right] = o \qquad (4.34)$$

B. Low-Energy Phonons

Following the same procedure, the general Boltzmann equation for low-energy phonons can be expressed as follows:

$$\frac{e}{\hbar} F[\frac{\gamma_i e\hbar}{m_i^*} + \beta_i \hbar^2 \frac{(k - K_i)}{m_i^*} \cos\theta] [1 - f_i(\vec{k})] f_i(\vec{k})$$

$$- 2\pi \sum_j D_{ij}^{\prime(s)} [f_i(\vec{k}) S_o^{\prime}(k)_{ij} - \frac{1}{\sqrt{4\pi}} T_o^{\prime o}(k)_{ij} - \sqrt{\frac{3}{4\pi}} \cos\theta T_1^{\prime o}(k)_{ij}] = o \tag{4.35}$$

where

$$D_{ij}^{\prime(s)} = \frac{D_{ij}^{(s)} K_B T}{\hbar v_s} \tag{4.36}$$

$$S_n^{\prime}(k)_{ij} = \int_j (\delta_+ + \delta_-) W_n^{\prime} (k, k') k'^2 dk' \tag{4.37}$$

$$W_n^{\prime} (k, k') = \int_{-1}^{1} [k^2 + k'^2 - 2kk'u]^{(r-1)/2} P_n(u) du \tag{4.38}$$

$$T_n^{\prime \ell}(k)_{ij} = \int_j (\delta_+ + \delta_-) W_n^{\prime} (k, k') Z_n^{\ell}(k')_{ij} k'^2 dk' \tag{4.39}$$

4.3 Analytical Solution of Boltzmann Equation

For the case of high energy phonons (or at low temperatures), it is clear that Eq. (4.34) with the integrals given in Appendix II has no simple solution. To obtain an analytical solution, we make the following assumptions

(i) $$f_i(\vec{k}) << 1 \tag{4.40}$$

This condition is well satisfied, since for nondegenerate semiconductors $\exp[\alpha+\beta E+(\gamma e\hbar k/m^*)\cos\theta]>>1$;

(ii) $$\left|\frac{2\gamma_j e\hbar k_j^+}{m_j^*}\right| << 1 \tag{4.41}$$

where k_j^+ is defined by

$$k_j^+ = (2m_j^*/h^2)^{1/2}\,(E + \hbar\omega_s - \Delta_j)^{1/2} + K_j \qquad (4.42)$$

In this expression we assumed the jth subband to be parabolic and its extremum to have an energy Δ_j

$$E - \Delta_j = \hbar^2 (k - K_j)^2 / 2m_j^* \qquad (4.43)$$

The condition given by Eq. (4.41) is equivalent to

$$|\gamma_j| << \frac{1}{2eV_j^+} \qquad (4.44)$$

where

$$V_j^+ = hk_j^+/m_j^* = \mu_j^+ F \qquad (4.45)$$

and μ_j^+ is the electron mobility in the jth subband. Therefore

$$|\gamma_j| << \frac{1}{2e\mu_j^+ F} \qquad (4.46)$$

This relation shows that condition (ii) is applicable for $|\gamma_j| = 0$ corresponding to $\vec{F} = 0$ up to extremely high values of $|\gamma_j|$ for any desired practical values of $\vec{F}$.

From Eqs. (4.40) and (4.41) we obtain the following useful relation

$$\frac{\sqrt{\pi} m_j^*}{e\hbar\gamma_j k_j^+} \,\ell n \left\{ e^{\frac{2e\hbar\gamma_j k_j^+}{m_j^*}} \left[\frac{1 + e^{\alpha_j + \beta_j (E + \hbar\omega_s) - \frac{e\hbar}{m_j^*}\gamma_j k_j^+}}{1 + e^{\alpha_j + \beta_j (E + \hbar\omega_s) + \frac{e\hbar}{m_j^*}\gamma_j k_j^+}} \right] \right\}$$

$$= \frac{\sqrt{\pi}\, m_j^*}{e\hbar\gamma_j k_j^+} \ln \{1 + (e^{\frac{2e\hbar\gamma_j k_j^+}{m_j^*}} - 1)\, f_j(E + \hbar\omega_s)\}$$

$$\simeq 2\sqrt{\pi}\, f_j\, (E + \hbar\omega_s) \qquad (4.47)$$

Using Eq. (4.47), the integrals $T_o^o(k)_{ij}$ and $T_1^o(k)_{ij}$ reduce to (see also Appendix II)

$$T_o^o\,(k)_{ij} \simeq f_j(E + \hbar\omega_s)\, \sqrt{\pi}\, \frac{(\frac{2m_j^*}{\hbar^2})k_j^{+2}}{(k_j^+ - K_j)}$$

$$X \left(\sum_{p=o}^{\infty} \frac{\Gamma(2p - \frac{r}{2})}{\Gamma(-\frac{r}{2})\Gamma(2p+1)(\frac{1}{2} + p)} [\{(\frac{2m_i^*}{\hbar^2})^{\frac{1}{2}}(E-\Delta_i)^{\frac{1}{2}}+K_i\}^2+k_j^{+2}]^{r/2-2p} \right. \qquad (4.48)$$

$$\left. X\; [2\{(\frac{2m_i^*}{\hbar^2})^{\frac{1}{2}}\,(E-\Delta_i)^{\frac{1}{2}} + K_i\}\, k_j^+]^{2p} \right)$$

and

$$T_1^o(k)_{ij} \simeq f_j(E + \hbar\omega_s)\, \frac{\sqrt{3\pi}\,(\frac{2m_j^*}{\hbar^2})\, k_j^{+2}}{(k_j^+ - K_j)} \cos\theta$$

$$X \left(\sum_{p=o}^{\infty} \frac{\Gamma(2p+1 - \frac{r}{2})}{\Gamma(-\frac{r}{2})\Gamma(2p+2)(\frac{3}{2} + p)} [\{(\frac{2m_i^*}{\hbar^2})^{\frac{1}{2}}(E-\Delta_i)^{\frac{1}{2}}+K_i\}^2+k_j^{+2}]^{r/2-2p-1} \right. \qquad (4.49)$$

$$\left. X\; [2\{(\frac{2m_i^*}{\hbar^2})^{\frac{1}{2}}\,(E-\Delta_i)^{\frac{1}{2}} + K_i\}k_j^+]^{2p+1} \right)$$

Therefore, Eq. (4.34) reduces to

$$L_i(E)f_i(E) = \sum_j H_{ij}(E)f_j(E + \hbar\omega_s) \qquad (4.50)$$

where

$$L_i(E) = \frac{e}{\hbar} F[\frac{\gamma_i e\hbar}{m_i^*} + \beta_i \hbar^2 \frac{(k - K_i)}{m_i^*} \cos\theta] - 2\pi \sum_j D_{ij}^{(s)} S_o(k)_{ij} \qquad (4.51)$$

and $$H_{ij}(E) = -\pi D_{ij}^{(s)} \frac{(\frac{2m_j^*}{\hbar^2}) k_j^{+2}}{(k_j^+ - K_j)}$$

$$\left(\sum_{p=o}^{\infty} \frac{\Gamma(2p - \frac{r}{2})}{\Gamma(-\frac{r}{2})\, \Gamma(2p+1) (\frac{1}{2} + p)} [\{(\frac{2m_i^*}{\hbar^2})^{\frac{1}{2}} (E-\Delta_i)^{\frac{1}{2}} + K_i\}^2 + k_j^{+2}]^{r/2-2p} [2\{(\frac{2m_i}{\hbar^2})^{\frac{1}{2}} (E-\Delta_i)^{\frac{1}{2}} + K_i\} k_j^+]^{2p} \right)$$

$$- 3\pi D_{ij}^{(s)} \frac{(\frac{2m_j^*}{\hbar^2}) k_j^{+2}}{(k_j^+ - K_j)} \cos^2\theta$$

$$\left(\sum_{p=o}^{\infty} \frac{\Gamma(2p + 1 - \frac{r}{2})}{\Gamma(-\frac{r}{2}) \Gamma(2p+2) (\frac{3}{2} + p)} \left[\{(\frac{2m_i^*}{\hbar^2})^{\frac{1}{2}} (E-\Delta_i)^{\frac{1}{2}} + K_i\}^2 + k_j^{+2}\right]^{r/2-2p-1} \right.$$
$$\left. \times \left[2\{(\frac{2m_i^*}{\hbar^2})^{\frac{1}{2}} (E-\Delta_i)^{\frac{1}{2}} + K_i\} k_j^+\right]^{2p+1} \right) \qquad (4.52)$$

It is clear that the above treatment can be applied to cases with any number of conduction subbands. However, we shall use GaAs as an example for the following treatment. There are two conduction subbands in GaAs, and they are located at the centre of the Brillouiu zone (Γ point) and at the edge of this zone at the symmetry points designated by X in the direction [100] [Ehrenreich, 1960]. By denoting the lower subband with the subscript 1 and the higher subband with the subscript 2, Eq. (4.50) becomes

$$L_1(E) f_1(E) = H_{11}(E) f_1(E + \hbar\omega_s) + H_{12}(E) f_2(E + \hbar\omega_s)$$
$$L_2(E) f_2(E) = H_{21}(E) f_1(E + \hbar\omega_s) + H_{22}(E) f_2(E + \hbar\omega_s) \qquad (4.53)$$

Therefore, Eqs. (4.53) can be written in matrix form as follows

$$\begin{bmatrix} f_1(E+\hbar\omega_s) \\ f_2(E+\hbar\omega_s) \end{bmatrix} = \begin{bmatrix} J_{11}(E) & J_{12}(E) \\ J_{21}(E) & J_{22}(E) \end{bmatrix} \begin{bmatrix} L_1(E)f_1(E) \\ L_2(E)f_2(E) \end{bmatrix} \tag{4.54}$$

where

$$[J_{ij}] = [H_{ij}]^{-1} \tag{4.55}$$

Thus, carrier distribution function for the first subband is

$$f_1(E+\hbar\omega_s) = J_{11}(E)L_1(E)f_1(E) + J_{12}(E)L_2(E)f_2(E) \tag{4.56}$$

This difference equation is simply a mathematical expression of the physical process that the change of the electron energy E by $\pm\hbar\omega_s$ through the absorption or emission of a phonon of energy $\hbar\omega_s$ causes a corresponding change of the values of the carrier distribution function. This is of course a natural consequence. Since the magnitude and directions of the phonon wave vectors are random, while their energy is discrete and equals $\hbar\omega$, it is convenient to change the argument of the carrier distribution function from wave vector dependence to energy dependence. Furthermore, f in Eq. (4.8) with the energy in the argument enables an easy calculation of Eq. (4.14) and the quantities $T_o^o(k)_{ij}$ and $T_1^o(k)_{ij}$ given by Eqs. (4.48) and (4.49), which lead to the conversion of the Boltzmann equation into the difference

equations.

If we confine ourselves to the electron energy $\Delta_1 < E < \Delta_2$, then $f_2(E) = 0$. This implies that $f_1(E)$ diminishes at $E \geq \Delta_2$. For this case, Eq. (4.56) becomes

$$f_1(E + \hbar\omega_s) = J_{11}(E)L_1(E)f_1(E) \tag{4.57}$$

By denoting

$$x = \frac{E}{\hbar\omega_s} \tag{4.58}$$

Eq. (4.57) becomes

$$f_1(x + 1) = J_{11}(x)L_1(x)f_1(x) \tag{4.59}$$

This is a difference equation which has the following solution

$$f_1(x) = Ae^{\frac{1}{\Box}\ln[J_{11}(x)L_1(x)]} \tag{4.60}$$

where $\Box$ is the difference operator and A is a normalization constant. Thus by combining Eqs. (4.8) and (4.60), we obtain

$$\ln A + \frac{1}{\Box}\ln[J_{11}(x)L_1(x)] = -\alpha_1 - \beta_1\hbar\omega_s x - \frac{\gamma_1 e\hbar}{m_1^*}\cos\theta[(\frac{2m_1^*\hbar\omega_s}{\hbar^2})^{\frac{1}{2}}(x-\frac{\Delta_1}{\hbar\omega_s})^{\frac{1}{2}} + K_1] \tag{4.61}$$

which gives

$$\ln[J_{11}(x)L_1(x)] = -\beta_1\hbar\omega_s - \tfrac{1}{2}\frac{\gamma_1 e\hbar}{m_1^*}\cos\theta\left(\frac{2m_1^*\hbar\omega_s}{\hbar^2}\right)^{\frac{1}{2}}\left(x - \frac{\Delta_1}{\hbar\omega_s}\right)^{-\frac{1}{2}} \quad \ldots \quad (4.62)$$

Therefore

$$\left(x - \frac{\Delta_1}{\hbar\omega_s}\right)\ell n\,[J_{11}(x)\,L_1(x)] = -\beta_1 E - \frac{1}{2}\frac{\gamma_1 e\hbar k}{m_1^*}\cos\theta + \beta_1\Delta_1 + \frac{1}{2}\frac{\gamma_1 e\hbar k_1}{m_1^*}\cos\theta \quad (4.63)$$

If we choose the coordinates of the E-k relationship such that $\Delta_1 = 0$ and $K_1 = 0$, we obtain

$$e^{-\beta_1 E - \frac{1}{2}\gamma_1\frac{e\hbar k}{m_1^*}\cos\theta} = \{J_{11}(E)L_1(E)\}^{E/\hbar\omega_s} \quad (4.64)$$

Since $f_1(E) \approx \exp[-\alpha_1-\beta_1 E-(\gamma_1 e\hbar k/m_1^*)\cos\theta]$, the carrier distribution function can be written in the form

$$f_1(E) = e^{-\alpha_1}\left\{J_{11}(E)\ \ L_1(E)\right\}^{nE/\hbar\omega_s} \quad 4.65)$$

where n is a factor taking a value between 1 and 2 depending on whether $\beta_1 E$ is larger or smaller than $(\gamma_1 e\hbar k/m_1^*)\cos\theta$. At low temperatures n is expected to be approximately equal to 1.

By applying the same argument in determining $L_1(E)$, we obtain the following relation for small values of θ

$$e^{\alpha_1} f_1(E) - \left\{\frac{H_{22}}{H_{11}H_{22} - H_{12}H_{21}}\left(-\frac{2eF}{n\hbar}\frac{\ell n[e^{\alpha_1} f_1(E)]}{\left(\frac{2m_1^* E}{\hbar^2}\right)^{\frac{1}{2}}\cos\theta} - \right.\right.$$

$$- 2\pi\sum_j D_{1j}^{(s)} S_o(E)_{1j})\}^{\frac{nE}{\hbar\omega_s}} = 0 \qquad (4.66)$$

It should be emphasized that Eq. (4.66) is unique because it reduces to Fermi-Dirac distribution function when $F \to o$ as $\gamma \to o$. This can be deduced from Eq. (4.64).

For large values of θ, Eq. (4.8) reduces to the Fermi-Dirac distribution function.

For the case of low-energy phonons (or at high temperatures) Eq. (4.53) becomes

$$\begin{aligned} L_1'(E)f_1(E) &= H_{11}(E)f_1(E+\hbar\omega_s) + H_{12}(E)f_2(E+\hbar\omega_s) \\ &\quad + H_{11}'(E)f_1(E-\hbar\omega_s) + H_{12}'(E)f_2(E-\hbar\omega_s) \\ L_2'(E)f_2(E) &= H_{21}(E)f_1(E+\hbar\omega_s) + H_{22}(E)f_2(E+\hbar\omega_s) \\ &\quad + H_{21}'(E)f_1(E-\hbar\omega_s) + H_{22}'(E)f_2(E-\hbar\omega_s) \end{aligned} \qquad (4.67)$$

where

$$L_i'(E) = \frac{eF}{\hbar}\left[\frac{\gamma_i e\hbar}{m_i^*} + \beta_i\hbar^2 \frac{(k-K_i)}{m_i^*}\cos\theta\right] - 2\pi\sum_j D_{ij}'^{(s)} S_o'(k)_{ij} \qquad (4.68)$$

and $H_{ij}'(E)$ can be obtained from Eq. (4.52) by replacing r with r-1, and k_j^+ with k_j^- which is given by

$$k_j^- = \left(\frac{2m_j^*}{\hbar^2}\right)^{1/2} (E - \hbar\omega_s - \Delta_j)^{1/2} + K_j \qquad (4.69)$$

In the energy range $\Delta_1 < E < \Delta_2$, we can set $f_2(E) = 0$ and $f_2(E-\hbar\omega_s) = 0$. Thus Eq. (4.67) reduces to

$$L_1'(E)f_1(E) = [H_{11}(E) - \frac{H_{12}(E)H_{21}(E)}{H_{22}(E)}]f_1\ (E + \hbar\omega_s)$$

$$+ [H_{11}'\ (E) - \frac{H_{12}(E)H_{21}'(E)}{H_{22}(E)}]f_1(E - \hbar\omega_s) \qquad (4.70)$$

If $f_1(E/\hbar\omega_s)$ is assumed to be in the form

$$f_1(\frac{E}{\hbar\omega_s}) = e^{\frac{\lambda E}{\hbar\omega_s}} \qquad (4.71)$$

it can be shown that the solution of Eq. (4.70) is given by

$$f_1(E)-\left(L_1(E)\pm\{L_1'^2\ (E)-4[H_{11}(E)- \frac{H_{12}(E)H_{21}(E)}{H_{22}(E)}][H_{11}'(E) - \frac{H_{12}(E)H_{21}'(E)}{H_{22}(E)}]\}^{\frac{1}{2}}\right)^{\frac{E}{\hbar\omega_s}} \left[2\{H_{11}(E) - \frac{H_{12}(E)H_{21}(E)}{H_{22}(E)}\}\right]^{-1} = o$$

$$(4.72)$$

4.4 Computed Results and Discussion

The solution of Eq. (4.66) shows that the quantity $e^{\alpha_1}f_1(E)$ can be expressed in the form

$$e^{\alpha_1}f_1(E) = f'(E) + c \qquad (4.73)$$

where c is a constant which depends on the applied field and can be determined by employing the following boundary condition

$$f_1(E) \to o \quad \text{as} \quad E \to \infty \tag{4.74}$$

In the following we shall confine ourselves to the carrier distribution function for the case of high-energy phonons (that is to say $\hbar\omega_s > K_B T$), since it is of direct interest to the study of electron transfer between conduction subbands in multivalley semiconductors at low temperatures.

For the purpose of demonstrating the above mentioned calculations we choose an n-type GaAs material as an example. In this semiconductor the bottom of the first valley in the conduction band is located at the centre of the Brillouin zone (000) with the electron effective mass $m_1^* = 0.067\ m_0$ and that of the second valley at (100) with $m_2^* = 0.35\ m_0$, where m_0 is the rest mass of the electron, the energy separation between these two valleys $\Delta_2 - \Delta_1$ being 0.36 eV. The value of the distribution function f'(E) has been computed under various conditions and the results are presented and discussed below.

The values of $D_{ii}^{(o)}$ and $D_{ij}^{(ij)}$ for n-GaAs are given by [Butcher, 1967]

$$D_{ii}^{(o)} = \frac{e^2\omega_o}{2\pi}\left(\frac{1}{\varepsilon_\infty} - \frac{1}{\varepsilon_o}\right) \simeq 10^{-15} \text{ M.K.S. units}$$

and

$$D_{ij}^{(ij)} = \frac{\overline{D}_{ij}^{2}}{8\pi^2 \rho\omega_{ij}} \simeq 10^{-22} \text{ M.K.S. units}$$

where ω_0 is the angular frequency of the optical phonons, ε_∞ and ε_0 are, respectively, the dielectric constants at infinite and zero frequencies; $\tilde{D}_{ij}$ is the deformation potential field for the transferred phonons between the ith and j^{th} subbands [Vassell and Conwell, 1966], which is taken to be 5×10^8 eVcm^{-1}; ρ_d is the density of the semiconductor and ω_{ij} is the phonon frequency at wave vector $\vec{K}_i - \vec{K}_j$. We choose the value of D_{ij} to be of the order of 10^{-18} mks units in order to examine the effect of mixed optical and intervalley scatterings since this value falls within the value of the upper and lower limits which correspond to these two types of scattering as discussed in section 4.2. A decrease of the value of D_{ij} corresponds to an increase in weight of the intervalley scattering, and in turn corresponds to an increase of electron transfer from the lower to the upper valley and consequently leads to current instabilities.

Figure 4.1 shows the carrier distribution function as a function of $E/\hbar\omega_s$ for applied electric fields of strengths 1 and 2 KV/cm. We chose C_{ij} in this case to be $2 \times 10^{-18} |\vec{k}-\vec{k}'|^{-2}$ and $\theta=0$. It should be expected that the tail of the distribution curve has a slope equal to $-E/K_BT$. From this fact one can realize that the case for n=1 corresponds to that for T=0°K, and the case for n=1.02 corresponds to that for T=30°K. We chose also the phonon energy $\hbar\omega_s = 0.01$ eV. From this figure the tail of curve (c)

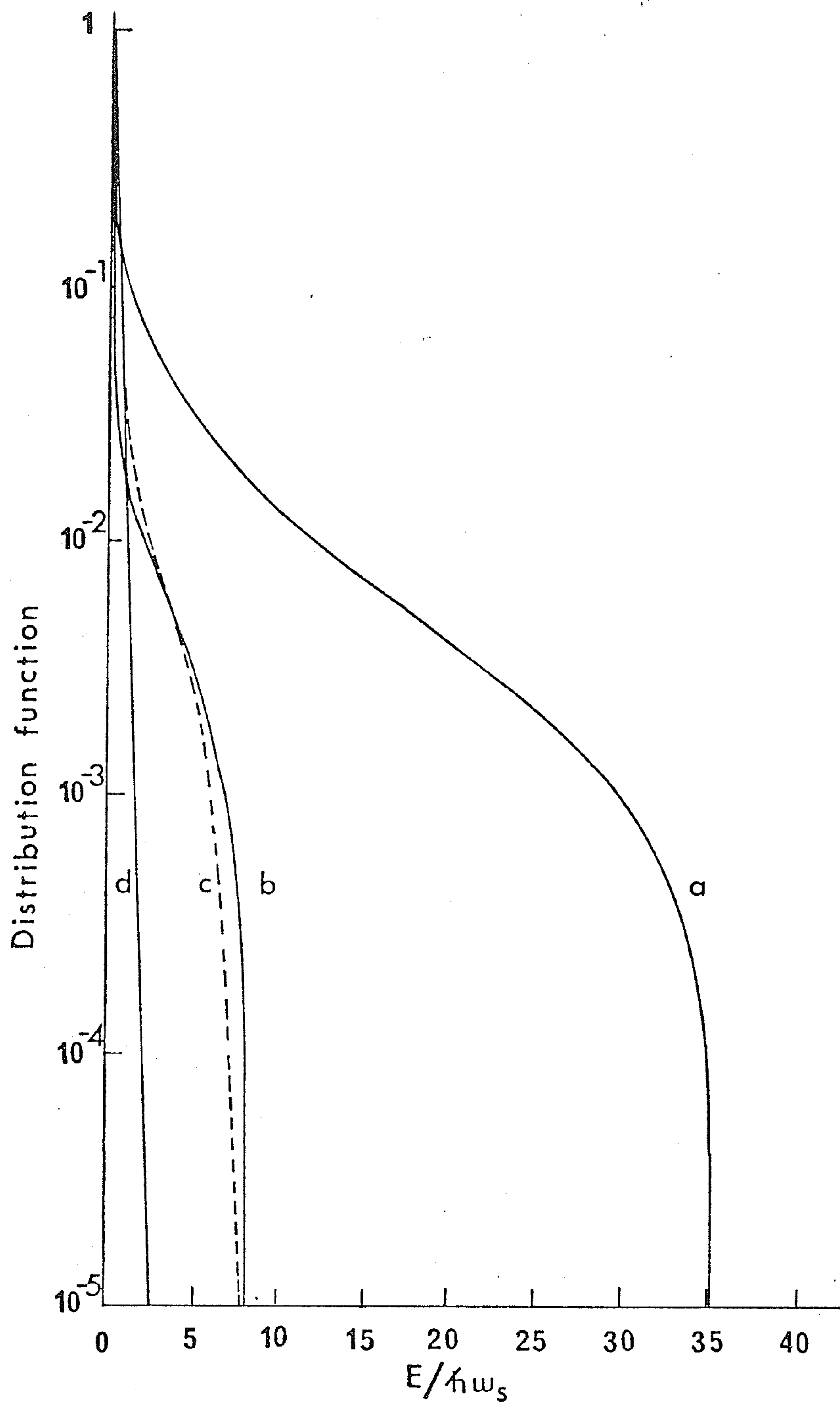

Fig. 4.1. Distribution function of electrons in (000) valley in n-GaAs for $C_{ij} = 2 \times 10^{-18}|\vec{k}-\vec{k}'|^{-2}$, $\theta = 0°$ and $\hbar\omega_s = 0.01$ eV. (a) F = 2 kV/cm, n = 1; (b) F = 1 kV/cm, n = 1; (c) F = 1 kV/cm, n = 1.02; (d) Maxwellian distribution at F = 0 and T = 30°K for comparison purposes.

is clearly parallel to the Maxwellian distribution curve (d) for the same temperature and phonon energy. By comparing curve (a) with curves (b) and (d) it is clear that the higher the applied electric field, the more electrons acquire higher energies.

In Figure 4.2 we replace the value of C_{ij} to $1 \times 10^{-18} |\vec{k}-\vec{k}'|^{-2}$. In this case the increase of the external field will cause a decrease in the distribution function throughout the whole energy range. This trend is just opposite to that shown in Fig. 4.1, indicating that there is a critical value of D_{ij} below which the distribution function reverses its trend of response to the applied field.

This phenomenon may be explained by the fact that when D_{ij} is large the coupling between electrons and the lattice is large and therefore the number of electrons transferring to the upper subbands is less and hence the increase of applied field F results in an increase of the number of electrons with high energies. But when D_{ij} is small, the coupling is small, and hence the probability of electron transfer to upper subbands increases. This is why in this case the trend of the change of f with F is reversed.

Figure 4.3 shows the effect of the parameter r. By changing r from -2 to -1.98 so that the scattering is a mixed scattering, and comparing the results with those in Fig. 4.2, it can be seen that the distribution function increases considerably with a slight decrease in the value of r, particularly in the low-energy region. This indicates the importance of mixed scattering processes.

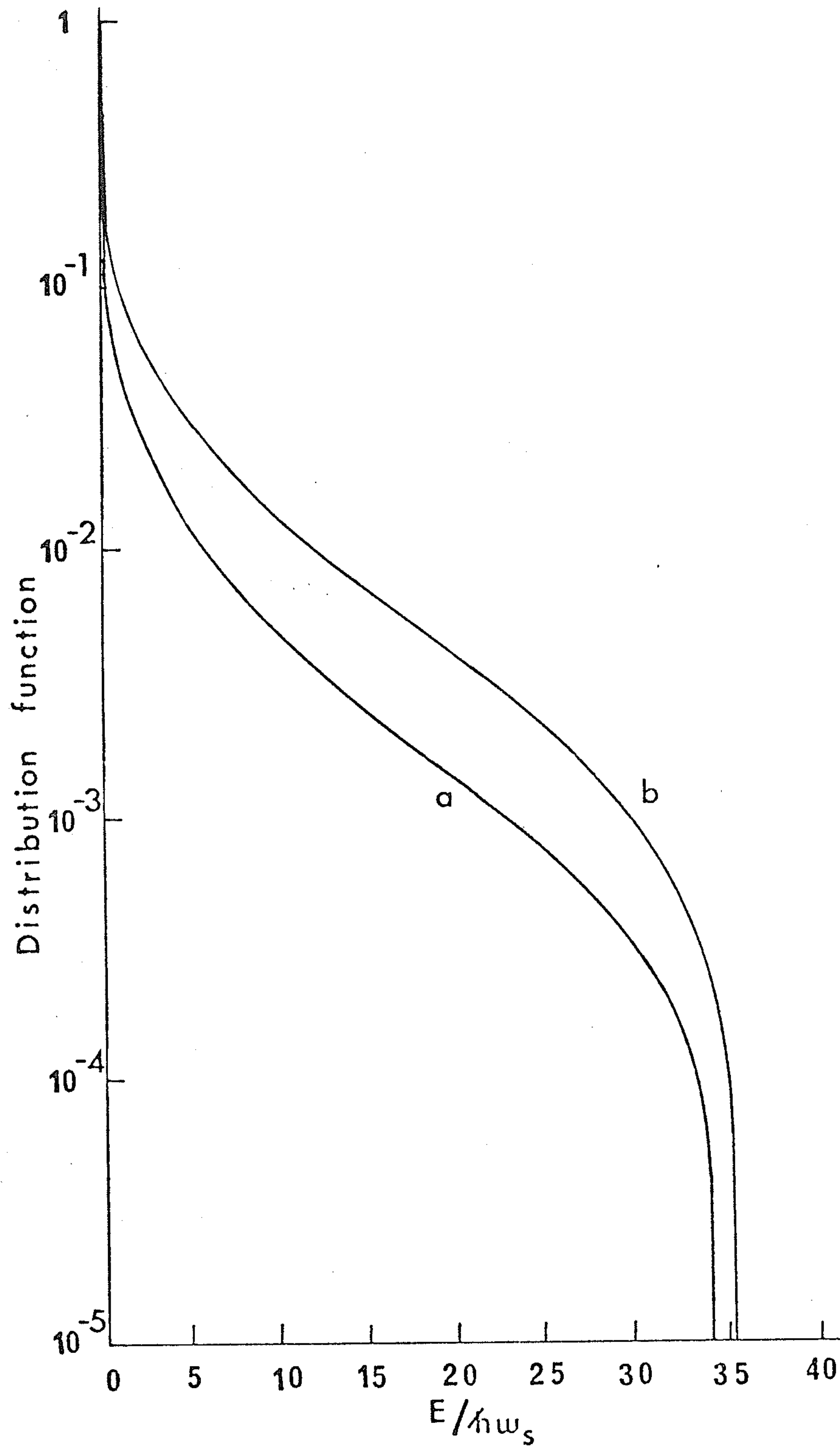

Fig. 4.2. Distribution function of electrons in the (000) valley in n-GaAs for $C_{ij} = 1 \times 10^{-18}|\vec{k}-\vec{k}'|^{-2}$, $\theta = 0°$, and $\hbar\omega_s = 0.01$ eV. (a) $F = 2$ kV/cm, $n = 1$; (b) $F = 1$ kV/cm, $n = 1$.

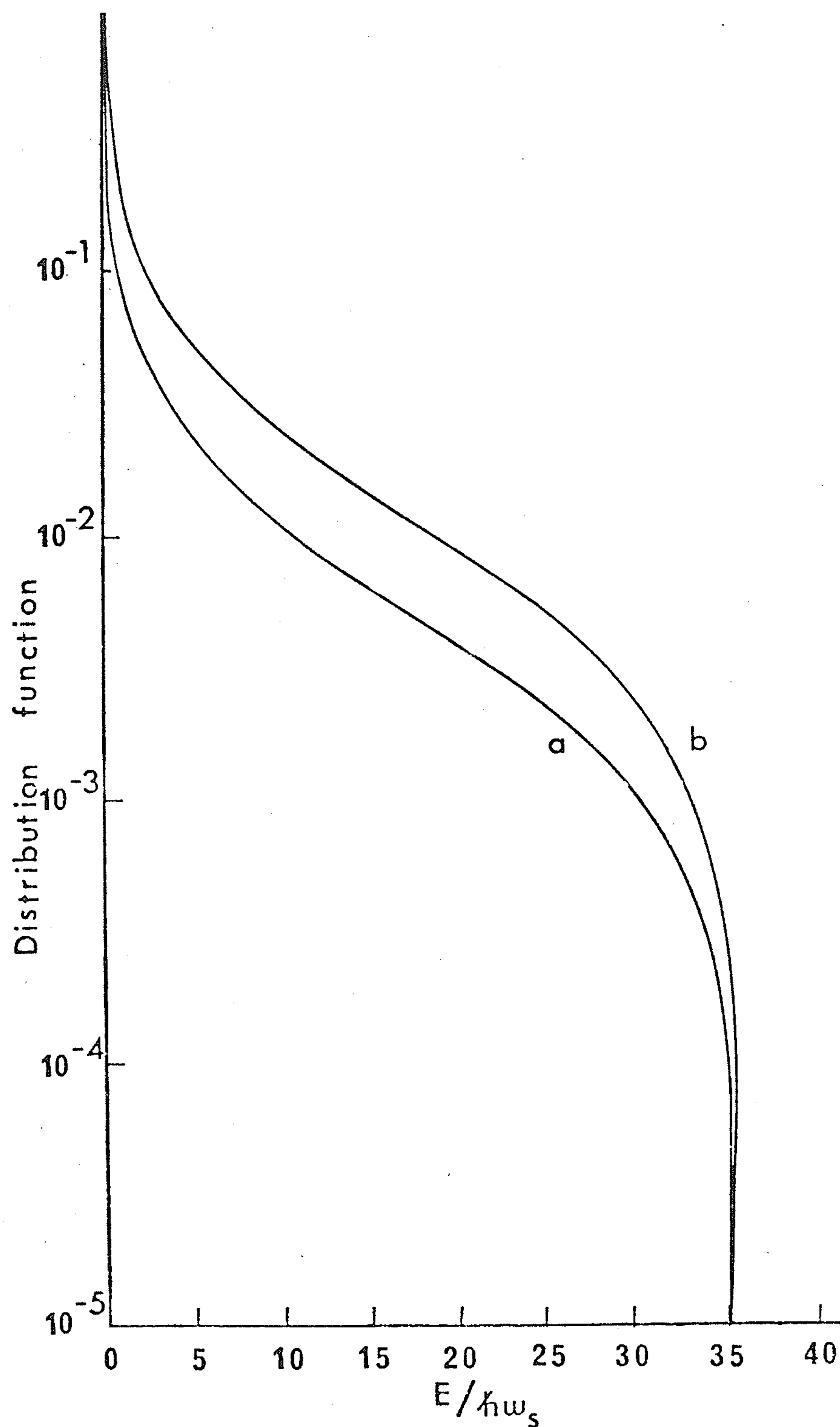

Fig. 4.3. Distribution function of electrons in the (000) valley in n-GaAs for $C_{ij} = 1 \times 10^{-18}|k-k'|^{-1.98}$, $\theta = 0°$ and $\hbar\omega_s = 0.01$ eV. (a) F = 2 kV/cm, n = 1; (b) F = 1 kV/cm, n = 1.

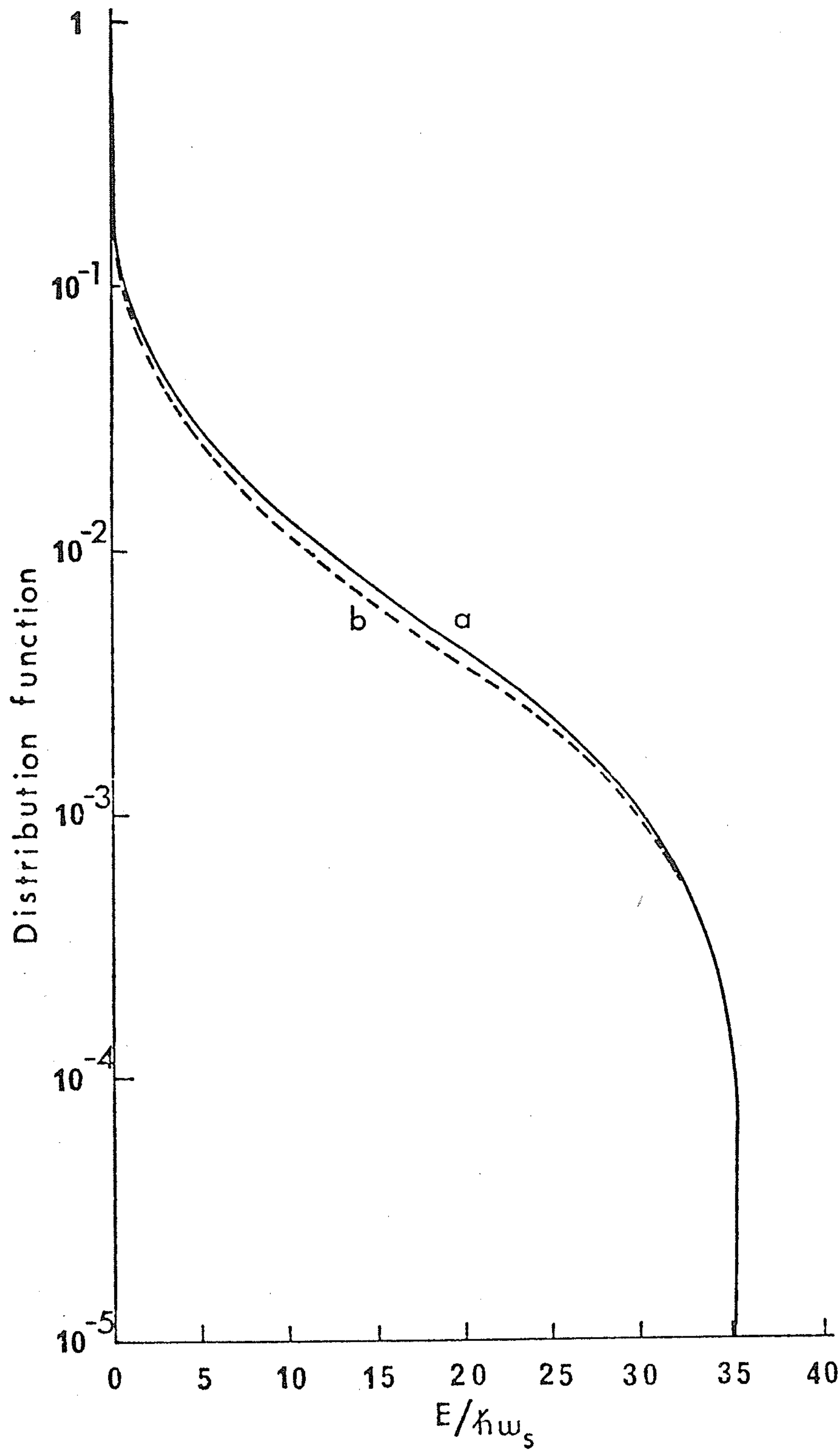

Fig. 4.4. Distribution function of electrons in the (000) valley in n-GaAs for $C_{ij} = 1 \times 10^{-18}|\vec{k}-\vec{k}'|^{-2}$, F = 1 kV/cm, $\hbar\omega_s$ = 0.01 eV and n = 1. (a) $\theta = 0°$; (b) $\theta = 10°$.

Figure 4.4 shows the effect of the angle θ. It is clear that the distribution function is not sensitive to a small variation of θ. This result can be seen directly from Eq. (4.8) and indicates that the maximum anisotropy approach [Baraff, 1964] in which the distribution function is represented by a delta function in the direction of the applied field is far from the actual situation.

However, for large values of θ ($\simeq\pi/2$), the distribution function will decrease strongly and tends to become the Maxwellian distribution.

Figure 4.5 gives the comparison between the results of the present calculations and the corresponding ones of Vassell and Conwell [1966] for F = 2.4 KV/cm. In order to use the mixed scattering, approximately similar to that used by Vassel and Conwell, we used $C_{ij} = 2 \times 10^{-18} |\vec{k}-\vec{k}'|^{-2}$, $\theta = 0°$ and n = 1.05 which corresponds approximately to T = 293°K. The results based on this calculation deviates markedly from the Maxwellian distribution much more than that of Vassell and Conwell especially at high energies. Based on Fig. 4.5, an appreciable portion of electrons have energies extending to the bottom of the upper subband. The main source of the disagreement is due to truncation of the expansion of the distribution function done by Varrell and Conwell, who used only two terms of Legendre series which has been proved not accurate by Law and Kao [1971], while the treatment of Wassef and Kao does not involve this approximation. So we can claim that our results are more accurate than theirs from theoretical analysis point of view.

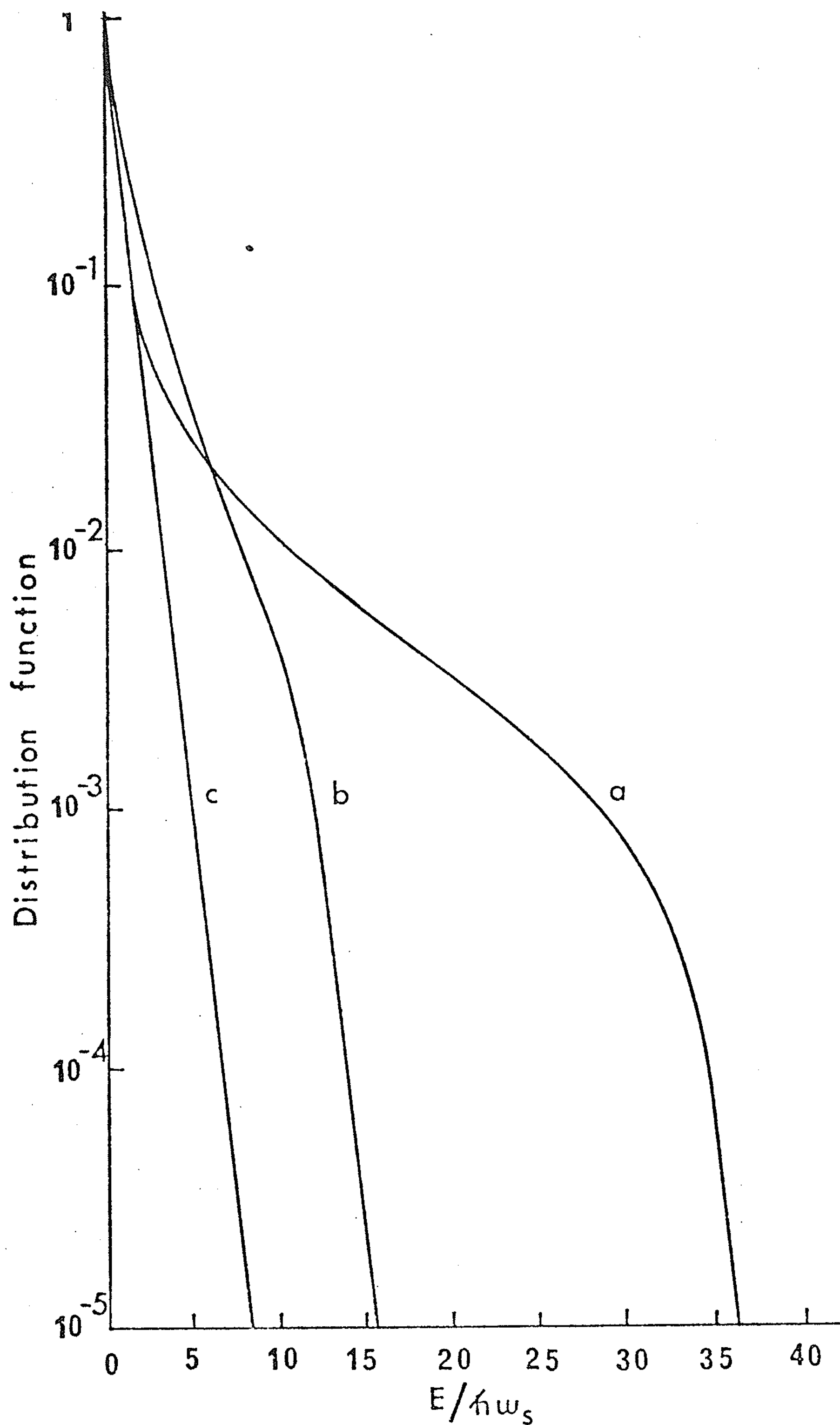

Fig. 4.5. Distribution function of electrons in the (000) valley in N-GaAs for $C_{ij} = 2 \times 10^{-18}|\vec{k}-\vec{k}'|^{-2}$, F = 2.4 kV/cm, $\hbar\omega_s$ = 0.01 eV, n = 1.05, and $\theta = 0°$. (a) Wassef and Kao; (b) Vassell and Conwell [1966]; (c) Maxwellian distribution (F = 0) at T = 293°K corresponding to n = 1.05 for comparison purposes.

CHAPTER 5

THE EFFECT OF NONPARABOLIC ENERGY BAND STRUCTURES ON THE HIGH-FIELD CARRIER DISTRIBUTION FUNCTIONS

In this chapter we first present a general distribution function based on the energy band structure developed in Chapter 3. The parameters used in this distribution function will be calculated in terms of some known physical quantities in Section 5.1. At certain high fields the distribution function turns to be a complex quantity. The calculation of this critical field for this occurrence and the physical interpretation of this feature will be given in Section 5.2.

5.1 Distribution Function of Carriers in Non-Parabolic Energy Band Structures

According to Eq. (3.34), the energy band structure for the ith sub-band can be written in the following form:

$$E_{\vec{k},i} - E_{o,i} = \frac{\hbar^4}{20\langle m^*\rangle_i^2 \, K_B T} |\vec{k} - \vec{K}_i|^4 \qquad (5.1)$$

where the extremum of the ith sub-band has an energy $E_{o,i}$ at a wave vector $\vec{K}_i$. For mathematical simplicity we will

consider the effective mass $\langle m^* \rangle_i$ to be isotropic and scalar. Thus, the distribution function of carriers in the ith subband given by Eq. (4. 8) can be written in the form

$$f_i(\vec{k}) = \frac{1}{1+\exp[\alpha_i+\beta_i(\frac{\hbar^4}{20\langle m^*\rangle_i^2}K_BT)|\vec{k}-\vec{K}_i|^4+\gamma_i(\frac{e\hbar}{\langle m^*\rangle_i})|\vec{k}-\vec{K}_i|\cos\theta]}$$

$$\simeq \exp[-\alpha_i - \beta_i' k'^4 - \gamma_i' k' \cos\theta] \qquad (5.2)$$

where

$$k' = |\vec{k}'| = |\vec{k}-\vec{K}_i|$$

$$\beta_i' = \beta_i \frac{\hbar^4}{20\langle m^*\rangle_i^2 K_B T} \qquad (5.3)$$

$$\gamma_i' = \gamma_i \frac{e\hbar}{\langle m^*\rangle_i}$$

In chapter 3 we have mentioned that Eq. (3.3.4) and hence Eq. (5.1) are valid for $0.01\ (\frac{2\pi}{a}) < k < 0.08\ (\frac{2\pi}{a})$. But since the distribution functions given in Fig.s 4.1 to 4.5 show that at high fields most of electrons occupy states in this range, we assume that the extension of Eq. (5.1) to the band edge would not introduce a serious error.

For a complete determination of the carrier distribution function given by Eq. (5.2), we have to determine α_i, β_i' and γ_i'. Three conditions are required to determine these three parameters for each subband. We may choose the following three conditions:

(i) the concentration of carriers in the ith subband

$$n_i = \int_{\vec{k} \leq \vec{k}_o} f_i(\vec{k}') \, d^3k' \tag{5.4}$$

(ii) the mobility of carriers in the ith subband

which can be calculated from the average drift velocity

$$<\vec{v}>_i = \frac{1}{n_i} \int_{\vec{k} \leq \vec{k}_o} \vec{v} \, f_i(\vec{k}') \, d^3k'$$

therefore

$$\mu_i = \frac{\hbar}{n_i <m^*>_i F} \int_{\vec{k} \leq \vec{k}_o} k' \cos\theta \, f_i(\vec{k}') \, d^3k' \tag{5.5}$$

$<\vec{v}>_i$ and $\vec{F}$ are taken in the z-direction.

(iii) the average effective mass of carriers in the ith subband defined by:

$$\frac{1}{<m^*>_i} = \frac{1}{n_i \hbar^2} \int_{\vec{k} \leq \vec{k}_o} \left(\frac{\partial^2 E}{\partial k^2}\right)_i f_i(\vec{k}') \, d^3k'$$

Therefore, using Eq. (5.1) we obtain

$$<m^*>_i = \frac{3\hbar^2}{5 n_i K_B T} \int_{\vec{k} \leq \vec{k}_o} k'^2 \, f_i(\vec{k}') \, d^3k' \tag{5.6}$$

To simplify matter we assume that the average dynamic effective mass given in Eq. (5.6) is equal to the average effective mass defined in Eq. (5.5).

The vector $\vec{k}_o$ is used as the radius of a sphere which contains all the carriers in the ith valley at zero temperature and zero external field. The vector $\vec{k}_o$ can be related to the carrier concentration n_i in the usual manner. It is well known that the wave vectors of carriers in a crystal can only take certain values in the reciprocal lattice given by

$$k = \frac{2\pi}{a}\frac{n}{M} \tag{5.7}$$

where n is a positive or negative integer and takes the values

$$-\frac{M}{2} < n \leq +\frac{M}{2} \tag{5.8}$$

and M is the number of unit cells in the fundamental domain of the crystal. Therefore, we have

$$n_i = \frac{2}{\Omega}\sum_{\vec{k}-\vec{k}_o} 1 = \frac{1}{(2\pi)^3}\int_0^{2\pi}\int_0^{\pi}\int_0^{k_o} k^2 \sin\theta \, d\phi \, d\theta \, dk \tag{5.9}$$
$$= \frac{k_o^3}{3\pi^2}$$

in which the spin degeneracy is included. At any temperature and field we can still use Eq. (5.9) as an approximate relation between k_o and n_i.

In Eq. (5.5) we assume the drift velocity to be in the direction of the applied field z-direction; in other words, the mobility μ_i is considered to be a scalar quantity. It is clear that the right hand sides of Eqs. (5.4) to (5.6) are proportional to the zero, first and second moments of

the wave vector $\vec{k}'$ with respect to the distribution function $f_i(\vec{k}')$. The solution of Eqs. (5.4) to (5.6) for α_i, β_i' and γ_i' is not a simple problem. However, with further approximation of the distribution function we can get a simple solution.

We begin with Eqs. (5.4) and (5.5) by setting the distribution function of the form e^{-x} to be $(1-x)$. This approximation is clearly valid for the major part of the energy spectrum as can be seen from Figs. 4.1 to 4.5. The multiplication of the distribution function with k'^2 in the integrand on the right hand side of Eq. (5.6) suggests the use of a better approximation for e^{-x} in this case, which may be expressed as

$$e^{-x} = 1 - x + \frac{x^2}{2} \qquad (5.10)$$

Then Eq. (5.4) becomes

$$n_i = \int_0^{2\pi}\int_0^{\pi}\int_0^{k_o} [1-\alpha_i-\beta_i' k'^4-\gamma_i' k' \cos\theta] \sin\theta k'^2 \, d\phi \, d\theta \, dk'$$

$$= \frac{4\pi}{3} k_o^3 [1 - \alpha_i - \frac{3}{7} k_o^4 B_i'] \qquad (5.11)$$

Similarly, Eq. (5.5) becomes

$$\frac{\mu_i n_i \langle m^* \rangle_i F}{\hbar} = - \frac{4\pi k_o^5 \gamma_i'}{15} \qquad (5.12)$$

However, using Eq. (5.10) as an approximation for the distribution function, Eq. (5.6) reduces to

$$\langle m^*\rangle_i = \frac{3\hbar^2}{5K_BTn_i}\int_0^{2\pi}\int_0^{\pi}\int_0^{k_o} k'^4\{1-(\alpha_i+\beta_i' k'^4+\gamma_i' k'\cos\theta)$$

$$+ \tfrac{1}{2}(\alpha_i+\beta_i' k'^4+\gamma_i' k'\cos\theta)^2\}\sin\theta\, d\phi\, d\theta\, dk' \qquad (5.13)$$

All the integrations on the right hand side of Eq. (5.13) can be carried out easily and the expression for γ_i' is thus given by

$$\gamma_i' = \{\frac{35K_BTn_i\langle m^*\rangle_i}{2\pi\hbar^2k_o^7} - 21[\frac{1}{5k_o^2}(1-\alpha_i)^2+\frac{1}{5k_o^2}$$

$$-\frac{2}{g}\beta_i'(1-\alpha_i)k_o^2 + \frac{1}{13}\beta_i'^2k_o^6]\}^{\frac{1}{2}} \qquad (5.14)$$

Substituting Eqs. (5.11) and (5.12) into Eq. (5.14) we obtain

$$(\frac{15\mu_i n_i\langle m^*\rangle_i F}{4\pi\hbar k_o^5})^2 - \frac{35K_BTn_i\langle m^*\rangle_i}{2\pi\hbar^2k_o^7} + 21[\frac{1}{5k_o^2}(\frac{3n_i}{4\pi k_o^3}+\frac{3}{7}k_o^4\beta_i')^2$$

$$+\frac{1}{5k_o^2} - \frac{2}{g}\beta_i' k_o^2(\frac{3n_i}{4\pi k_o^3}+\frac{3}{7}k_o^4\cdot\beta_i') + \frac{1}{13}\beta_i'^2k_o^6] = 0 \qquad (5.15)$$

which can be written in the form

$$C_1\beta_i'^2 + C_2\beta_i' + C_3 = 0 \qquad (5.16)$$

where

$$C_1 = 333.18\, n_i^2$$

$$C_2 = -0.13\, n_i^{2/3}$$

$$C_3 = (C_4\frac{\mu_i\langle m^*\rangle_i F}{n_i^{2/3}})^2 - C_5T\frac{\langle m^*\rangle_i}{n_i^{4/3}} + \frac{C_6}{n_i^{2/3}} \qquad (5.17)$$

$C_4 = 3.82 \times 10^{32}$ MKS units

$C_5 = 7.89 \times 10^{42}$ MKS units

$C_6 = 4.2$

The solution of Eq. (5.16) can readily be found as follows:

$$\beta_i' = \frac{-C_2 \pm (C_2^2 - 4C_1C_3)^{\frac{1}{2}}}{2C_1} \qquad (5.18)$$

It is clear that under certain conditions β_i' becomes a complex quantity and so does the distribution function f_i. This condition can be deduced from Eq. (5.18) and is given by

$$4C_1C_3 > C_2^2 \qquad (5.19)$$

since C_3 is a function of the field F; therefore, we can calculate the critical field beyond which the condition (5.19) is satisfied. This critical field is given by

$$F_C = C_7 \frac{n_i^{1/3}}{\mu_i \langle m^* \rangle_i} \left(C_8 \frac{T \langle m^* \rangle_i}{n_i^{2/3}} - 1\right)^{\frac{1}{2}}$$

$$\simeq C_9 \frac{T^{\frac{1}{2}}}{\mu_i \langle m^* \rangle_i^{\frac{1}{2}}} \qquad (5.20)$$

where

$C_7 = 2.62 \times 10^{-33}$ MKS units

$C_8 = 1.879 \times 10^{42}$ MKS units

$C_9 = 3.59 \times 10^{-12}$ MKS units

It should be mentioned here that the constants C_4 to C_9 contains only $\hbar$, K_B and some numerical constants.

As an example we may estimate the value of F_C for GaAs at room temperature by choosing

$<m^*>_1 = 0.072\ m_o$ [Ehrenreich, 1960]

and

$\mu_1 = 0.68\ m^2/vsec$ [Hasty, Stratton and Jones, 1968] where the subscript 1 refers to the lower conduction subband. Therefore, Eq. (5.20) gives $F_C = 3.4$ kV/cm.

5.2 Possible Interpretation of the Complex Distribution Function

It should be noted that the term $\left| C_5\, T \frac{<m^*>_i}{n_i^{4/3}} \right|$ is always larger than the term $\left| \frac{C_6}{n_i^{2/3}} \right|$ in Eq. (5.17), thus at fields $F < F_c$, B_i' given in Eq. (5.18) is always real. However, for $F \geq F_c$, B_i' becomes complex. In this case there may be two possible explanations:

(a) It is clear that the critical field F_c is very high and at this field the approximation $e^{-x} \simeq 1 - x + \frac{x^2}{2}$ might not be satisfactory and thus the approximate distribution function does not apply for fields larger than F_c.

(b) The complex distribution function can also be interpreted physically in a way similar to the case of an electron entering a forbidden energy band for which the wave vector $\vec{k}$ and consequently the carrier distribution function becomes a complex quantity [Spenke, 1958]. In our case, the complex distribution function implies that the carriers cannot have energies beyond a certain critical level determined by the field F_C for a certain band structure. Of course, carriers having energies higher than this critical level must behave

differently. One of the following mechanisms may play a role in the behaviour of such high energy carriers:

(1) the carriers at certain energy levels may transfer from a lower to a higher conduction subband at or beyond the critical applied field F_C. In this case both of the lower and higher subbands will contribute to the current flow in the semiconductor and we may write

$$J = g(n_1\langle v\rangle_1 + n_2\langle v\rangle_2) \tag{5.22}$$

where the subscript 2 refers to the higher subband. Using expressions similar to Eq. (5.5) we may calculate the critical field for the onset of current instabilities in the usual manner by applying the criterion

$$\frac{dJ}{dF} = 0 \; ; \tag{5.23}$$

(2) for semiconductors containing coulombic repulsive trapping centres then the carriers with energies beyond certain high level will tend to be trapped. This implies that no carriers can exist with an energy beyond this level;

(3) in the case of double injection from electrodes in semiconductors, the current density equation is written in the form

$$J = J_n + J_p \tag{5.24}$$

where J_n is the current density due to electrons and J_p is that due to holes. The electron-hole recombination constant is proportional to the average velocity of

carriers. Therefore, when the carriers gain energy in the applied field, they cannot have energy higher than that necessary for the electron-hole recombination process.

It should be noted that F_C is the field in which some carriers may start to have energies beyond a certain critical level and that it may not be the critical field for the onset of current instabilities, the criterion of which is $\frac{dJ}{dF} = 0$. To determine the critical field for the onset of current instabilities, the mechanisms to cause the instabilities must be taken into account.

CHAPTER 6

CONCLUSIONS

The energy band structures and the carrier distributors function calculations are two major problems which have to be solved before theoretical analysis of any electrical properties of a solid can be carried out. In this thesis we have presented new approaches. These approaches remove some shortcomings existing in the previous methods dealing with these problems. In this chapter we shall summarize and discuss our approaches and contributions to these problems:

6.1. The energy band structure

An expression for the energy band structures of crystals has been derived. This expression has the following advantages:

(a) The expression is of simple form and requires only two parameters for the complete determination of the energy band structure. These parameters are the energy splitting and the effective mean at the band extremum. which can easily be determined experimentally.

(b) No assumptions are needed concerning the lattice potential. The involvement of the lattice potential is considered to be the major shortcomings of most previous methods since the knowledge of lattice potential is not available.

(c) The expression can be applied easily to study either temperature or pressure effect or the energy band structures.

It should be noted that the general expression for the wave function given in Eq. (3.22) does not involve any kind of approximations. To obtain a close form of analytic solution for $E_{\vec{K}}$ as a function of K we have

made only one approximation, that is $E_{\vec{K}} - V(\vec{r}) < \frac{\hbar^2 K^2}{2m}$. Because of this assumption, our expression [Eq. (3.43)] is valid for the range of the values of K from $K = 0.01(2\pi/a)$ to $K = 0.08(2\pi/a)$. Within this range the calculation should be accurate to $\pm 1\%$. However, for $K < 0.01(2\pi/a)$ the band structure is close to a parabolic structure. The band structure for $0.01(\frac{2\pi}{a}) < K < 0.08(\frac{2\pi}{a})$ are of great importance to the study of properties of semiconductors at normal temperatures. From the computed results we can draw the following conclusions:

(i) The energy band structure is far from the parabolic profile for any crystalling solids (Fig.3.1). This non-parabolic feature should be taken into account when studying electrical properties of solids.

(ii) The energy band structure is very sensitive to temperature. The E-K curve tends to shift towards higher K as the temperature is increased. Again, this temperature effect should also be taken into account when studying electrical properties of solids at various temperatures.

(iii) The discrepancy between our results and that of Pollak, Higginbotham and Condona may be attributed to the different approximations used in the two different approaches. But we would like to say that the approximation used in our approach would introduce much less errors.

6.2. The Carrier Distribution Function

The problem concerning the carrier distribution function in semiconductors has been rigorously solved analytically without any approximations involved. The general expression can be used to determine the carrier

distribution functions at low and high fields for degenerate and non-degenerate semiconductors with parabolic and non-parabolic energy band structures. With some approximations our expression reduces to other well known forms of distribution functions used by previous investigators and in this way it can be shown that the use of these approximate distribution functions by the previous investigators may result in some errors.

We have used the general expression to study some effects on the distribution function. To obtain a relatively simple solution, we feed back the general expression for f into the Boltzmann equation and make the following assumptions:

(a) The semiconductor is nondegenerate.

(b) The energy band structure is parabolic.

(c) The external applied field $\vec{F}$ is uniform across the semiconductor sample.

(d) The honon distribution function is not disturbed by the existance of carrier flow.

The effect of scattering parameters, temperature, high fields and the angle relative to the direction of the applied field can be deduced easily from the expressions obtained. The computed results are summarized as follows:

(i) The carriers are in general spread over a wider range of energy rather than has been expected before by other investigators

(ii) Both the deformation potential and extreme applied electric field affect greatly the carrier distribution.

(iii) The distribution function is insensitive to small angles relative to the direction of the applied field ($0 < \theta < 10°$). However, for large angles ($\theta \approx \frac{\pi}{2}$) the distribution function tends to

approach the Fermi-Dirac distribution.

(iv) The disagreement between the results of Wassef and Kao [1972] and those of Vassell and Conwell [1966] is attributed mainly to the approximation used. Vassell and Conwell used only two terms of the Legandre series for the distribution function, but Wassef and Kao did not use any approximation.

Using the expression for the energy band structure and feeding it back to that for the carrier distribution function, it is found that there exists a critical field under certain conditions beyond which the distribution function becomes a complex quantity. In the case where the approximations used in the work holds, this complex distribution function can be attributed to the fact that there exists an upper energy level beyond which the carriers cannot occupy energy states steadily. The physical interpretation of this feature is that the carriers having energies beyond a certain energy level may transfer to a higher subband, may be trapped in trapping centers, or disappear through electron-hole recombination; all of these processes tend to decrease the number of high energy carriers.

APPENDIX I: EVALUATION OF ε

The distribution function $f(\vec{k})$ may be written in the form

$$f(\vec{k}) = \text{constant} \times \exp\left[-\frac{\hbar^2}{2 < m^* > k_B T}(k_x^2 + k_y^2 + k_z^2)\right] \quad (I.1)$$

where $<m^*>$ is the average effective mass of the electron. Thus

$$\int_{-\infty}^{\infty}\int_{-\infty}^{\infty}\int_{-\infty}^{\infty} \exp\left[-\frac{\hbar^2}{2 < m^* > k_B T}(k_x^2 + k_y^2 + k_z^2)\right] dk_x dk_y dk_z$$

$$= \left(\frac{2 < m^* > k_B T}{\hbar^2}\right)^{3/2} \pi^{3/2} \quad (I.2)$$

setting $G_N = |\vec{G}_N|$, we obtain

$$\frac{\partial^2}{\partial k_x^2}\left[\frac{(k_x^2 + k_y^2 + k_z^2)^2}{(2k_x G_N - G_N^2)}\right] = \frac{4}{(2k_x G_N - G_N^2)^3}$$

$$\times \{6 G_N^2 k_x^4 - 8 G_N^3 k_x^3 + 3 G_N^4 k_x^2$$

$$+ (k_y^2 + k_z^2)(G_N^4 + 2 G_N^2 (k_y^2 + k_z^2))\} \quad (I.3)$$

By introducing the normalized quantities

$$s_x = \frac{k_x}{G_N}, \quad s_y = \frac{k_y}{G_N}, \quad s_z = \frac{k_z}{G_N} \quad (I.4)$$

Eq. (I.3) becomes

$$\frac{\partial^2}{\partial k_x^2}\left[\frac{(k_x^2 + k_y^2 + k_z^2)^2}{(2k_x G_N - G_N^2)}\right] = \frac{4}{(2 S_x - 1)^3}$$

$$\times \{6 S_x^4 - 8 S_x^3 + 3 S_x^2 + S_y^2 + S_z^2 + 2 S_y^4 + 2S_z^4 + 4 S_y^2 S_z^2\} \qquad (I.5)$$

For large N and small $\vec{k}$, we find that S_x, S_y and $S_z << 1$. Therefore, we may neglect terms involving any of them having powers higher than 2. With this approximation Eq. (I.5) reduces to

$$\frac{\partial^2}{\partial k_x^2}\left[\frac{(k_x^2 + k_y^2 + k_z^2)^2}{(2k_x G_N - G_N^2)}\right] \simeq \frac{-4}{G_N^2} (3k_x^2 + k_y^2 + k_z^2) \qquad (I.6)$$

Hence, we have

$$\int_{-\infty}^{\infty}\int_{-\infty}^{\infty}\int_{-\infty}^{\infty} - \frac{4}{G_N^2} (3k_x^2 + k_y^2 + k_z^2) \exp\left[- \frac{\hbar^2}{2 < m^* > k_B T} (k_x^2 + k_y^2 + k_z^2)\right] dk_x dk_y dk_z$$

$$= - \frac{10 \pi^{3/2}}{G_N^2} \left(\frac{2 < m^* > k_B T}{\hbar^2}\right)^{5/2} \qquad (I.7)$$

and Eq. (I.3) reduces to

$$\frac{1}{m_N} = - \frac{1}{10 k_B T} \frac{\hbar^2 G_N^2}{< m^*_{\vec{G}_N} >^2} \qquad (I.8)$$

In this thesis $< \frac{1}{m^*_{\vec{G}_N}} > = \frac{1}{<m^*_{\vec{G}_N}>} = \frac{1}{<m^*>}$

Thus, we obtain

$$\frac{E_{\vec{k},N} - E_{o,N}}{\mathcal{E}} = \frac{1}{5\, k_B T} \left(\frac{\hbar^2 G_N^{\,2}}{2 < m^*_{\vec{G}_N} >} \right)^2 \tag{I.9}$$

which is termed the "vertical scale".

APPENDIX II

Evaluation of Integrals Defined in Eqs. (4.27) - (4.31)

(a) The integral $W_n(k,k')$ can be put in the form:

$$W_n(k, k') = (k^2 + k'^2)^{\frac{r}{2}} \int_{-1}^{1} [1 - (\frac{2kk'}{k^2+k'^2}) u]^{\frac{r}{2}} P_n(u)\, du \qquad (II.1)$$

Since $(\frac{2kk'}{k^2+k'^2})u$ is always less than unity we can write

$$[1 - (\frac{2kk'}{k^2+k'^2})u]^{\frac{r}{2}} = 1 - \frac{r}{2} (\frac{2kk'}{k^2+k'^2})u + \frac{\frac{r}{2}(\frac{r}{2} - 1)}{2!} (\frac{2kk'}{k^2+k'^2})^2 u^2$$

$$- \frac{\frac{r}{2}(\frac{r}{2} - 1)(\frac{r}{2} - 2)}{3!} (\frac{2kk'}{k^2+k'^2})^3 u^3 + \ldots$$

$$= \sum_{p=o}^{\infty} \frac{\Gamma(2p - \frac{r}{2})}{\Gamma(- \frac{r}{2})\ \Gamma(2p + 1)} \left(\frac{2kk'}{k^2+k'^2}\right)^{2p} u^{2p}$$

$$+ \sum_{p=o}^{\infty} \frac{\Gamma(2p + 1 - \frac{r}{2})}{\Gamma(- \frac{r}{2})\ \Gamma(2p + 2)} \left(\frac{2kk'}{k^2+k'^2}\right)^{2p+1} u^{2p+1} \qquad (II.2)$$

Legendre function $P_n(u)$ is an even or odd function according to whether n is even or odd integer, respectively. Therefore, the integration in Eq. (II.1) will be twice the integration from 0 to 1 if we take the first summation on the right-hand side of Eq. (II.2) with $P_{n\ even}$ and the second summation on the right-hand side of Eq. (II.2) with $P_{n\ odd}$ such that the integrand in Eq. (II.1) is always an

even function, otherwise the integration will vanish.

Therefore, if q is a positive integer we get

$$(k, k') = (k^2+k'^2)^{\frac{r}{2}} \sum_{p=o}^{\infty} \frac{\Gamma(2p - \frac{r}{2})}{\Gamma(-\frac{r}{2})\ \Gamma(2p+1)} \left(\frac{2kk'}{k^2+k'^2}\right)^{2p} \frac{(-1)^q \Gamma(q-p)\Gamma(\frac{1}{2} + p)}{\Gamma(-p)\Gamma(q+\frac{3}{2}+p)} \tag{II.3}$$

$$1\ (k, k') = (k^2+k'^2)^{\frac{r}{2}} \sum_{p=o}^{\infty} \frac{\Gamma(2p+1-\frac{r}{2})}{\Gamma(-\frac{r}{2})\ \Gamma(2p+2)} \left(\frac{2kk'}{k^2+k'^2}\right)^{2p+1} \frac{(-1)^q \Gamma(q-p)\ \Gamma(\frac{3}{2}+p)}{\Gamma(q+\frac{5}{2}+p)\ \Gamma(-p)} \tag{II.4}$$

As a special case we examine the behaviour of the integrals W_n for polar optical scattering [Conwell and Vassell, 1968] for which r = -2.

$$\begin{aligned} W_n\ (k, k') &= \frac{1}{2kk'} \sum_{m=0}^{\infty} (2m + 1)\ Q_m\left([k^2 + k'^2]/2kk'\right) \int_{-1}^{1} P_m(u)\ P_n(u)\ du \\ &= \frac{1}{kk'}\ Q_n\left([k^2 + k'^2]/2kk'\right) \end{aligned} \tag{II.5}$$

where Q_n are Legendre functions of the second kind. From the characteristics of $Q_n(\ [k^2 + k'^2]/2kk'\ )$ for $[k^2 + k'^2]/2kk' > 1$ it can be shown that we need consider only W_o and W_1 since the value of W_n decreases rapidly for n greater than 1. In general cases in which r is arbitrary, the integrals W_{2q} and W_{2q+1} given in Eqs. (II.3) and (II.4) have the same features as the aforementioned case, and therefore we consider only W_o and W_1. These are given by

$$W_o(k, k') = (k^2+k'^2)^{\frac{r}{2}} \sum_{p=o}^{\infty} \frac{\Gamma(2p - \frac{r}{2})}{\Gamma(-\frac{r}{2})\ \Gamma(2p+1)\ (\frac{1}{2}+p)} \left(\frac{2kk'}{k^2+k'^2}\right)^{2p} \tag{II.6}$$

and

$$W_1(k, k') = (k^2+k'^2)^{\frac{r}{2}} \sum_{p=o}^{\infty} \frac{\Gamma(2p+1-\frac{r}{2})}{\Gamma(-\frac{r}{2})\ \Gamma(2p+2)\ (\frac{3}{2}+p)} \left(\frac{2kk'}{k^2+k'^2}\right)^{2p+1} \qquad \text{(II.7)}$$

This shows that the summation over n for the scattering term in Eq. (4.26) will contain only the first two terms: n=0 (ℓ=0) and n=1 (ℓ= -1,0,0). Therefore, in the following integrals we shall consider these two values of n only.

(b) The integrals y_n^ℓ can be readily obtained if only the values 0 and 1 for n are considered. The results are

$$y_o^0 = 2\sqrt{\pi} \qquad \text{(II.8)}$$

$$y_1^{-1} = 0 \qquad \text{(II.9)}$$

$$y_1^o = 0 \qquad \text{(II.10)}$$

$$y_1^1 = 0 \qquad \text{(II.11)}$$

(c) Since the integrals y_n^ℓ are multiplied by $S_n(k)_{ij}$ in Eq. (4.26) and from the results given by Eqs. (II.8) through (II.11), we conclude that it is necessary only to calculate $S_o(k)_{ij}$. The result is given by

$$S_o(k)_{ij} = \frac{1}{2} \frac{\left(\frac{2m_j^*}{\hbar^2}\right)^{\frac{1}{2}}}{(E-\hbar\omega_s-\Delta_j)^{\frac{1}{2}}} \left[\left(\frac{2m_j^*}{\hbar^2}\right)^{\frac{1}{2}} (E-\hbar\omega_s-\Delta_j)^{\frac{1}{2}} + K_j\right]^2$$

$$\times \sum_{p=0}^{\infty} \frac{\Gamma(2p-\frac{r}{2})}{\Gamma(-\frac{r}{2})\,\Gamma(2p+1)\,(\frac{1}{2}+p)} \left[\{(\frac{2m_i^*}{\hbar^2})^{\frac{1}{2}}(E-\Delta_i)^{\frac{1}{2}}+K_i\}^2 + \{(\frac{2m_j^*}{\hbar^2})^{\frac{1}{2}}(E-\hbar\omega_s-\Delta_j)^{\frac{1}{2}}+K_j\}^2\right]^{\frac{r}{2}-2p}$$

$$\times \left[2\,\{(\frac{2m_i^*}{\hbar^2})^{\frac{1}{2}}(E-\Delta_i)^{\frac{1}{2}}+K_i\}\,\{(\frac{2m_j^*}{\hbar^2})^{\frac{1}{2}}(E-\hbar\omega_s-\Delta_j)^{\frac{1}{2}}+K_j\}\right]^{2p} \qquad \text{(II.12)}$$

(d) The integrals $Z_n^{\ell}(k')_{ij}$ for $n=0$ and $\ell=0$ is

$$Z_o^o(k')_{ij} = \frac{\sqrt{\pi}\, m_j^*}{e\hbar\gamma_j k'}\, \ln\left\{ e^{\frac{2e\hbar\gamma_j k'}{m_j^*}} \frac{(1+e^{\alpha_j+\beta_j E' - \frac{e\hbar\gamma_j k'}{m_j^*}})}{(1+e^{\alpha_j+\beta_j E' + \frac{e\hbar\gamma_j k'}{m_j^*}})} \right\} \qquad \text{(II.13)}$$

The integrals $Z_1^{\pm}(k')_{ij}$ will vanish due to the integration over the angle ϕ'. The remainder integration of this group is

$$Z_1^o(k')_{ij} = \sqrt{3\pi}\,(\frac{m_j^*}{e\hbar\gamma_j k'})^2 \Bigg[2(\alpha_j+\beta_j E')(\frac{e\hbar\gamma_j k'}{m_j^*})$$

$$-\left\{\sum_{t=0}^{\infty} \frac{2(-1)^t}{t^2\, t!}\, e^{-t(\alpha_j+\beta_j E')}\left(\left[1+t(\alpha_j+\beta_j E')\right]\sinh\frac{te\hbar\gamma_j k'}{m_j^*} - \frac{te\hbar\gamma_j k'}{m_j^*}\cosh\frac{te\hbar\gamma_j k'}{m_j^*}\right)\right\}$$

$$-(\alpha_j+\beta_j E')\ln\left\{ e^{\frac{2e\hbar\gamma_j k'}{m_j^*}} \frac{(1+e^{\alpha_j+\beta_j E' - \frac{e\hbar\gamma_j k'}{m_j^*}})}{(1+e^{\alpha_j+\beta_j E' + \frac{e\hbar\gamma_j k'}{m_j^*}})} \right\}\Bigg] \qquad \text{(II.14)}$$

(e) The integrals $T_n^{\ell}(k)_{ij}$ for $n=0$ and $\ell=0$ is

$$T_o^o(k)_{ij} = \frac{1}{2}\,\frac{(\frac{2m_j^*}{\hbar^2})}{k_j^+ - K_j}\, k_j^{+\,2}$$

$$\times \frac{\sqrt{\pi}\, m_j^*}{e\hbar\gamma_j k_j^+}\, \ln\left\{ e^{\frac{2e\hbar\gamma_j k_j^+}{m_j^*}} \frac{(1+e^{\alpha_j+\beta_j(E+\hbar\omega_s) - \frac{e\hbar\gamma_j k_j^+}{m_j^*}})}{(1+e^{\alpha_j+\beta_j(E+\hbar\omega_s) + \frac{e\hbar\gamma_j k_j^+}{m_j^*}})} \right\}$$

$$\times \sum_{p=o}^{\infty} \frac{\Gamma(2p-\frac{r}{2})}{\Gamma(-\frac{r}{2})\ \Gamma(2p+1)\ (\frac{1}{2}+p)} [\{(\frac{2m_i^*}{\hbar^2})^{\frac{1}{2}}(E-\Delta_i)^{\frac{1}{2}}+K_i\}^2+k_j^{+\ 2}]^{\frac{r}{2}-2p}$$

$$\times [2 \left\{ (\frac{2m_i^*}{\hbar^2})^{\frac{1}{2}} (E-\Delta_i)^{\frac{1}{2}} + K_i \right\} k_j^+]^{2p}$$

$$\text{(II.15)}$$

where

$$k_j^+ = (\frac{2m_j^*}{\hbar^2})^{\frac{1}{2}} (E + \hbar\omega_s - \Delta_j)^{\frac{1}{2}} + K_j \qquad \text{(II.16)}$$

The integrals $T_1^{\pm}(k)_{ij}$ will vanish since $Z_1^{\pm}(k')_{ij}=0$. Therefore, the last integral in this group is given by

$$T_1^o(k)_{ij} = \frac{1}{2} \frac{(\frac{2m_j^*}{\hbar^2})\ k_j^{+\ 2}}{k_j^+ - K_j}$$

$$\times \left(\sum_{p=o}^{\infty} \frac{\Gamma(2p+1-\frac{r}{2})}{\Gamma(-\frac{r}{2})\ \Gamma(2p+2)\ (\frac{3}{2}+p)} [\{(\frac{2m_i^*}{\hbar^2})^{\frac{1}{2}}(E-\Delta_i)^{\frac{1}{2}}+K_i\}^2+k_j^{+2}]^{\frac{r}{2}-2p-1} \right.$$

$$\left. \times [2\ \{(\frac{2m_i^*}{\hbar^2})^{\frac{1}{2}}(E-\Delta_i)^{\frac{1}{2}}+K_i\}\ k_j^+]^{2p+1} \right)$$

$$\times \sqrt{3\pi}\left(\frac{m_j^*}{e\hbar\gamma_j k_j^+}\right)^2 \Bigg\{ 2\,\{\alpha_j + \beta_j (E+\hbar\omega_s)\}\,\{\frac{e\hbar\gamma_j k_j^+}{m_j^*}\}$$

$$- \left[\sum_{t=o}^{\infty} \frac{2\,(-1)^t}{t^2\, t!}\, e^{-t\left[\alpha_j+\beta_j(E+\hbar\omega_s)\right]} \left(\left\{1+t\left[\alpha_j+\beta_j(E+\hbar\omega_s)\right]\right\} \sinh \frac{te\hbar\gamma_j k_j^+}{m_j^*} - \frac{te\hbar\gamma_j k_j^+}{m_j^*} \cosh \frac{te\hbar\gamma_j k_j^+}{m_j^*} \right)\right]$$

$$- \left[\alpha_j+\beta_j(E+\hbar\omega_s)\right] \ln\left[e^{\frac{2e\hbar\gamma_j k_j^+}{m_j^*}} \frac{\left(1 + e^{\alpha_j+\beta_j(E+\hbar\omega_s)-\frac{e\hbar\gamma_j k_j^+}{m_j^*}}\right)}{\left(1 + e^{\alpha_j+\beta_j(E+\hbar\omega_s)+\frac{e\hbar\gamma_j k_j^+}{m_j^*}}\right)} \right] \Bigg\}$$

(II.17)

REFERENCES

Baraff, G.A., "Maximum anisotropy approximation for calculating electron distribution; application to high field transport in semiconductors," Phys. Rev. 133, A26-A33 (1964).

Bardeen, J. and Shockley, W., "Scattering of electrons in crystals in the presence of large electric fields," Phys. Rev. 80, 69-71 (1950).

Bartling, J.Q. and Craig, R.A., "Method of executing the tight-binding method of energy-band calculation," Phys. Rev. B3, 3170-3172 (1971).

Bassani, F. and Yashimine, M., "Electronic band structure of group IV elements and of III-V compounds," Phys, Rev. 130, 20-33 (1963).

Bloch, F., "Uber die quantenmechanik der elektronen in kristallgittern," Z. Physik 52, 555-600 (1929).

Butcher, P.N., "The Gunn effect," Reports on Progress in Physics 30, 97-148 (1967).

Callaway, J., Energy Band Theory, Academic Press, New York, Chapter 2 (1964).

Cardona, M. and Pollak, F.H., "Energy band structure of Germanium and Silicon: the $\vec{k} \cdot \vec{p}$ method," Phys. Rev. 142, 530-543 (1966).

Cohen, M.L. and Bergstresser, T.K., "Band structures and pseudopotential form factors for fourteen semiconductors of the diamond and zinc-blende structures," Phys. Rev. 141, 789-796 (1966).

Cohen, M.H. and Heine, V., "Cancellation of kinetic and potential energy in atoms, molecules and solids," Phys. Rev. 122, 1821-1826 (1961).

Conwell, E.M., High Field Transport in Semiconductors, Solid State Physics, Supplement G, Academic Press, New York (1967).

Conwell, E.M. and Vassell, M.O., "High-field distribution function in GaAs," IEEE Trans. Electron Devices ED-13, 22-27 (1966).

Conwell, E.M. and Vassell, M.O., "High-field transport in n-GaAs," Phys. Rev. 166, 979-821 (1968).

Curby, R.C. and Ferry, D.K., "Mobility of hot electrons in n-type InAs," Phys. Rev. B3, 3379-3389 (1971).

Dresselhaus, G., "Spin-orbit coupling effects in zinc blende structures," Phys. Rev. 100, 580-586 (1955).

Ehrenreich, H., "Transport of electrons in intrinsic InSb," J. Phys. Chem. Solids 9, 129-148 (1959).

Ehrenreich, H., "Band structure and electron transport of GaAs," Phys. Rev. 120, 1951-1963 (1960).

Elliott, R.J., "Spin orbit coupling in band theory-character tables for some double space groups," Phys. Rev. 96, 280-287 (1954).

Falicov, L.M., "Orthogonalized plane waves and pseudo-potentials," Metallurgical Society Conferences Vol. 45, Gordon and Breach, Science Publishers (1968).

Fawcett, W., Boardman, A.D. and Swain, S., "Monte Carlo determination of electron transport properties in GaAs," J. Phys. Chem. Solids 31, 1963-1990 (1970).

Folberth, O.G., Z. Naturforsch. 10a, 502. The discussion on this reference can be found in Madelung, 1964 .

Fröhlich, H. and Paranjape, B.V., "Dielectric breakdown in solids," Proc. Phys. Soc. 69, 21-32 (1956).

Grünbaum, F. (editor), The Boltzmann Equation, Courant Institute of Mathematical Sciences, New York (1972).

Hamermesh, M., Group Theory and Its Application to Physical Problems, Addison-Wesley Publishing Company, Inc., Mass., U.S.A. (1962).

Hasty, T.E., Stratton, R. and Jones, E.L., "Effect of nonuniform conductivity on the behaviour of Gunn effect samples," J. Appl. Phys. 39, 4623-4632 (1968).

Herman, F., "Band structures of semiconductors," Electronic Structures in Solids, Second Chania Conf., Crete, Plenum Press, New York (1969).

Herring, C., "A new method for calculating wave functions in crystals," Phys. Rev. 57, 1169-1177 (1940).

Hilsum, C., "Mixed scattering in III-V compounds," Proc. Internal. Conf. on Phys. Semi., Kyoto, 532-536 (1966).

Howarth, D.J. and Sondheimer, E.H., "The theory of electronic conduction in polar semiconductors," Proc. Roy. Soc. A29, 53-74 (1953).

Huang, K., Statistical Mechanics, John Wiley and Sons, Inc., New York (1963).

Kane, E.O., "Band structure of Indium Antimonide," J. Phys. Chem. Solids 1, 249-261 (1957).

Kane, E.O., "The $\vec{k} \cdot \vec{p}$ method," Semiconductors and Semimetals Vol. 1, Academic Press, New York, Chapter 3 (1966).

Kogan, Sh. M., "On the theory of hot electrons in semiconductors," Soiet Physico - Solid State (English trans.) 4, 1813-1819 (1963).

Kohn, W. and Rostoker, N., "Solution of the Schrödinger equation in periodic lattices with application to metallic lithium," Phys. Rev. 94, 1111-1120 (1954).

Korringa, J., "On the calculation of the energy of a Bloch wave in a metal," Physica 13, 392-400 (1947).

Kurosawa, T., "Monte Carlo calculation of hot electron problem," Proc. Internal. Conf. on Phys. Semi., Kyoto, 424-426 (1966).

Law, H.C. and Kao, K.C., "Analytical solutions of the Boltzmann transport equation. I. carrier transport phenomena in nondegenerate semiconductors at low fields," Phys. Rev. B4, 2524-2534 (1971).

Long, D., "Energy band structures of mixed crystals of III-V compounds," Semiconductors and Semimetals Vol. 1, Academic Press, New York, Chapter 5 (1966).

Loucks, T.L., Augmented Plane Wave Method, Frontiers in Physics, W.A. Benjamin, Inc., Hew York (1967).

Madelung, O., Physics of III-V Compounds, John Wiley and Sons, Inc., New York (1964).

Mazo, R.M., Statistical Mechanical Theories of Transport Processes, The International Encyclopedia of Phys. Chem. and Chem. Phys., Pergamon Press, Oxford (1967).

Messiah, A., Quantum Mechanics, North-Holland Publishing Company, Amsterdam, Vol. 2, Chapter 19 (1965).

Novikova, S.I., "Thermal expansion," Semiconductors and semimetals Vol. 2, Academic Press, New York, Chapter 2 (1966).

Parmenter, R.H., "Symmetry properties of the energy bands of the zinc blende structure," Phys. Rev. 100, 573-579 (1955).

Pendry, J.B., "The cancellation theorem in pseudopotential theory," J. Phys. C.: Solid State Physics 4, 427-434 (1971).

Phillips, J., "Energy band interpolation scheme based on a pseudopotential," Phys. Rev. 112, 685-695 (1958).

Phillips, J. and Kleinman, L., "New method for calculating wave functions in crystals and molecules," Phys. Rev. 116, 287-294 (1959).

Pollak, F.H., Higginbotham, C.W. and Cardona, M., "Band structure of GaAs, GaP, InP and AlSb: the $\vec{k} \cdot \vec{p}$ method," Proc. Internal. Conf. on Phys. Semi. Kyoto, 20-26 (1966).

Rees, H.D., "Calculation of the distribution functions by exploiting the stability of the steady state," J. Phys. Chem. Solids 30, 643-655 (1969).

Ridley, B.K. and Watkins, T.B., "The possibility of negative resistance in semiconductors," Proc. Phys. Soc. 78, 293-304 (1961).

Rode, D.L., "Electron mobility in direct-gap polar semiconductors," Phys. Rev. B2, 1012-1024 (1970).

Rode, D.L., "Electron transport in InSb, InAs and InP," Phys. Rev. B3, 3287-3298 (1971).

Ruch, J.G. and Kino, G.S., "Transport properties of GaAs," Phys. Rev. 174, 921-931 (1968).

Sharma, S.K., "Attenuation and amplification of acoustic waves in nondegenerate semiconductors in the presence of dc fields," Phys. Rev. B3, 3279-3282 (1971).

Sladek, R.J., "Pressure dependence of the resistivity and Hall effect in n-GaAs," Bull. Am. Phys. Soc. A9, 258-268 (1964).

Slater, J.C., "Electronic energy bands in metals," Phys. Rev. 45, 794-801 (1934).

Slater, J.C., "Wave functions in a periodic potentials," Phys. Rev. 51, 846-851 (1937).

Spenke, E., Electronic Semiconductors, McGraw-Hill Book Company, Inc., New York (1958).

Wassef, W.A. and Kao, K.C., "High-field distribution function of carriers in semiconductors," Phys. Rev. B6, 1425-1435 (1972).

Wigner, E. and Seitz, F., "On the constitution of metallic sodium," Phys. Rev. 43, 804-810 (1933).

Żukotyński, S. and Grynberg, M., "On the theory of transport phenomena with anisotropic scattering," Phys. Stat. Sol. 9, 549-553 (1965).